



Commission of the European Communities

technical steel research

Reduction of ores

Coal injection into the blast furnace



Report

EUR 8544 EN

Blow-up from microfiche original

Commission of the European Communities

technical steel research

Reduction of ores

Coal injection into the blast furnace

S. BORTZ

ESTEL-HOOGOVS
Building 3G 25
PO Box 10 000
NL-1970 CA IJMUIDEN

Contract No 7210.AA/601
(1.7.1981 - 1.5.1982)

FINAL REPORT

Directorate-General
Science, Research and Development

1983

EUR 8544 EN

**Published by the
COMMISSION OF THE EUROPEAN COMMUNITIES
Directorate-General
Information Market and Innovation
Bâtiment Jean Monnet
LUXEMBOURG**

LEGAL NOTICE

Neither the Commission of the European Communities nor any person acting on behalf of the Commission is responsible for the use which might be made of the following information

ZUSAMMENFASSUNG

Es wurde die Verbrennung von Kohlenstaub unter Bedingungen untersucht, die das Einsprühen in einen Hochofen simulieren. Vier Kohlesorten wurden erprobt und die Auswirkungen von Kohleeinsatz, Blastemperaturen von 900°C bis 1200°C, Feinheit der Kohle, Einblaslage und Momentum auf die Verbrennung dieser Kohlesorten durch Sichtbarmachen und Messungen beschrieben.

Die Leistung der Kohle war von der Kohlequalität abhängig. Die anderen Parameter, insbesondere der Kohledurchsatz, übten ebenfalls einen starken Einfluss auf die Verbrennungsgeschwindigkeit aus. Es bestehen Hinweise dafür, dass die rasche Verbrennung (<10 min) von der Pyrolysegeschwindigkeit abhängig ist, wobei das Ausbringen flüchtiger Stoffe erheblich über den Werten der Analyse von Fettkohle liegt. Die Verbrennung der ausgestossenen flüchtigen Bestandteile war unbefriedigend und führte zu Russbildung. Dieses Problem wurde noch durch einen hohen Kohleeinsatz verstärkt. Die Holzkohleverbrennung war bei allen vier Testkohlesorten langsam, was einen Hinweis dafür darstellt, dass die Annahme der vollständigen Verbrennung im Laufringbereich des Hochofens wahrscheinlich falsch ist, ausser bei sehr begrenztem Kohleeinsatz.

RESUME

On a étudié la combustion du charbon pulvérisé dans des conditions simulant l'injection dans un haut fourneau. Quatre charbons différents ont été testés et les effets de la mise au mille du charbon, des températures du vent de 900 à 1200°, de la finesse du charbon, de la position et de la cadence d'injection, sur la combustion de ces charbons ont été déterminés par observation visuelle et mesurés.

On s'est aperçu que la performance des charbons dépendait étroitement des stades de la houille. Les autres paramètres, notamment la vitesse d'écoulement du charbon influent eux aussi fortement sur la vitesse de combustion. Les résultats montrent que le stade initial de la combustion (< 10 ms) est caractérisé par des taux de pyrolyse qui déterminent une production de matières volatiles nettement en excès par rapport aux résultats de l'analyse immédiate effectuée sur les charbons bitumineux. On a constaté que la combustion des matières volatiles rejetées était limitée par la réaction, d'où formation de suie. Ce problème se trouve amplifié avec un charbon dont la mise au mille est élevée. La combustion des résidus pour les quatre charbons testés est lente, indiquant que l'hypothèse d'une combustion complète dans la zone des canalisations d'un haut fourneau est probablement fausse, sauf pour des mises au mille très réduites.

<u>TABLE OF CONTENTS</u>	<u>Page</u>
NOMENCLATURE	I
ABSTRACT	II
1. INTRODUCTION	1
1.1 Background	1
1.2 Objectives	2
2. EXPERIMENTAL ARRANGEMENTS	3
2.1 Instrumentation	3
2.2 Coal preparation and composition	3
2.3 Furnace and air preheater	4
2.4 Tuyere and blow pipe	4
2.5 Input conditions	5
3. EXPERIMENTAL RESULTS	6
3.1 Presentation of data	6
3.2 Measurement techniques and interpretation	7
3.3 Elk Creek measurement results	9
3.4 Armco coal	15
3.5 Norwich Park coal	16
3.6 Preussag coal	17
3.7 Heavy fuel oil	18
3.8 Additional experiments	19
4. COMPARISON OF THE IFRF SIMULATION TO BLAST FURNACE CONDITIONS	20
4.1 Blast furnace	20
4.2 Wall temperature and raceway geometry	20
5. SUMMARY AND CONCLUSIONS	22
REFERENCES	
TABLES	
FIGURES	
PHOTOS	

NOMENCLATURE

<u>Symbol</u>	<u>Definition</u>
AR	Armco coal
AP	Axial position
A ₀	Weight percent of ash in the input coal
A ₁	Local weight percent of ash in the flame
C ₀	Weight percent of carbon in the input coal
c ₁	Local weight percent of carbon in the flame
C _x	Burnout, total carbon
C _f	Burnout, fixed carbon (uncorrected for Q-factor)
C _{CO2}	Oil burnout, based on the local CO ₂ concentration
EC	Elk Creek coal
F	Fine grind of the coal
HP	Horizontal position
h ₀	Weight percent of hydrogen in the input coal
h ₁	Local weight percent of hydrogen in the flame
H _x	Burnout, hydrogen
I	Injector
NP	Norwich Park coal
N	Normal grind of the coal
P	Preussag coal
Q	Ratio of true volatile yield to proximate volatile matter
SR	Stoichiometric ratio
T _b	Blast temperature
T _x	Burnout, total
V ₀	Weight percent of volatiles in the input coal
V ₁	Local weight percent of volatiles in the flame
Z _x	Burnout, volatiles

ABSTRACT

Combustion of pulverised coal under conditions simulating injection into a blast furnace was studied. Four coals were tested and the effects of coal rate, blast temperatures from 900 °C to 1200 °C, coal fineness, injection position and momentum, on the combustion of these coals were characterized through visualization and measurements.

The performance of the coals was very dependent on the coal rank. The other parameters, particularly coal flow rate, also had a strong influence on the combustion rate. Indications are that the early combustion (<10 ms) is determined by pyrolysis rates with volatile yields significantly in excess of the proximate analysis being measured for the bituminous coals. The combustion of the expelled volatile matter was found to be mixing limited, leading to soot formation. This problem was amplified with a high coal rate. The char combustion for all four test coals was slow, indicating that an assumption of complete combustion in the raceway region of a blast furnace is probably invalid, except at very reduced coal rates.

1. INTRODUCTION

1.1 Background

The rising cost and reduced availability of fuel oil and natural gas has made coal an attractive blast furnace injectent. Despite fuel handling and flow monitoring problems inherent in a solid injection system the use of coal is becoming more common.

Because of the immense difficulties in performing combustion related measurements under actual blast furnace conditions, knowledge about combustion in a blast furnace is extremely limited. It is believed that it is important for solid fuel injectents to be consumed before leaving the zone of a blast furnace known as the raceway. This belief has arisen from problems with soot collection in the flue gas cleaning plants and raceway blockages encountered during heavy fuel oil injection.

The raceway is a cavity formed in the blast furnace charge by forces generated from the hot blast. Several people have measured the size and shape of the chamber in operating blast furnaces. An endoscope was used by Greuel et al. [1], to investigate the raceway region. The picture of this region resulting from their investigation is shown in figure 6. This chamber takes the shape of a curved hose expanding in diameter with distance. A typical length for this chamber appears to be between 1.0 and 1.5 meters long. Estimating the average blast velocity in the raceway at 200 m/s the residence time of a small particle traveling with the gas would only be about 10 ms.

This time is much shorter than in normal furnaces where pulverised coal is used (cement kilns and boilers). In these type of furnaces the residence time is on the order of seconds. This short residence time in the raceway region is clearly an important factor in determining the percentage of coal combustion that will occur. Particularly the heterogenous combustion of coal is a relatively slow process, although burn-out times as fast as 20 ms have been reported for optimum conditions in coal engines [2].

However, it is clear, that in a blast furnace, conditions such as heating rate, mixing particle size, and other fuel properties must be optimized to achieve a reasonable level of burn-out in the raceway region. The effect of some parameters on burn-out times, for example particle sizes, are reasonable well understood. However, intrinsic coal properties such as reactivity and the devolatilization process under high heating rates are not as well understood, and also have an important role in determining combustion times.

The blast furnace provides a simple but effective means of burning coal. The blast air is preheated to temperatures which at some facilities exceeds 1200 °C. The blast air is then injected at a high velocity, of about 200 m/s, into the raceway region. The current method of coal injection is to mix the coal directly with this hot blast as described in figure 3. This results in extremely fast, convective heating of the coal particles, accelerated to an even faster rate through the high initial slip velocity between the coal and blast air.

Also if ignition occurs while the slip velocity is still high, the combustion rate of the coal can be enhanced by the increased oxygen availability at the particle surface.

The potential inefficiency in the blast furnace injection system, is the current method of mixing the coal with the blast air. The coal with cold transport air is injected through a straight pipe as showed in figure 3. Although some mixing of the coal with the blast air will result from the existance of a high initial velocity component of the coal jet in the direction normal to that of the blast air, this mixing is directional in nature. The remainder of the mixing process must occur through turbulent diffusion. The poor global mixing resulting from this system would be expected to generate local fuel rich regions and a delay in the heterogenous and volatile combustion. However, the desire to remain with a simple system combined with the impracticality of a complex injector due to the abbrasive nature of coal is the reason for chosing a single axial pipe injection system in a blast furnace.

It was to clarify the combustion process of coal under these special conditions of very high heating rates, about 10^6 °C/sec, with relatively poor mixing that this trial was performed. The experiments were conducted in the IFRF furnace rather than an actual blast furnace in order to facilitate visualization of the flames and to make possible measurements at accurately known spatial locations. The conditions in the raceway region of a blast furnace were simulated as well as possible (see table 6). If it was not feasible to simulate an important condition, an attempt to predict possible effects resulting from these deviations is made.

1.2 Objectives

The overall purpose of this programme was to understand the influence of some variable parameters on the combustion of pulverized coal under conditions simulating injection into a blast furnace. A full scale blow pipe and water cooled tuyere were used and the correct blast temperature and velocity were reproduced.

The parameters which were varied, were deliberately restricted to parameters which could be altered in a blast furnace system namely:

- coal type and particle size;
- air blast temperature;
- coal flow rate;
- coal injection parameters (position of coal lance, injector size).

Through visual observation and in-flame measurements of gas composition, and temperature as well as solid sampling, it was intended to develop a "picture" of the combustion process in a blast furnace raceway, and to indicate to what extent that process could be influenced through the variation of these parameters. In order to assist in extrapolating these results to actual conditions in a blast furnace, heavy fuel oil was also used as an injectent. Also for that purpose the coal presently being used in the blast furnaces situated in the Armco steelworks was selected as one of the test coals.

2. EXPERIMENTAL ARRANGEMENTS

2.1 Instrumentation

Standard IFRF techniques were applied for flue gas and detailed flame measurements. Here, only a list of instrumentation employed is outlined, as detailed information on the construction and principle of operation of these instruments are given in various IFRF publications [3].

- . Gas temperatures were measured with a suction pyrometer employing a Pt-Rh6, Pt-Rh30 thermocouple. In addition a fixed suction pyrometer was used to measure the flue gas temperature.
- . Gas concentrations were sampled with an IFRF "B" probe. The "B" probe utilizes bronze filters with pore sizes of 5-7 μ . The gases were analysed using a gas chromatograph and also various single specific instruments (CO_2 , O_2 , CO , NO_x).
- . Solid samples were also collected with the "B" probe. In-flame gas velocities were approximated by Prandtl probe measurements in the blast air jet and whenever possible solid sampling was done under near isokinetic conditions.

2.2 Coal preparation and composition

The IFRF pulverized fuel preparation plant includes a combined drying and pneumatic transport system for raw coal. The coal is pulverized in a ball mill and fed pneumatically into storage bunkers. From the storage bunkers the coal is delivered via a rotary valve into a pressurized, microprocessor controlled gravimetric feeding system. This pressurized feeder is a new system for the IFRF, and it gives more flexibility than the old atmospheric screw feeder-ejector mechanism.

The basic components of the new system are a pressurized weigh bunker, variable speed rotary valve, and electronic controls. By maintaining the pressure in the bunker above the required delivery pressure, the motive force for the coal transport is independent of the transport air. This allows a much higher ratio of coal to transport air than is possible with an ejector. The actual coal feed rate is then controlled by a variable speed rotary valve. The speed of the rotary valve is set by a microprocessor which monitors the rate of weight loss in the bunker and adjusts the speed of the valve to achieve a preset coal delivery rate. This new system can deliver from 100 kg/hr to 1000 kg/hr with coal to transport air ratios as high as 10 kg/kg. A schematic of the coal dosing system can be seen in figure 4.

For this trial the mass flow of transport air was kept constant at 50 kg/hr. This results in a mass ratio of coal to transport air of about 6/1 for the stoichiometric condition, and 3/1 for the reduced coal flow rate case.

The proximate and ultimate analysis of the four coals are shown in table 1. The numbers are reported on a dry (df) and dry-ash free (daf) basis. Also in this table more complete information about the four test coals can be found. The composition of the coals after devolatilization is shown as weight percentages of the original coal (fixed elements). The ash composition, the petrographic analysis, calorific values and other coal properties giving information about the rank and plasticity can also be found in table 1.

Particle size distributions for the four pulverized coals are shown in table 2. Unfortunately the size distributions are not identical. The ball mill used for grinding the coal does not give very much flexibility in changing the size distribution for a given coal. Consequently the final mean particle size is a function of the Hardgrove index of the coal. Also in this table a comparison between the two grindings obtained for the Elk Creek coal are shown. It should be noted that the fine grind of the Elk Creek coal compares reasonable well to the Norwich Park coal. This similarity will be used to compare the burn-out data from the two coals.

2.3 Furnace and air preheater

The trial was executed in the IFRF furnace number 1, which has a square cross-section of 4 m² and a length of 6.25 m, (see figure 1). The first 2 meters were uncooled to best simulate real blast furnace conditions, with the final 4.25 meters lined with cooling tubes to reduce the flue gas temperature to an acceptable level.

The desired blast air temperatures were obtained in a two step process, as indicated in figure 2. Firstly, the combustion air was indirectly heated to about 400 °C, by the existing IFRF air preheater. This air was then injected together with natural gas into a special precombustor furnace where combustion raised the temperature of the "air" to the desired level. Oxygen was added to this flue gas mixture to restore the oxygen content of the blast air back to a nominal value of 21.0%. It was also possible with this system to enrich the blast to levels above 21.0% O₂. Reduced blast temperatures were achieved by reduction of the natural gas input into the precombustor. This method results in a variation with temperature of the CO₂ and H₂O concentrations in the blast air. A list of the variation of blast composition with temperature is shown in table 3.

2.4 Tuyere and blow pipe

A full-scale blow pipe and water-cooled tuyere was used for these trials. A blow pipe previously used for oil injection on a Hoogovens blast furnace was obtained and modified for coal injection. The oil injection port was left unchanged and six possible positions for coal injection were provided. At three axial locations, an arrangement was made so that either a 16 mm or 32 mm lance could be inserted to variable depths inside the blow pipe. Figure 3 shows the position of the coal injectors on the blow pipe.

The different axial positions were used to enable the residence time of the coal, before exiting from the tuyere, to be varied. All injectors including the oil lance were at an angle of 18° with respect to the axis of the blow pipe.

The oil injection was performed at the standard position, resulting in the tip of the oil lance being located at the center of the inlet of the tuyere. The oil pipe had an exit diameter of 10 mm. Thermocouples were installed in both diameter coal lances to measure the lance tip temperature during operation. A photograph of the modified blow pipe can be seen in plate 5.

2.5 Input conditions

Input conditions for the various flames produced in this trial are listed in table 5. A set of standard inputs were pre-selected for these experiments and consisted of the following:

- blast temperature 1200 °C;
- blast velocity 200 m/s;
- coal flow rate to give a stoichiometric ratio (SR) equal to one;
- blast oxygen concentration 21%.

These standard inputs were then varied to enable the influences of a particular or combination of parameters to be evaluated. When the blast temperature was decreased the mass flow of the blast was increased to keep the velocity at about 200 m/s. The stoichiometric ratio was altered by reduction of the coal rate, consequently decreasing the thermal input. The coal transport air was maintained at 50 kg/hr independent of the coal rate.

3. EXPERIMENTAL RESULTS

3.1 Presentation of data

The data collected during this trial are presented in the form of tables, figures and photographs. All measured flames are listed in table 5. This table provides an easily accessible and concise list of input conditions for each flame, according to flame number. This list should be used to supplement the figures, where because of space limitations, complete information about the flame is not always supplied.

. Flame tables

In tables 7-24 a complete listing of measured gases, solids and temperatures are given. Each table corresponds to a particular flame, and the measured values are listed by axial and radial position. Also in these tables burn-out related quantities calculated from the chemical analysis of the solid samples are shown. These quantities have been calculated according to the following procedures, the limitations of which are discussed in the subsequent section on measurement techniques.

$$C_x = \frac{\text{Mass loss of carbon}}{\text{Carbon in the input coal}}$$

$$= 1 - \frac{C_1}{C_0} \cdot \frac{A_0}{A_1} = \text{Carbon burn-out}$$

$$H_x = \frac{\text{Mass loss of hydrogen}}{\text{Hydrogen in the input coal}}$$

$$= 1 - \frac{H_1}{H_0} \cdot \frac{A_0}{A_1} = \text{Hydrogen burn-out}$$

$$T_x = \frac{\text{Mass loss of total combustibles}}{\text{Total combustibles in the input coal}}$$

$$= \frac{1 - \frac{A_0}{A_1}}{1 - A_0} = \text{Total combustible burn-out}$$

$$Z_x = \frac{\text{Mass loss of volatiles}}{\text{Volatiles in the input coal}}$$

$$= 1 - \frac{V_1}{V_0} \cdot \frac{A_0}{A_1} = \text{Volatile burn-out}$$

$$C_f = \frac{\text{Mass loss of "fixed" combustibles}}{\text{Fixed combustibles in the input coal}}$$

$$= \frac{1 - V_o + \frac{A_o}{A_1} (V_1 - 1)}{1 - A_o - V_o} = \text{"Fixed" combustible burn-out}$$

. Figures

The data contained in the flame tables have been plotted in figures 8-36. In order to make these figures more independent the following flame identification scheme has been used. Where two or more flames are being compared according to a particular variable, that variable is shown next to the flame number. The variables have been labelled according to the following system; coal type (EC = Elk Creek, AR = Armco, NP = Norwich Park, P = Preussag); blast temperature (T_b); stoichiometric ratio (SR); coal fineness (N = normal, F = fine) and injector number (I). For example F-15 (SR = 1) and F-18 (SR = 2) indicates the figure which is showing the effect of stoichiometric ratio, where F-15 has a nominal stoichiometric ratio of 1 and F-18 a value of 2. Where a figure pertains to a single flame, complete information about that flame is given. For example F-15 (EC, $T_b = 1200$, SR = 1, N, I2) means flame F-15 has the following nominal inputs; the Elk Creek coal, a blast temperature of 1200 °C, a stoichiometric ratio of one, the grind of the coal is normal, and injector 2 was used. If more detailed information about the input conditions is required the flame list can be consulted.

3.2 Measurement techniques and interpretation

. Solids

The devolatilization and char combustion of the coal has been followed using standard ash tracer techniques. The solid material collected at various positions in the flame is analyzed for relevant quantities, in this case carbon, hydrogen, ash, and volatiles. From this analysis and the assumption of consistent ash behavior, various burn-out related quantities can be calculated. Here, consistent ash behavior implies that the total mass of ash as measured by standard analysis techniques remains constant and uniformly distributed.

An important point in the interpretation of these results is that the burn-out quantities relate only to a loss in weight of solid material. Particularly for volatile matter, this expelled material may not have undergone combustion, but only pyrolysis. For this reason the quantities C_x , H_x , T_x , Z_x and C_f are defined in terms of mass loss rather than burn-out. However, for the sake of simplicity and convention these parameters will be referred to as burn-out in the text.

The interpretation of the fixed carbon burn-out, C_f , is subject to another problem. The calculation is dependent on an accurate determination of the percentage volatile matter in the original coal. However, this measurement is performed by standard techniques under slower heating rates and to a much lower final temperature than found in this trial. It is a well established fact that both an increased heating rate and/or a high final temperature can considerably enhance the volatile yield, [2] and [5]. The ratio of actual volatile yield to the ASTM result is known as the Q-factor and values exceeding two have been measured. This implies that a substantial percentage of the weight calculated as fixed carbon burn-out may actually be expelled as volatile matter, when subjected to the high (10^6 °C/s) heating rates and combustion elevated temperatures found in this trial. When this parameter, C_f , has been plotted, it is only to emphasize a difference in the amount of fixed carbon measured in the partially combusted samples from two flames, not to imply that a certain percentage of fixed carbon has burned.

Gases

The measurement of gas composition is more direct than that of solid composition and probably less subject to error. However, the relationship of the gas measurements to burn-out is somewhat obscured by the large concentration gradients of the coal in the combustion air. The concentration of gases produced by combustion is a function of both particle concentration and particle burn-out. In order to correlate burn-out directly with the gas concentration measurements it is also necessary to have particle concentration measurements. However, due to the difficulties of accurately measuring particle concentration, combined with the time limitations of this trial they were not performed.

The CO_2 gas concentration cannot be directly compared for different blast temperature flames. This is a result of the variation of CO_2 content in the blast air with temperature (table 3).

Temperatures

The important consideration in the interpretation of the temperature measurements is that they relate to the gas and not to the particle temperatures.

Finally it must be remembered that all probes used here are intrusive, they alter the flame by their presence. This is particularly important in an unignited coal jet where turbulence caused by the probe may ignite the coal. For this reason neither gas nor solid samples were normally collected in the flame upstream of the ignition front. Sometimes temperature measurements were attempted in these regions, however they were performed with a unshielded thermocouple to avoid local ignition.

3.3 Elk Creek measurement results

. Injectors

The first parameter to be investigated was the effect of injector position and/or diameter. The back injectors, 3 and 6 (see figure 3) were quickly eliminated as practical positions because of slag formation on the hot wall of the blowpipe. The remaining four injectors were evaluated by collecting solids at an axial distance of 1.9 meter from the tuyere exit. The samples were then quickly analyzed for ash at the research station and the respective burn-out was calculated. The results from these tests are shown in table 4. They show that the injector position or diameter has only a small effect on burn-out at this axial location, although the 16 mm injector at the middle position appears to give slightly improved results over the 32 mm injector.

Photographs of the flames produced with injectors 1, 2, 4, 5 can be seen in Plate 1 and 2. The length of the furnace opening shown in these photographs is about 2 meters. The four photographs are all taken with a shutter speed of 1/500 sec. with the aperture set automatically to produce similar exposures. With all four injectors the general combustion process appears, in general, similar. The coal jet is always ignited inside the tuyere. There is a very bright initial flame region of about 1.5 meters in length. After this highly radiating region a cloud of particles continues downstream.

This very bright initial region probably results from high concentration of soot-like material, combined with rapid combustion of volatile matter [4]. This emissive region eventually disappears, as the concentration of this condensed material is reduced through oxidation and/or agglomeration. This process is perhaps better illustrated by photograph 10 in Plate 3. Here the ignition of the coal jet has been delayed through reduction of the blast temperature and now individual tracks of these bright sooting regions are visible as random ignitions occur.

The photograph of the flame produced with injector 2, photograph 4, seems to be slightly different from those of the other injectors. The furnace wall is clearly visible except directly behind the bright region for photographs 3, 5 and 6. It is only for injector 2, that the wall is obscured by what appears to be a very dense particle cloud, downstream of the bright initial region.

In order to verify and explain these observations and measurements injectors 2 (16 mm) and 5 (32 mm) were chosen for more detailed analysis. Axial and radial measurements of solids, gas and temperature were collected for the flames produced with these different size injectors. These injectors were chosen rather than 1 or 4 for several reasons. The middle injection position is favored by blast furnace personnel, and is the position that is used at Armco. The use of the middle position also simplifies the comparison of the coal combustion with the oil because of the similarity in axial location of these two injectors.

In figure 8a the total burn-out rate, T_x , and devolatilization rate, Z_x , are plotted for both injectors. In this figure the axial solids burn-out is plotted against axial position. Also on the burn-out figures an approximate residence time calculated from the coal injection point is shown on the upper horizontal scale. The residence time calculation is based on the blast jet velocities and assumes the particles behave as a gas, and also isothermal flow. The use of the large lance, injector 5, apparently slows down the initial devolatilization process. This perhaps is a result of the reduced mixing with the hot blast because of the lower fuel velocity. However, after an axial distance of 1.5 meter the burn-out curves are reasonable similar.

Based on results generated by various investigators and the general burn-out trends measured in this trial, the following interpretation of these burn-out measurements seems probable. The extremely high heating rates ($106\text{ }^\circ\text{C/s}$) and particle temperatures elevated by volatile combustion should significantly enhance the proximate volatile matter yield. Low rank bituminous coals typically yield 65 to 70% volatile matter, when subjected to conditions similar to those found here (Kobayashi, Howard and Sarofim [5] and Essenhigh [2]). The heterogeneous (char) combustion will be limited by the short residence time in the blast, approximately 2 ms, before the volatile combustion consumes the available oxygen. During this 2 ms period the particles must first heat up to ignition temperature, reducing the time for char combustion even more. The 10 ms ignition time measured for the Preussag coal gives an indication of the time required for heterogeneous ignition, figure 30. This ignition delay for the Preussag coal which contains only 4% volatiles, although it is probably less reactive than the other coals, supports the viewpoint that the ignition front for the bituminous coals, occurring after about 2 ms, is volatile ignition. This viewpoint is also supported by the recent work of Mclean [4] who observed the ignition and devolatilization behavior of pulverized coal particles injected into $1700\text{ }^\circ\text{K}$ gases. He also found, for bituminous coals, an abrupt region of gas phase volatile combustion that corresponded to the ignition point. This is a very critical observation, since as can be seen in the gas measurements for F-15 and F-18 (figures 17a, b) the oxygen concentration in the bright region of volatile combustion is almost zero. The rate of char combustion in this oxygen depleted region will be extremely slow. This indicates the initial burn-out ($t < 10\text{ ms}$) is primarily a result of pyrolysis. The combustion of char and soot occurs after about 10 ms when the devolatilization is nearly complete, and oxygen again becomes available through turbulent mixing.

An initially contradictory result is seen in the temperature measurements, figure 21a, for the two flames F-13 and F-15. Even though the axial burn-out curves (Z_x) show much quicker devolatilization with the smaller injector the initial gas temperature is higher for the large injector.

A partial explanation for these results is seen in the gas measurements. In figure 17a, the measured gas species for the 16 mm injector are shown. When compared with 17b, the 32 mm lance, a significantly higher concentration of CO₂ is seen for the large lance. This indicates that although more material has been devolatilized through the use of the small lance, because of a localized oxygen deficiency the greater mass of volatile matter cannot be completely oxidized. This gives rise to the greater early concentrations of CO and H₂ generated with the 16 mm injector.

Some further insight into the combustion process can be achieved through a comparison of the carbon to hydrogen ratio of the residual solid material collected on the flame axis. With injector 2 (16 mm) an elevated C/H mass ratio is seen during the first meter of the flame, when compared to injector 5. This suggests that larger quantities of condensed material, in the form of soot, are present. The C/H mass ratio of soot formed from rapid pyrolysis of a bituminous coal has been measured to be about 300 [4]. The C/H ratio of the Elk Creek char appears to be about 80. This number has been obtained by noting the C/H ratios at 5 meter axial distance for the high stoichiometric ratio flames (F-18, F-23, F-26). Here any soot should be rapidly oxidized and the solids collected near the exit of the furnace should provide a reasonable determination of the C/H ratio in the Elk Creek char. It is speculated that the condensed matter is formed in the following sequence of events. First light gases, CO and CH₄, are released from the coal particles, mix with the hot blast and through combustion reduce the local oxygen concentration. Then heavy tars are ejected and undergo condensation reactions in the oxygen depleted blast, forming soot-like structures. Other investigators have measured up to 25% of the expelled volatile matter condensing into soot [8]. The presence of soot can be detected through measurement of the C/H ratio in the sampled solids. If large amounts of the condensed material are captured in the filter, the carbon/hydrogen ratio of the collected solids should be increased.

The effect of ejector momentum, for the Elk Creek coal, seems to be as follows. A higher injection velocity appears to increase particle heating rates which promote much quicker devolatilization and pyrolysis. However, due to poor mixing, large fuel rich regions are created which delay combustion and promote soot formation. By delaying the devolatilization rate to better match the fuel and air mixing rate, more efficient combustion can result. However, it should be remarked that these processes seem to be very dependent on both coal type and stoichiometric ratio.

. Stoichiometric ratio, Elk Creek coal

In figure 8b, the effect of stoichiometric ratio on the coal burn-out is shown. The difference in inputs between F-15 and F-18 are coal rates of 290 and 140 kg/hr respectively. The greatest effect of stoichiometric ratio is observed on the char burn-out.

The high concentration of oxygen, figure 18a, increases the rate of char combustion, with a significant effect apparent after about 1 meter (10 ms). The axial temperature profiles for these two flames are shown in figure 21a. Here the initial temperatures are about the same, but because of the reduced coal rate for F-18 the peak temperature is reduced. It is informative to examine the axial behavior of the C/H ratios, figure 12b, for flame 18. The initial value is already very high at 25 cm and then rises to a remarkably high value at 50 cm, before beginning a rapid descent. This again documents the effect seen for F-15, where quick devolatilization resulted in a high C/H ratio in the collected solid and presumably a high soot concentration. However, if the oxygen concentration is high the soot-like material is rapidly oxidized and the C/H mass ratio returns to below 100, as observed for F-18.

The visible effect of stoichiometric ratio can be observed in Plate 2, photographs 7 and 8. Here, for the fine grind Elk Creek coal the bright sooting region is clearly smaller for F-26, although not necessarily less emissive. Also following this region the furnace wall is visible, evidently showing the reduced concentration of soot and char for the higher stoichiometric ratio.

. Blast temperature, Elk Creek coal

The effect of blast temperature is best introduced by the series of photographs 9, 10 and 11 shown in plate 3: In photograph 9 a decrease in luminosity is seen with a blast temperature of 1030 °C when compared with photo 4. A region of lower intensity just downstream of the tuyere precedes the commencement of the brighter region. At 990 °C and with a stoichiometric ratio of two, a sudden change in behavior is apparent. The bright sooting region of volatile combustion is gone except for random ignition of either separate or small groups of particles. These flashes seem to relate to gas phase ignition, when locally flammable gas concentrations are achieved.

As the blast temperature is reduced still further to 930 °C, photograph 11, these ignition flashes disappear, and a diffuse, almost transparent flame can be seen at about 2 meter downstream of the tuyere. Also in this photograph burning coal particles being entrained backwards into the blast jet are seen. Judging from the large diameter and brightness of these particle paths, the particles seem to be surrounded by condensed material. The exposure time for this photograph is 1/15 second.

The axial burn-out measurements, figures 9a and 9b, show an initial time lag in the devolatilization with the reduced blast temperature. However, even though the devolatilization process is slower, the total combustion, T_x , is improved. The cause of this anomaly is not completely clear, but there seem to be two reasonable explanations for this behavior. The first possible explanation is, because of the delayed devolatilization a significant amount of char combustion has occurred before volatile combustion consumed the locally available oxygen.

The second interpretation of the decreased burn-out for F-15 is, the 1200 °C blast temperature aggravated a situation where devolatilization preceded fuel-air mixing, resulting in rapid cracking of the volatiles into soot-like material. This soot-like material should then reappear in the solid sample as carbon. This second explanation seems to be supported by the C/H mass ratios plotted in figure 12. Here, the C/H ratio is lower, even after Z_x is similar, indicating lower soot concentrations for the reduced blast temperature flame F-22.

Another phenomenon that becomes evident under reduced blast temperature conditions, is an interaction between particle concentration and ignition. It has been well documented that high particle concentrations reduce ignition temperatures, the cooperative effect [2]. This explains the reduced initial burn-out for F-23 when compared to F-22, figure 9b. As the blast temperature is lowered to near the ignition limit, a change in particle concentration results in a large change in ignition behavior.

The axial gas temperatures, figure 21a, show a sizable increase in the initial heat release for the reduced blast temperature flame. This information seems to indicate that under these very special conditions the early combustion was actually improved by reducing the blast temperature. The magnitude of the initial temperature difference, about 400 °C, is surprising. Perhaps a partial explanation can be seen in the radial burn-out and gas species for F-15 (1200 °C blast) and F-22 (1030 °C blast) figures 13 and 16 respectively. The 1200 °C blast temperature flame, figure 16, shows an increased burn-out off axis (+ 5 cm). Here, when the blast temperature is far above the critical ignition temperature, the combustion efficiency is increased because of the greater oxygen availability off axis, see the section on radial burn-out measurements. However, for the reduced blast temperature condition the ignition is delayed in regions where the coal concentration is low (off axis). This results in a reduced consumption of oxygen in the annular region surrounding the high concentration region of coal in the center and possibly could increase the amount of volatile combustion on the blast jet axis as that oxygen becomes available in the central region through turbulent mixing.

Also on figure 9b, the burn-out measurements corresponding to flame F-42 are shown. This is the flame shown in plate 3, where the Elk Creek coal burned without an emissive flame. Measurements were not taken prior to 1 meter because of the rapid ignition caused in this region by the insertion of the B-probe. With a blast temperature of 930 °C, the reduced devolatilization rate is evident. However, the level of total combustion at one meter is similar to the higher blast temperature flames. This high level of initial burn-out can again be explained by a complete inhibition of soot formation. The total burn-out curve for F-42 appears to parallel the volatile burn-out curve lacking the rapid char burn-out shown by flames F-18 and F-23.

. Coal fineness, Elk Creek coal

Flames F-25 and F-15, SR = 1, and F-26 and F-18, SR = 2, differ only by the size distribution of the input coal, see figure 2. The burn-out measurements for the fine-grind Elk Creek coal are shown in figures 10 and 11a. When the stoichiometric ratio is near one (figure 10) the burn-out appears to be very strongly inhibited during the first 10 ms. The effect is strong enough to create an initial decrease in the carbon burn-out. It is clear from these figures that the eventual effect of the smaller particle size is to increase the rate of char combustion. With a stoichiometric ratio of one the effect of particle size on char combustion can be seen in the increased burn-out rate for times greater than about 15 ms. When the oxygen availability is greater (SR = 2), see figure 11a, the beneficial effect of the fine grinding is observed earlier. The temperature measurements, figure 21, support these conclusions. As was observed with F-15, a very low initial temperature was recorded for F-25. This temperature then rapidly increases until it ultimately achieves the highest peak temperature of the Elk Creek flames. The high peak temperature was also observed for flame F-26, which for both flames is a result of the increased rate of char combustion. The effect of a smaller particle size is clearly to accelerate char combustion. However, the use of a finer grind did not significantly improve the early devolatilization controlled burn-out.

. Oxygen concentration, Elk Creek coal

At a reduced blast temperature the blast air was enriched with oxygen to a level of 23%. For this condition, F-40, axial solids and gases were measured. The burn-out is plotted, with flame F-22, in figures 11a. Unfortunately the blast temperature was slightly lower for F-40 than for F-22. This probably has caused the apparent ignition delay observed for the oxygen enriched flame. The small amount of oxygen enrichment used here shows little effect on the combustion rate of the Elk Creek coal.

. Radial burn-out measurements, Elk Creek coal

In figures 13-16, radial gas, burn-out, and temperature measurements for four flames have been plotted. In all these figures very sharp radial gradients for all these quantities are evident. This demonstrates one of the sampling difficulties encountered during this trial. Small misalignments of the sampling probes result in large measurement errors. This problem is maximized in the first section of the flame where the gradients are the sharpest. This emphasizes the importance of accurate probe positioning in achieving meaningful results.

Flames F-15 and F-25 (figures 13 and 14) are both plotted as examples of typical radial gradients measured for high fuel loadings (SR = 1).

They demonstrate how the fuel concentrated at the center of the hot blast jet has depleted the local oxygen. However, the lower concentrations of coal off axis, where more oxygen is available shows a higher burn-out level.

For lower stoichiometric ratios, figure 15, the increased particle concentration on axis results in maximum burn-out. For this stoichiometric ratio, where oxygen availability is not as critical, other factors favourable on axis, temperature and particle concentration, accelerate combustion. Also when the blast temperature is lowered to near the ignition temperature of the particles, burn-out on axis is favoured. Again, gas temperature and particle concentration, not oxygen concentration seem to be the important factors when the blast temperature is reduced.

3.4 Armco coal

The Armco coal was chosen as a test coal because of its current successful use at the Armco blast furnaces. Although both the Armco and Elk Creek are high volatile bituminous coals, they exhibit different fluidity and swelling behaviors, see table 1. These differences are attributable to the lower rank of the Armco coal, as compared to the Elk Creek coal. The Armco blast furnaces utilize a blast temperature of 950 °C, so the influence of blast temperature was chosen as the important test parameter for this coal.

Photographs of the various Armco flames are shown in plate 4. Photograph 13 shows the Armco flame under standard conditions. When compared to the flame produced with the Elk Creek coal, photograph 4, the Armco flame is less bright. This difference is perhaps not significant in these photographs, but to the eye the difference in brightness was dramatic. Photograph 14, shows the Armco coal injected into 930 °C blast air. The visible ignition point is about 0.75 meter downstream of the tuyere exit. Photographs 15 and 16 document the effect of stoichiometric ratio on the Armco coal. An interesting observation is the relationship between particle concentration and the visual ignition point (volatile ignition). With a blast temperature of 930 °C, a downstream shift of this point occurs as the stoichiometric ratio is changed from one to two.

The burn-out measurements, for the Armco flame with 1200 °C preheat are shown in figure 22. When compared to the Elk Creek coal, two interesting phenomena are seen. First, devolatilization of the Armco coal is slower than the Elk Creek coal. However, the Armco coal exhibits a remarkable improvement in the initial degree of total combustion. The fixed carbon burn-out is shown in figure 22b to amplify the magnitude of the difference in behavior between the two coals, not to imply initial char burn-out has occurred.

An effect of this significant improvement in early combustion is seen in the temperature measurements, figure 35. The gas temperature on the tuyere axis initially exceeded 1850 °C for F-28. The suction pyrometer can not measure temperatures above 1850 °C, thus the actual temperature is not known.

The reason for the extreme difference in performance demonstrated by these two coals appears to be related to the devolatilization behaviors of the two coals. The relatively non-emissive flame and the low C/H mass ratios shown in figure 34 both are explained by postulating a reduced volatile cracking behavior from the Armco coal. A problem in sampling, resulting from ash vaporization, is probably at least partially responsible for the decrease in burn-out observed for flame F-28 between 0.25 m and 1.5 m. The high gas temperature combined with the low ash content of the Armco coal compound the problems of computing burn-out using the ash tracer method.

The burn-out results for the reduced temperature Armco flame (930 °C), F-29, are shown together with the reduced temperature Elk Creek flame (1030 °C) in figure 23. Here the two coals compare reasonably well. The ignition point for the Armco coal is shifted downstream as a result of the lower blast temperature used. However, after ignition occurs, the burn-out degree of the two coals is very similar. The axial temperatures for the two coals are compared in figure 36. The rapid heat release demonstrated by the high blast temperature Armco flame is also seen at the reduced blast temperature.

Several distinct differences between the first 15 ms of combustion for the Elk Creek and Armco coals were observed. At high blast temperatures the devolatilization of the Elk Creek coal was completed earlier than with the Armco coal. However, it appears that this early devolatilization for the Elk Creek coal is accompanied by poor combustion resulting in high concentrations of unburned gases, soot, and reduced flame temperatures. The Armco coal was more efficient in conversion of its devolatilization products into the final products of combustion. The Armco coal also allowed the use of a 930 °C blast temperature without a significant reduction in burn-out.

3.5 Norwich Park coal

The Norwich Park coal was chosen as a test coal for several reasons. It has a relatively low volatile content and provided an indication of the importance of that parameter, and is also a higher rank coal which would normally produce a low reactivity char. It also has the desirable feature of being a currently available type of coal.

Measurements with the Norwich Park coal are somewhat more limited than with the other coals. Several problems with the coal feeding system, combined with sampling problems caused by the higher ash content of the coal created a situation where only axial measurements were possible.

Photographs of the two measured flames with the Norwich Park coal can be seen in plate 5. Visually they appear similar to the Elk Creek flames, however not as bright. As observed with the Elk Creek coal the furnace back wall is obscured with a particle cloud.

The burn-out measurements shown in figures 27 and 28, demonstrate an initial burn-out similar to that measured for the Elk Creek flames (in these figures the Norwich Park coal has been compared to the fine grind Elk Creek coal because of their similar initial size distribution). This is surprising due to the much higher rank and lower proximate volatile matter content of the Norwich Park coal. The Norwich Park shows an improved initial performance when compared to the Elk Creek coal on the basis of temperatures, figure 35. For both stoichiometric ratios the temperature in the first 50 cm of the flame is significantly higher for the Norwich Park coal. However this initially better combustion performance shown by the Norwich Park coal disappears during the period of soot and char combustion. Also the burn-out rate of the Norwich Park coal does not appear to be strongly influenced by the stoichiometric ratio. The total burn-out at an axial distance of 2.8 meter is about 70% for both stoichiometric ratios (figures 27 and 28).

When the Norwich Park coal was compared to the Elk Creek coal the following differences were observed. The initial burn-out level was lower for the Norwich Park coal, but the difference was much less than the difference between the volatile matter of the two coals, (as given by the proximate analysis). The char burn-out was slower for the Norwich Park coal and was not strongly affected by stoichiometric ratio. The Norwich Park coal gave a significantly earlier peak gas temperature than did the Elk Creek coal.

3.6 Preussag coal

The Preussag coal was chosen because of its high rank. It clearly is classified as an anthracite and should be less reactive than the other coals tested. Also the Chinese have demonstrated success with the injection of an anthracite into blast furnaces, and information relating the combustion of this type coal to more reactive coals would be valuable.

The low flame temperatures and low ash concentrations encountered with the Preussag coal simplified measurements and enabled three flames to be studied. The burn-out measurements for the baseline, reduced load, and reduced blast temperature flames are shown in figure 30. The initial region of the Preussag flame is difficult to characterize. In figure 30 this region is shown with a dotted line. The actual burn-out in this region, if any, is hard to determine because of a systematic sampling problem resulting in a decreasing ash concentration. This probably results from a selective loss of ash into the filter pores as described by Kobayashi, et al. [5]. Combining the information from the gas, solids, and temperature measurements (figures 30, 31 and 35) the ignition positions of the three anthracite flames can be approximated, at about 1 meter downstream of the tuyere's exit. The ignition position is approximately the same with the reduced blast temperature flame, F-39, however the final burn-out level is decreased. Similar to the Norwich Park coal, the final char burn-out level seems to be unaffected by the stoichiometric ratio, when the blast temperature is 1200 °C.

A photograph of the Preussag flame is shown in plate 5. There is no flash of volatile combustion, and only a jet of coal is visible. The combustion takes place primarily as char burn-out, without any noticeable gas phase combustion.

The slow rate of heat release generated by the Preussag coal gives rise to the temperature profiles in figure 35. For both stoichiometric ratios the initial rate of heat loss exceeds that of heat production and the gas temperature drops. For a high coal rate, figure 35a, the ignition of the coal reverses this trend and the temperature slowly increased. For a lower coal rate (figure 35b) the temperature decrease continues even after ignition.

A clear difference between the Preussag and the other test coals was observed. The Preussag coal did not lose a large percentage of its mass as volatile matter. This causes the lack of a visible gas combustion region and an ignition delay.

3.7 Heavy fuel oil

Heavy fuel oil was used as an injectant to generate data that can be correlated with existing experience of oil injection into blast furnaces. The oil was injected with a standard straight pipe injector (10 mm exit) situated in the normal oil injection position. This resulted in the same axial position of the oil injector as was used with either coal injector 2 or 5.

Photographs of the two measured oil flames are shown in plate 1. Photograph 1, with 1200 °C blast temperature, indicates that most of the combustion has occurred before an axial distance of 1.5 meter. This region is then followed by a region of final gas and soot combustion which extends beyond two meters. When the blast temperature is reduced to 950 °C the ignition is delayed until about 0.5 meter downstream of the tuyere exit. The combustion appears less intense, with a large percentage of the burn-out occurring further downstream.

The temperature measurements for F-14, figure 35a, show the long time required before the peak temperature was reached. This can be related to the very poor mixing between the oil and air. The oil is initially in a concentrated liquid jet which needs a relatively long time to vaporize. It is this vaporization, or atomization, time that initially limits the oil combustion. The mixing of the hot blast with the oil jet is important both to provide oxygen for combustion and for gasification. The oil is injected with an extremely low velocity and that mixing is initially very slow.

To assist in comparing the oil flames with the coal flames, a burn-out related quantity, C_{CO_2} , has been calculated. This number was calculated by correcting the measured CO_2 concentration for the CO_2 in the blast air and then normalizing it by the CO_2 content resulting from complete combustion of the oil.

This scheme assumes uniform mixing between the oil and combustion air. This assumption is certainly invalid in the earlier parts of the flame, but in the latter section of the flame C_{CO_2} should be a reasonable indication of burn-out. The results of these calculations appears in figure 32. Here, the reduced blast temperature appears to shift the oil burn-out to longer times. After about 2.8 meters the degree of burn-out appears to be the same for both blast temperatures.

3.8 Additional experiments

Several other parameters were briefly examined to determine their influence on visual flame characteristics. The influence of reduction in the blast velocity was one parameter investigated. This was accomplished by reducing both the Elk Creek coal and blast rates to 70% of the standard conditions. The visual effect of this experiment was a shortening of the bright region of volatile combustion.

As another extra test, an double wall injection lance was tested. This lance was constructed with a 16 mm x 20 mm pipe inside a 35 mm x 26 mm pipe. These dimensions were chosen to give equal areas for the central and annular openings. The annular space was used to supply cooling air for the inside coal transport pipe. This type of injector enables the coal-transport air supply to be interrupted without danger of overheating to the inside pipe. The injector was inserted in the position of lance number five and the flame was observed as the extra cooling air was varied between 0-50 kg/hr, with the other furnace inputs under standard conditions and with Elk Creek coal. Independent of the cooling air flow rate, the flame produced was visually similar to flame F-13.

The final supplementary experiment involved the measurement of lance temperature. These temperatures were measured with thermocouples welded to the inside surface of the injector, just prior to the exit. With 50 kg/hr air and 300 kg/hr coal the temperatures measured were 140 °C and 310 °C, for the 16 and 32 mm lances respectively. With only 50 kg/hr air the temperature recorded for the small lance rose to 230 °C.

4. COMPARISON OF THE IFRF SIMULATION TO BLAST FURNACE CONDITIONS

An important aspect of the IFRF coal injection trials lays in the possibility of extending the data produced under the simulated conditions to the combustion of coal during actual blast furnace operation. In table 6, a list of the main parameters which effect the combustion of pulverised coal through control of the mixing, heating rate, heat losses, residence time or other mechanisms is shown. The parameters are separated into two categories. Category 1 consists of parameters where the agreement between the compared parameters should permit direct extension of the data acquired during the IFRF trials. This does not imply direct transfer of the data is possible to state, for example, the burn-out in a blast furnace at 1.0 meter, but should enable the qualitative effect of a reduction of coal rate or other variable to be evaluated. This lack of direct correlation is a result of the parameters listed in category 2. They alter the conditions controlling the combustion process in the IFRF simulation from that which would be found in an actual blast furnace. In order to assist in the application of the data generated during the IFRF trial to coal injection into a blast furnace, the general influence of the parameters listed in category 2 will be discussed.

4.1 Blast pressure

The operation of the IFRF furnace at near atmospheric pressure instead of typical blast pressure will indirectly effect the ignition and combustion of the coal particles. Pressures of the magnitude found in blast furnace raceways have been experimentally shown to exhibit only marginal effect on the reaction rate of coal with oxygen [2]. There will also be an interaction between volatile release and pressure, but at the relatively low pressures found in blast furnaces the effect should be small [6]. Pressure does, or can, affect the reaction in other ways. Rates of heat transfer, and aerodynamics are affected by the pressure. The increased gas density of the pressurized blast air will increase the rate of heat transfer to the coal particles, when compared to the atmospheric conditions of the IFRF trial. This combined with the greater drag force on the coal particles also resulting from the increased blast density, will result in a situation of reduced global mixing and higher heating rates. These phenomena may enhance the rate of early soot formation by the creation of even greater fuel rich zones, than was generated at atmospheric pressure. This again indicates the need for a more efficient mixing system than is now used.

4.2 Wall temperature and raceway geometry

Perhaps the greatest discrepancy between the conditions found in the IFRF furnace and those in a blast furnace are the boundary conditions outside the tuyere. In the IFRF furnace the coal-blast mixture exits from the tuyere into a large, relatively cold (1100 °C) chamber. This permits large quantities of air to be entrained into the base of the blast jet. This recirculating gas is about 1200 °C and contains char particles from latter parts of the flame. The gas mixes with the blast air and coal and quickly reduces the average gas temperature in the jet.

It also has the effect of dilution of the blast air with combustion products. This dilution effect reaches the jet axis at an axial distance of about six tuyere diameters (0.9 m) [7].

In a blast furnace the blast jet is confined by the raceway, with wall temperatures of about 2000 °C (figure 6). This confinement will reduce the amount of gases entrained into the jet and the elevated temperatures in the raceway region will result in the entrained gases being much hotter than in the IFRF furnace. This will have a large effect on the radial burn-out profiles that were measured during these trials, and after about one meter will also affect the axial burn-out. However, the raceway walls are permeable which might allow gases rich in CO to be drawn into the root of the blast jet from the burden surrounding the raceway. If this phenomenon occurs it will slow down the rate of soot and char combustion as the additional CO entrained into the blast jet consumes oxygen. Without more detailed information about the physical and chemical processes occurring in a raceway these effect cannot be properly evaluated.

The general influence on the combustion of coal from the higher temperature surroundings in a blast furnace raceway is probably positive. This is particularly applicable to char combustion where the reaction rate increases exponentially with particle temperature. However, it is not believed that elevated particle temperatures alone will significantly alter the results measured during the first meter of combustion. Particularly for low stoichiometric ratios, the combustion in the early section of the flame is clearly mixing limited. However, another important phenomenon occurring in a blast furnace raceway might help assist in the mixing of the coal and hot blast. Large pieces of coke have been observed dropping into the blast jet and then transported with the blast into the rear of the raceway (Greuel et al. [1]). If the frequency of these disturbances is great enough, the increased turbulence in the blast jet should significantly increase the fuel and air mixing. Unfortunately without detailed information about the motion of coke in the raceway the magnitude of this effect also cannot be quantified.

In summary, the following modifications in the combustion results found in this trial would be expected under actual blast furnace conditions. For the bituminous coals any sooting behavior would be increased by the higher blast pressure. The conditions in a blast furnace raceway are capable of significantly accelerating the char combustion of these coals, but in order to take advantage of these conditions the mixing must be improved. The combustion of an anthracite should be enhanced in blast furnace conditions. Here, where the lack of volatile combustion prevents both sooting behavior and a quick consumption of oxygen, the higher heating rate and favorable surroundings in a raceway should both reduce the ignition delay and increase the combustion rate.

5. SUMMARY AND CONCLUSIONS

Table 25 lists the various flames and the total burn-out measured for each flame at axial positions of 1.0 and 1.5 meters. These distances correspond with typical lengths observed for blast furnace raceways [1], and this table provides a convenient method to compare the influences of the various parameters on the coal combustion within this region.

- Effect of coal type

Coal rank was found to have a significant influence on the initial combustion region. The coal properties important in determining the behavior of the coal, under conditions of a high heating rate combined with poor mixing, appear to be extremely complex. The devolatilization process is believed to be the determining factor for the early combustion behavior.

The Armco coal which is the lowest rank coal tested, gave the best performance. It exhibited an ability to efficiently convert its devolatilization products to CO_2 and H_2O with a corresponding high energy release. The Elk Creek coal, which is also a high volatile bituminous coal, demonstrated a very poor early performance when injected into the 1200°C blast air. This reduced performance is attributed to a cracking tendency of the Elk Creek volatile matter. It is believed that this sooting and cracking behavior of the Elk Creek coal is caused by a high percentage of tars contained in its volatile matter.

The high rank bituminous coal, Norwich Park, gave a very good early performance ($t < 5$ ms) comparable to that of the Elk Creek coal. However, the total burnout at 1 m ($t = 10$ ms) is clearly lower than that of the high volatile coals, see table 25. The highest rank coal tested (Preussag) demonstrated the poorest performance. The ignition time was approximately 10 ms with a slow char reaction rate after ignition.

If the combustion performance is to be evaluated on the basis of burn-out in the first 10 ms of combustion, the Armco coal is superior. It also demonstrated an ability to retain its high level of performance at blast temperatures lower than the other test coals.

- Effect of stoichiometric ratio

For the bituminous coals a higher stoichiometric ratio (low coal rate) resulted in a slightly enhanced initial burn-out. This appears to be related to a decreased rate of soot formation combined with an increased rate of soot and char oxidation. A more substantial effect of stoichiometric ratio was seen on the downstream char combustion. An increased downstream oxygen concentration, resulting from a reduced coal rate, increased the rate of char combustion. This effect was observed to be stronger for the low rank coal, Elk Creek, than for the high rank coals, Preussag and Norwich Park. The use of a higher stoichiometric ratio and/or a better mixing system should result in both less soot formation and quicker oxidation of char and soot.

To improve the combustion efficiency at lower stoichiometric ratios it is clear that an improved mixing system must be implemented. The burn-out data presented in table 25 demonstrates that with the current injection system the greatest possibility to improve the performance of the bituminous coals is through control of the stoichiometric ratio. The total burn-out at AD = 1.5 m for the Elk Creek flames was improved by about 30% through a change in stoichiometric ratio from one to two (table 25).

- Effect of blast temperature

The two high volatile bituminous coals, the Armco and Elk Creek, were tested at a reduced blast temperature. For both coals a decrease in the devolatilization rate was measured when the blast temperature was reduced. However, it was found that the performance of the coal was not significantly impaired until a critical temperature was reached. An improvement in burn-out efficiency was actually measured for the Elk Creek coal when the blast temperature was reduced from 1200 °C to 1030 °C. This improvement is evidently related to a reduced soot concentration for the 1030 °C blast temperature case. The Elk Creek coal exhibited a sudden change in the visual flame, at a blast temperature just below 1000 °C. Below this temperature the very bright initial region of volatile combustion disappeared. This visual change probably occurs when the rate of devolatilization is slow enough to prevent fuel rich regions and soot formation. The Armco coal exhibited a different behavior. As the blast temperature was reduced to 900 °C the bright volatile combustion region remained, but was delayed.

The combustion rate of the Preussag coal was directly influenced by the blast temperature. Here, the heat release is low and the initial gas temperature has a large effect on the downstream gas temperatures. This is the probably cause of the reduced reaction rate measured when the Preussag coal was injected into the 1000 °C blast.

For the high volatile coals it can be concluded that the blast temperature is not directly important until a critical temperature is reached. This critical temperature is a function of the coal type. If this temperature is approached, the ignition characteristics become interrelated with coal concentration.

- Effect of particle size

For the Elk Creek coal the effect of particle mean size was examined. The use of a finer particle size demonstrated little effect on the devolatilization process. The major advantage was observed in the char combustion region, when the small size distribution resulted in a faster burn-out. For a high coal rate (SR = 1) the benefit of a finer particle size was not observed until after an axial distance of 1.5 m. With a stoichiometric ratio of 2 the effect was seen significantly earlier. The fine grind, SR = 2, flame F-26, exhibited the highest level of burn-out for all the Elk Creek flames at both AD = 1.0 and AD = 1.5 meter.

To improve the early combustion performance with finer grinding for a high coal rate (SR = 1), the coal and blast air mixing would have to be improved, creating a higher concentration of oxygen available for char combustion during the first 10 ms.

- Effect of injector position and size

The middle injection position was found to give optimum results. The use of injectors further back on the blow pipe should be avoided because of possible slag build-up on the hot refractory surface. The injector diameter appears to effect the initial combustion through alteration of the mixing and heating rates of the pulverised coal. However, the influence of injector diameter was not significant if the burn-out at one meter or beyond is the important criterion. Particularly with the high momentum injector (16 mm), the ability to shift the depth of injector insertion was important. This enabled the coal jet to be centered in the tuyere exit, and also any impingement of coal on the wall of the blow pipe or tuyere to be avoided.

REFERENCES

- [1] GREUEL, HILLNHÜTTER, KISTER, KRÜGER
Untersuchung der Bewegungsvorgänge vor Blastformen eines Hochofens
mit einem Endoskop.
Stahl und Eisen, 94, nr. 12, 1974

- [2] ESSENHIGH
Chemistry of coal utilization, second volume
Chapter 19, Fundamentals of coal combustion, John Wiley and Sons, 1981

- [3] CHEDAILLE and BRAUD
Industrial Flames, volume one
Measurements in flames, Edward Arnold Publishers, London 1972

- [4] MCLEAN, HARDESTY and POHL
Direct observations of devolatilizing pulverised coal particles in
a combustion environment
Eighteenth Symposium (International) on Combustion,
The Combustion Institute, 1982

- [5] KOBAYASHI, HOWARD and SAROFIM
Coal devolatilization at high temperatures
Sixteenth Symposium (International) on Combustion,
The combustion Institute, 1976

- [6] SUUBERG, PETERS and HOWARD
Product compositions and formation kinetics in rapid pyrolysis of
pulverised coal - implications for combustion
Seventeenth Symposium (International) on Combustion,
The Combustion Institute, 1978

- [7] BEER and CHIGIER
Combustion Aerodynamics
Applied Science Publishers Ltd., 1972

- [8] MCLEAN, POHL and HARDESTY
Experimental observations of the early stages of combustion of indi-
vidual coal particles
Paper presented at the International Conference of Coal Science,
Düsseldorf, September 1981

T A B L E S
=====

	Elk Creek % (mass)		Armco % (mass)		Norwich Park % (mass)		Preussag % (mass)	
	(db)	(daf)	(db)	(daf)	(db)	(daf)	(db)	(daf)
Ash	6.3	-	3.3	-	10.8	-	3.9	-
Volatiles	30.9	33.0	37.7	38.9	15.9	17.8	4.1	4.3
C	79.90	85.3	79.92	82.7	79.19	88.7	89.63	93.2
H	5.14	5.48	5.42	5.6	4.06	4.55	3.07	3.2
O	6.55	7.0	8.72	9.0	3.61	4.05	2.02	2.1
S	0.61	0.65	0.73	0.75	0.46	0.52	0.56	0.58
N	1.43	1.52	1.55	1.60	2.03	2.27	1.34	1.39
Ash	6.30	-	3.3	-	10.8	-	3.9	-
Fixed C	59.35		57.9		68.97		87.0	
Fixed H	0.96		0.97		1.40		1.81	
Fixed O	1.34		1.48		1.50		1.36	
Fixed N	1.37		1.39		1.89		1.39	
Fixed S	0.43		0.49		0.41		0.64	
Ash composition (%)								
MgO	1.0		1.3		0.4		1.10	
Al ₂ O ₃	28.0		27.2		33.30		25.20	
SiO ₂	55.3		36.9		56.60		33.30	
P ₂ O ₅	0.23		0.37		0.67		1.30	
CaO	1.5		4.70		0.90		2.60	
TiO ₂	1.5		1.30		1.80		0.70	
Fe ₂ O ₃	8.3		20.50		4.70		28.30	
Na ₂ O	0.46		0.75		0.35		1.20	
K ₂ O	2.50		0.80		0.84		1.60	
Maceral Group (%)								
Vitrinite	63.0		69.0		77.0		71.0	
Exinite	11.0		16.0		0.0		0.0	
Inertinite	23.0		12.0		18.0		27.0	
Gross cal. value (daf) KJ/kg	35234		34902		36007		35629	
Fluidity Index ddp _m	3650		330		6		0	
Dilatation %	75		30		10		no contraction	
Statistical mean reflectance R _m	0.88		0.82		1.54		3.67	

TABLE 1 - COAL ANALYSIS

	Preussag	Armco	Norwich park	Elk Creek normal	Elk Creek fine
% > 250 μ	1.2	2.3	0.8	0.8	0.4
% > 150 μ	7.8	10.3	6.2	7.0	5.4
% > 100 μ	22.9	21.0	16.3	16.0	15.2
% > 75 μ	33.9	31.0	23.0	26.4	24.7
% > 40 μ	49.5	46.0	38.0	45.5	38.2
% > 20 μ	70.9	63.5	48.7	60.8	54.3

TABLE 2 - COAL SIZE DISTRIBUTIONS

Fuel	BLAST CHARACTERISTICS					SR*	THEORETICAL FLUE GAS SPECIES (DAY)		
	T °C	% O ₂	% N ₂	% CO ₂	% H ₂ O		% CO ₂	% O ₂	% N ₂
Fuel oil	1200	21.0	67.5	4.4	8.4	1.0	22.4	0	77.5
	950	21.0	71.7	2.8	5.3	1.0	20.0	0	80.0
Elk Creek	1200	21.0	67.5	4.4	8.4	1.0	24.9	0	75.1
	1000	21.0	70.4	3.2	6.3	2.0	14.7	11.5	73.8
	950	21.0	71.7	2.8	5.3	1.0	23.1	0	76.8
Armco	1200	21.0	67.5	4.4	8.4	2.0	13.1	11.3	75.6
	950	21.0	71.7	2.8	5.3	1.0	22.3	0	77.5
	1200	21.0	67.5	4.4	8.4	2.0	12.6	11.2	76.3
	950	21.0	71.7	2.8	5.3	1.0	24.9	0	75.1
Norwich Park	1200	21.0	67.5	4.4	8.4	2.0	14.7	11.5	73.8
	1200	21.0	67.5	4.4	8.4	1.0	22.3	0	77.5
						2.0	12.6	11.2	76.3
						1.0	25.2	0	74.7
Preussag	1200	21.0	67.5	4.4	8.4	2.0	14.8	11.4	73.7
						1.0	25.8	0	74.1
						2.0	15.2	11.4	73.4

TABLE 3 - VARIATION OF THEORETICAL FLUE GAS SPECIES WITH BLAST TEMPERATURE

*Stoichiometric Ratio = m³ Blast/m³ Stoichiometric

Flame no.	Injector no.	Blast Temp. °C	Blast velocity m/s	% Combustion-AD= 1.9 m
3	2	1150	221	78.1
4	1	1140	223	72.8
5	4	1180	228	74.0
6	5	1173	226	71.2

TABLE 4 - EFFECT OF INJECTION POSITION AND MOMENTUM ON BURNOUT (AD = 1.9 m)

Flame no.	Blast temp. °C	Blast vel. m/s	Blast O ₂ %	Blast rate kg/hr	Fuel*	Fuel rate kg/hr	SR	Measured flue gas				Injector no.
								O ₂ %	CO ₂ %	CO	NO _x Ppm	
F-3	1146	221	21.1	3162	EC	300	1.01	4.2	24.0	-	580	2
F-4	1138	223	21.2	3154	EC	300	1.03	5.1	21.6	10 ppm	810	1
F-5	1183	228	20.7	3175	EC	300	1.02	4.2	24.0	25 ppm	720	4
F-6	1173	226	21.1	3175	EC	300	1.02	3.9	24.0	40 ppm	670	5
F-7	1147	148	21.5	2110	EC	200	1.02	2.2	21.0	125 ppm	460	5
F-13	1164	211	21.5	2977	EC	290	0.98	1.2	23.8	0.01 %	480	5
F-14	1197	214	21.5	2943	HFO	195	1.05	2.7	21.2	100 ppm	530	oil
F-15	1185	205	21.0	2841	EC	290	0.94	1.8	20.0	150 ppm	400	2
F-18	1179	220	21.3	3058	EC	140	2.1	10.0	13.5	185 ppm	440	2
F-22	1036	216	21.3	3335	EC	310	1.03	1.0	21.5	270 ppm	370	2
F-23	1030	213	21.1	3332	EC	150	2.14	10.0	11.2	200 ppm	460	2
F-25	1180	213	21.2	2978	ECF	280	1.02	1.1	23.5	0.1 %	400	2
F-26	1179	217	21.2	3033	ECF	150	1.94	11.6	14.0	10 ppm	460	2
F-28	1210	217	21.0	2964	AR	280	1.01	0.8	21.0	0.1 %	280	2
F-29	940	195	21.3	3253	AR	300	1.03	1.5	19.4	700 ppm	500	2
F-34	950	195	21.4	3230	HFO	213	1.09	1.2	18.0	-	350	oil
F-35	1200	212	21.3	2903	NP	140	2.05	10.1	14.0	120 ppm	340	2
F-36	1219	214	21.0	2899	NP	290	0.99	1.0	22.0	280 ppm	300	2
F-37	1219	218	21.2	2955	P	300	0.90	4.0	20.5	220 ppm	180	2
F-38	1200	218	21.2	2997	P	155	1.76	11.0	15.0	160 ppm	60	2
F-39	1060	210	21.5	3183	P	155	1.87	15.0	8.0	0.07 %	66	2
F-40	1020	214	23.1	3367	EC	300	1.08	2.3	19.5	105 ppm	500	2
F-42	930	194	21.1	3235	EC	150	2.08	12.0	10.6	280 ppm	120	2

*EC = Elk Creek coal
ECF = Elk Creek fine grind
AR = Aranco coal
NP = Norwich Park coal
P = Preussag coal
HFO = Heavy Fuel Oil

TABLE 5 - FLAME LIST

Operating parameter	Proposed Hoogovens BF 7	IFRF trial
<u>CATEGORY 1</u>		
Blast velocity (m/s)	190	200
Blast temperature (°C)	1300	1200
Tuyere diameter (m)	0.15	0.15
Coal lance diameter (mm)	32/16	32/16
Injector velocity (m/s)	4/11-16/45	18/61
Coal rate {kg(daf)/Nm ³ blast}	0.03-0.09	0.051/0.11
Coal fineness	80%<74 μ	70%<74 μ
<u>CATEGORY 2</u>		
Blast pressure (barg)	3.5	0
Wall temperature (°C)	2000	1200
Flame confinement	Raceway	Furnace

TABLE 6 - COMPARISON OF OPERATING PARAMETERS BETWEEN THE IFRF TRIAL AND A BLAST FURNACE

FLAME NUMBER : 13

COAL TYPE : EC
 SR : 0.98
 BLAST O₂ CONCENTRATION : 21.5

BLAST TEMPERATURE : 1170
 FURNACE WALL TEMPERATURE : 1074

VELOCITY : 211
 INJECTOR NUMBER : 5

AD	HIP	GAS ANALYSIS %						SOLID ANALYSIS %						DERIVED QUANTITIES					TEMP. °C
		CO ₂	O ₂	CO	H ₂	CH ₄	C ₂ H ₄	Vol.	Ash	C	H	C _x	H _x	T _x	Z _x	C _f			
25	0	17.0	0.7	6.66	2.93	0.7	0.15	12.8	10.5	79.5	2.1	40.3	75.4	42.7	75.1	26.7	1340		
25	5	10.7	13.6	0.16				12.6	11.0	78.3	2.1	43.9	76.6	45.6	76.6	30.3			
25	10							5.1	23.3	64.5	0.5	78.2	97.4	77.9	95.5	69.2			
50	0																1440		
75	0	16.9	2.8	1.7	0.4			8.4	11.2	80.1	1.3	43.6	85.7	46.7	84.7	28.0	1505		
75	5							5.1	13.1	81.6	0.6	50.9	94.4	55.4	92.0	37.3			
75	10							3.6	20.2	75.1	0.2	70.7	90.8	73.4	96.4	62.1			
100	0	18.0	1.73	1.73	0.5												1595		
150	0	17.6	1.4	0.6				4.6	14.0	80.0	0.6	54.9	94.5	58.7	93.3	41.7	1510		
150	10							4.9	16.2	79.4	0.5	61.4	96.2	65.2	93.8	51.1			
150	15							2.4	22.9	72.6	0.2	75.0	98.9	77.3	97.8	67.2			
280	0	18.0	1.9	0.2				2.9	23.1	73.2	0.28	75.0	98.5	77.6	97.4	67.9	1310		
280	10							3.5	21.6	74.9	0.41	72.7	97.7	75.6	96.7	65.2			
280	20							2.7	20.1	75.4	0.2	70.4	98.9	73.2	97.2	61.4			
500	0	18.0	2.0	0.1				6.3	32.1	60.6	0.6	85.1	97.7	85.8	96.0	80.7	1207		

Table 7

FLAME NUMBER : 14

COAL TYPE : HFO
 SR : 1.05
 BLAST O₂ CONCENTRATION : 21.5

BLAST TEMPERATURE : 1200
 FURNACE WALL TEMPERATURE : 1045

VELOCITY : 214
 INJECTOR NUMBER : -

AD	HIP	GAS ANALYSIS %						SOLID ANALYSIS %				DERIVED QUANTITIES					TEMP. °C
		CO ₂	O ₂	CO	H ₂	CH ₄	C ₂ H ₄	Vol.	Ash	C	H	C _x	H _x	T _x	Z _x	C _f	
25	0	14.0	7.2	3.0	1.3	0.2	0.3										1390
25	5	7.2	1.2	16.6	9.0	3.2	4.5										
25	10	6.0	21.8	0.4													
25	15	9.8	15.9	0.5													
25	20	19.3	3.5	0.07													
50	0	16.3	1.0	6.7	2.9	0.5	0.5										1504
50	5																1150
50	10																1104
75	0	17.3	1.78	3.9	1.6	0.2											1554
150	0	19.2	0.8	3.5	1.3												1672
150	5																1424
280	0	19.6	2.2	0.4													1307

Table 8

FLAME NUMBER : 15

COAL TYPE : EC
 SR : 0.94
 BLAST O₂ CONCENTRATION : 21.0

BLAST TEMPERATURE : 1185
 FURNACE WALL TEMPERATURE : 1050

VELOCITY : 205
 INJECTOR NUMBER : 2

AD	HP	GAS ANALYSIS %						SOLID ANALYSIS %				DERIVED QUANTITIES					TEMP. °C
		CO ₂	O ₂	CO	H ₂	CH ₄	C ₂ H ₄	Vol.	Ash	C	H	C _x	H _x	T _x	Z _x	C _f	
25	0	14.1	0.7	9.5	4.2	1.0	0.2	6.4	12.3	81.8	0.8	47.5	92.3	52.1	89.4	33.7	1160
25	5	15.3	1.6	6.6	2.5	0.8	0.2	10.2	15.3	77.7	1.3	59.9	89.5	62.8	86.4	51.2	
25	-5	12.0	11.0	0.3	-	-	-										
50	0																1502
75	0	19.2	2.6	0.9				3.2	14.0	81.5	0.4	54.1	96.5	58.7	95.3	40.7	1556
75	5							15.2	11.5	78.2	2.1	46.3	77.6	48.3	73.1	36.1	
75	10							16.8	13.4	76.2	1.7	55.1	84.4	56.5	74.4	47.7	
150	0	20.7	2.0	100p				2.7	15.0	80.6	0.3	57.6	97.5	61.9	96.3	45.0	1485
150	5							3.8	14.7	80.3	0.5	56.9	95.8	60.9	94.7	44.3	
150	10							3.7	26.7	68.8	0.4	79.6	98.1	81.5	97.1	73.8	
280	0	20.2	2.2	100p				3.9	20.0	74.1	0.6	70.8	96.3	73.1	96.0	61.8	1271
280	20							13.4	19.6	70.9	2.1	71.5	86.8	72.4	86.1	65.7	
500	0	20.7	2.8	100p				6.5	32.6	57.1	0.7	86.2	97.3	86.1	95.8	81.3	1165

Table 9

FLAME NUMBER : 18

COAL TYPE : EC
 SR : 2.10
 BLAST O₂ CONCENTRATION : 21.3

BLAST TEMPERATURE : 1177
 FURNACE WALL TEMPERATURE : 986
 VELOCITY : 220
 INJECTOR NUMBER : 2

AD	HP	GAS ANALYSIS %						SOLID ANALYSIS %					DERIVED QUANTITIES					TEMP. °C
		CO ₂	O ₂	CO	H ₂	CH ₄	C ₂ H ₄	Vol.	Ash	C	H	C _x	H _x	T _x	Z _x	C _f		
25	0	18.0	6	0.75				3.6	13.5	82.9	0.31	51.5	97.1	56.9	94.6	38.4	1210	
25	2.5	12.0	13.5	0.27														
25	5.0	7.0	19.3	0.05														
25	10.0	11.2	14.5	15p														
25	20.0	10.0	13.5	10p														
25	30.0	12.8	12.7	10p														
25	40.0	13.5	12.3	10p														
50	0	13.1	10.8	0.46				4.6	14.2	80.7	0.16	55.2	98.6	59.4	93.4	42.6	1310	
50	5	7.2	17.5	0.14														
50	10	8.1	17.2	280p														
75	0	13.8	10.2	0.5				3.0	13.0	82.4	0.19	50.0	98.2	55.0	95.3	35.2	1380	
75	5	8.8	16.5	0.2														
75	10	9.0	16.2	260p														
75	20	12.0	14.0	110p														
75	30	12.6	12.2	85p														
75	40	12.0	13.5	100p														
100	0	12.2	11.0	0.33				3.3	14.8	79.7	0.48	57.5	96.0	61.3	95.5	44.5	1380	
100	5																	
100	10	9.0	14.5	0.05				3.4	39.5	56.8	0.14	88.6	99.5	90.0	98.0	85.5		
100	15							3.4	55.3	41.0	0.03	94.1	99.9	95.0	99.0	93.0		
100	20	10.4	12.2	0.04														
150	0	12.0	11.2	0.2				5.0	22.5	71.9	0.66	74.8	96.4	76.8	95.5	67.7	1215	
280	0	12.2	11.4	0.06				5.9	33.8	59.1	0.88	86.2	96.8	86.8	96.4	82.1	1065	
500	0	9.0	12.6	250p														

Table 10.

FLAME NUMBER : 22

COAL TYPE : EC
 SA : 1.03
 BLAST O₂ CONCENTRATION : 21.3

BLAST TEMPERATURE : 1027
 FURNACE WALL TEMPERATURE : 1038

VELOCITY : 216
 INJECTOR NUMBER : 2

AD	HP	GAS ANALYSIS %						SOLID ANALYSIS %					DERIVED QUANTITIES					TEMP. °C
		CO ₂	O ₂	CO	H ₂	CH ₄	C ₂ H ₄	Vol.	Ash	C	H	C _x	H _x	T _x	Z _x	C _f		
25	0	12.0	2.5	0.6	3.5	0.96	0.29	10.4	14.7	76.2	1.6	59.1	86.5	61.0	85.6	48.9	1605	
50	0	15.57	3.04	3.3	0.87	0.2	-	2.9	15.7	79.4	0.5	60.1	96.1	63.9	96.2	48.0	1610	
50	5	11.97	2.04	9.97	4.61	1.19	0.32	7.7	12.8	78.7	1.1	51.5	89.5	54.2	87.7	37.7	1230	
75	0	16.9	3.8	1.2	0.3			7.3	15.3	77.6	1.1	60.0	91.2	62.8	90.3	49.3	1600	
100	0	14.8	4.5	0.5				4.7	15.6	77.5	0.8	60.8	93.7	63.6	93.9	48.7	1550	
100	5	12.8	3.6	3.3				6.8	12.9	80.9	1.0	50.5	90.5	54.6	89.3	37.6	1456	
100	10	13.5	1.4	4.2				9.5	16.0	76.7	0.9	62.2	93.1	64.6	87.9	53.3	1320	
100	15	14.6	1.5	3.6														
100	20	14.0	6.5	0.45													1177	
150	0	15.8	3.0	0.47				5.4	15.3	79.7	0.7	58.9	94.4	62.8	92.8	48.0	1470	
280	0	16.5	2.0	0.2				3.2	24.1	70.5	0.4	76.9	97.9	78.8	97.2	69.8	1270	
500	0	15.2	3.0	0.1				7.4	38.4	55.9	0.5	88.5	98.4	89.2	96.1	85.8	1160	

Table 11

COAL TYPE : BC
 SR : 2.14
 BLAST O₂ CONCENTRATION : 21.3

BLAST TEMPERATURE : 1023
 FURNACE WALL TEMPERATURE : 1011

VELOCITY : 213
 INJECTOR NUMBER : 2

AD	HP	GAS ANALYSIS						SOLID ANALYSIS					DERIVED QUANTITIES					TEMP. °C
		CO ₂	O ₂	CO	H ₂	CH ₄	C ₂ H ₄	Vol.	Ash	C	H	C _x	H _x	T _x	Z _x	C _f		
25	0	5.24	13.5	3.27	1.62	0.6	0.2	13.0	11.2	77.5	2.5	45.4	72.6	46.7	76.3	32.1	1074	
50	0							3.8	13.8	81.5	0.7	53.4	93.7	58.0	94.4	40.1	1278	
50	5							9.4	13.4	77.9	1.3	54.1	88.1	56.5	85.7	42.2	998	
75	0	13.5	6.2	1.6	0.3			5.2	13.9	80.7	0.7	54.2	93.8	58.4	92.4	41.5	1288	
100	0	15.0	3.5	1.3				7.3	14.5	78.9	1.2	57.1	89.8	60.4	89.7	45.9	1271	
100	5	15.0	1.3	4.2				7.3	15.9	76.8	1.3	61.9	89.9	64.4	90.6	51.5	1108	
100	10	13.5	7	0.6				6.2	26.0	68.1	0.6	79.4	97.2	80.9	95.1	73.8	1051	
100	15	9.0	13.5	0.2				8.2	19.3	73.8	1.2	69.8	92.3	71.9	91.3	62.3	1189	
150	0	10.4	10.5	0.3				4.5	37.9	59.1	0.76	87.7	97.5	89.0	97.6	84.8	1043	
280	0	10.0	11.2	0.03														
500	0	11.8	11.4	75P													973	

Table 12

FLAME NUMBER : 25

COAL TYPE : ECP
 SR : 1.1
 BLAST O₂ CONCENTRATION : 21.2

BLAST TEMPERATURE : 1180
 FURNACE WALL TEMPERATURE : 1047

VELOCITY : 213
 INJECTOR NUMBER : 2

AD	HP	GAS ANALYSIS A							SOLID ANALYSIS A					DERIVED QUANTITIES					TEMP. °C
		CO ₂	O ₂	CO	H ₂	CH ₄	C ₂ H ₄	Vol.	Ash	C	H	C _x	H _x	T _x	Z _x	C _f			
25	0	19.8	1.5	5.03	1.6	0.2		6.8	12.4	82.3	0.63	47.6	93.7	52.5	80.8	34.6	1155		
25	5	15.2	8.0	1.0				14.3	34.6	55.9	1.86	87.6	93.4	87.3	91.6	85.2	1128		
25	-5	11.2	0.1	0.5															
25	10																		
50	0	18.5	3.2	4.5	1.6	0.5	0.2	6.5	11.8	82.4	0.9	44.9	91.2	49.7	80.7	30.5	1275		
75	0	15.9	0.5	9.0	3.9	0.8	0.2	5.9	12.1	83.1	0.61	45.8	93.8	51.1	90.0	32.0	1535		
75	5	18.3	1.3	5.6	2.0	0.4	0.1	9.1	12.5	80.6	1.21	49.1	88.1	52.9	85.1	37.0	1330		
75	-5	18.5	1.5	4.5															
75	10							12.3	20.3	71.2	1.5	72.3	90.9	73.6	87.6	66.7	1265		
100	0	21.0	1.5	2.5				4.8	12.7	82.0	0.74	49.1	92.8	53.7	92.3	34.8	1685		
150	0	21.3	2.5	1.2				3.7	14.6	81.1	0.42	56.2	96.5	60.6	94.8	43.8	1590		
280	0	21.8	3.2	0.08				3.4	28.8	65.1	0.13	82.2	99.4	83.3	97.6	76.4	1365		
500	0	21.0	3.2	120p				6.3	40.7	53.1	0.37	89.7	98.9	90.2	96.8	86.9	1270		

Table 13

FLAME NUMBER : 26

COAL TYPE : ECF
 SR : 1.94
 BLAST O₂ CONCENTRATION : 21.2

BLAST TEMPERATURE : 1179
 FURNACE WALL TEMPERATURE : 967

VELOCITY : 217
 INJECTOR NUMBER : 2

AD	IIP	GAS ANALYSIS %						SOLID ANALYSIS %					DERIVED QUANTITIES					TEMP. °C
		CO ₂	O ₂	CO	H ₂	CH ₄	C ₂ H ₄	Vol.	Ash	C	H	C _x	H _x	T _x	Z _x	C _f		
25	0	17.2	1.2	2.5				6.3	14.7	78.4	0.94	57.9	92.1	61.0	91.2	46.0	1170	
25	5	9.0	15.0	0.6				3.8	13.0	83.6	0.26	55.0	94.0	55.0	94.0	35.8	965	
50	0							4.6	15.4	79.8	0.48	59.1	96.2	63.0	93.9	47.8	1295	
75	0	16.2	3.2	0.3				5.3	15.7	78.0	0.51	60.8	96.0	63.9	93.1	49.5	1540	
75	5	13.8	1.6	1.8				3.9	12.7	83.3	0.45	48.2	95.6	53.7	93.7	34.1	1155	
75	10							13.5	11.6	79.9	1.29	45.7	86.3	48.7	76.2	35.2	1075	
100	0	12.2	9.7	0.25				5.2	20.3	75.1	0.61	70.8	96.3	73.6	94.0	63.2	1490	
150	0	11.8	9.8	0.12				4.2	26.7	67.1	0.54	80.2	97.5	81.5	96.7	74.0	1320	
280	0	12.0	10.0	300p				3.3	52.0	43.5	0.16	93.4	99.6	93.8	98.7	91.3	1140	
500	0	10.4	11.0	130p				5.7	48.6	45.8	0.51	92.5	98.7	93.0	97.6	90.5	1045	

Table 14

FLAME NUMBER : 28

COAL TYPE : AR
 SR : 1.01
 BLAST O₂ CONCENTRATION : 21.0

BLAST TEMPERATURE : 1210
 FURNACE WALL TEMPERATURE : 1081

VELOCITY : 217
 INJECTOR NUMBER : 2

AD	HP	GAS ANALYSIS %						SOLID ANALYSIS %					DERIVED QUANTITIES					TEMP. °C
		CO ₂	O ₂	CO	H ₂	CH ₄	C ₂ H ₄	Vol.	Ash	C	H	C _x	H _x	T _x	Z _x	C _f		
25	0	17.2	3.0	0.6				23.5	9.4	81.1	1.8	64.4	88.5	67.1	78.1	60.1	>1850	
25	5	8.8	15.3	0.2				25.7	12.0	71.0	3.7	75.5	81.2	75.0	81.3	71.0		
25	10	16.4	5.5	0.5														
50	0	17.5	2.6	2.4				11.3	8.8	84.3	1.3	60.4	90.8	64.6	88.8	49.2	>1850	
75	0	18.8	1.0	0.8				18.3	7.6	82.7	1.2	55.0	90.2	58.5	78.9	45.5	1720	
75	5	16.4	5.0	0.5				19.4	7.6	81.0	2.3	55.9	81.5	58.5	77.7	46.3	1380	
75	10	15.0	7.5	0.2				18.4	11.2	77.0	2.6	71.6	85.8	72.9	85.6	64.8	1288	
100	0	18.8	1.7	0.6				14.5	8.9	83.4	1.1	61.3	92.5	65.1	85.7	51.9	1670	
150	0	19.0	2.1	0.6				14.7	8.3	81.5	1.0	59.5	92.6	62.3	84.5	48.0	1555	
280	0	20.5	1.6	0.3				5.7	14.6	79.0	0.6	77.6	99.7	80.0	96.6	69.5	1351	
500	0	21.0	1.2	0.1				9.3	19.1	71.0	0.98	84.6	96.0	85.5	95.7	79.0	1255	

Table 15

FLAME NUMBER : 29

COAL TYPE : AR
 SR : 1.03
 BLAST O₂ CONCENTRATION : 21.3

VELOCITY : 195
 INJECTOR NUMBER : 2

BLAST TEMPERATURE : 941
 FURNACE WALL TEMPERATURE : 1094

AD	HP	GAS ANALYSIS %						SOLID ANALYSIS %					DERIVED QUANTITIES					TEMP. °C
		CO ₂	O ₂	CO	H ₂	CH ₄	C ₂ H ₄	Vol.	Ash	C	H	C _x	H _x	T _x	Z _x	C _f		
50	0																	1110
50	5																	907
75	0	5.23	16.2	0.4				11.7	7.7	81.1	2.01	56.5	84.1	59.1	86.7	41.5		1221
75	5																	1163
100	0	17.2	3.5	1.3				13.3	8.5	80.9	2.14	60.7	84.6	63.3	86.3	48.5		1720
100	5	11.0	4.5	8.1	2.8			21.7	5.7	80.6	3.35	41.6	64.2	43.5	66.7	28.0		
100	10	9.3	5.3	10.2	4.6			26.4	6.1	78.7	4.25	46.7	57.5	47.5	62.1	38.1		
100	15	15.4	2.7	4.5	1.2													
150	0	17.8	2.9	0.5				7.0	9.4	83.6	1.42	63.3	90.8	67.1	93.5	50.3		1595
150	5	18.6	1.0	1.0														
150	10	17.8	0.2	2.5				13.2	6.5	83.3	2.1	47.0	80.3	50.9	82.2	30.9		
150	20	19.5	0.2	0.8														
280	0	17.0	2.9	0.6				4.0	12.9	81.1	0.73	74.0	96.5	77.0	97.3	64.0		1420
500	0	19.4	1.6	0.1				4.8	22.0	70.8	0.71	87.2	98.1	88.4	88.2	82.2		1300

Table 16

COAL TYPE : HFO VELOCITY : 195
 SR : 1.09 BLAST TEMPERATURE : 950
 BLAST O₂ CONCENTRATION : 21.4 FURNACE WALL TEMPERATURE : -
 INJECTOR NUMBER : -

AD	HP	GAS ANALYSIS %						SOLID ANALYSIS %					DERIVED QUANTITIES					TEMP. °C
		CO ₂	O ₂	CO	H ₂	CH ₄	C ₂ H ₄	Vol.	Ash	C	H	C _x	H _x	T _x	Z _x	C _f		
25	0	6.1	14.6	0.67	0.41	0.1	0.49											
50	0	5.9	12.7	5.4	2.8	0.9	2.5											
50	5	5.3	17.6	-														
75	0	5.9	3.4	8.6	2.6	0.7	1.6											
100	0	10.8	1.7	7.1	2.7	0.8	1.1											
100	5	7.0	10.4	2.5	0.8	0.2	0.6											
100	10	11.2	10.0	0.4														
150	0	14.8	1.0	3.1														
280	0	17.0	1.3	0.6														
500	0	18.0	1.5	160p														

Table 17

COAL TYPE : NP
 SR : 2.05
 BLAST O₂ CONCENTRATION : 21.3

BLAST TEMPERATURE : 1212
 FURNACE WALL TEMPERATURE : 964

VELOCITY : 212
 INJECTOR NUMBER : 2

AD	HIP	GAS ANALYSIS %						SOLID ANALYSIS %				DERIVED QUANTITIES					TEMP. °C
		CO ₂	O ₂	CO	H ₂	CH ₄	C ₂ H ₄	Vol.	Ash	C	H	C _x	H _x	T _x	Z _x	C _f	
25	0																1351
50	0	14.6	7.0	1.5				5.5	20.3	73.2	1.81	56.8	77.6	53	81.6	46.1	1342
75	0	14.2	8.5	1.2				5.1	20.6	72.7	1.68	50.8	76.2	53	83.2	46.9	1340
100	0							4.2	19.4	74.2	1.56	47.8	78.6	50	87.0	41.0	
150	0	14.2	8.1	0.3				2.6	24.0	70.8	0.93	59.7	89.7	61	92.6	54.9	1200
280	0	12.0	12.4	150p				2.9	28.8	65.4	0.76	69.0	92.9	70	93.2	65.1	1026
500	0	10.8	11.8	110p				2.1	36.9	58.9	0.52	78.3	96.2	79	96.1	75.6	993

Table 18

COAL TYPE : NP
 SR : 0.99
 BLAST O₂ CONCENTRATION : 21.0

BLAST TEMPERATURE : 1218
 FURNACE WALL TEMPERATURE : 1052

VELOCITY : 214
 INJECTOR NUMBER : 2

AD	HIP	GAS ANALYSIS %						SOLID ANALYSIS %						DERIVED QUANTITIES					TEMP. °C
		CO ₂	O ₂	CO	H ₂	CH ₄	C ₂ H ₄	Vol.	Ash	C	H	C _x	H _x	T _x	Z _x	C _f			
25	0																	1530	
25	5																	1690	
50	0	14.4	2.0	0.6				3.7	18.9	75.7	1.2	45.3	82.7	48.0	86.7	39.7			
50	5	13.8	10.5	0.4															
75	0	17.0	1.5	0.6				3.8	17.9	76.2	1.36	41.9	79.8	44.5	85.6	35.5			
75	5	17.2	6.0	0.4															
100	0	18.0	3.5	0.5				2.6	18.4	76.2	1.2	43.5	82.6	46.3	90.4	36.7			
150	0	19.5	3.2	0.3				2.8	18.4	76.9	0.9	42.9	85.9	46.3	89.7	36.9			
280	0	20.5	2.0	0.1				1.6	29.5	67.8	0.5	68.7	95.4	71.1	96.3	65.6			
500	0	20.5	1.0	0.3				1.1	34.9	62.2	0.4	75.6	96.8	77.4	97.8	73.0			

Table 19

AD	HIP	GAS ANALYSIS %						SOLID ANALYSIS %						DERIVED QUANTITIES					TEMP. °C
		CO ₂	O ₂	CO	H ₂	CH ₄	C ₂ H ₄	Vol.	Ash	C	H	C _x	H _x	T _x	Z _x	C _f			
25	0	6.0	20.2	0.4				4.7	4.9	86.0	2.07	23.6	46.3	21.2	8.7	21.8	1167		
25	5	7.2	19.3	0.05			4.3	11.1	79.7	1.71	1.71	68.7	81.2	67.5	63.1	67.7			
25	10	16.5	9.3	150p			4.1	5.5	85.9	2.29	2.29	32.2	49.2	30.3	29.0	3.0			
50	0	6.0	20.3	0.3			3.2	4.6	87.3	1.53	1.53	17.4	57.7	15.8	33.8	15.0	1106		
75	0	8.5	17.2	0.3			3.1	4.1	87.4	1.70	1.70	7.2	47.3	5.1	28.1	4.0	1063		
75	5	9.2	16.2	0.2			4.8	4.7	85.7	2.28	2.28	20.6		17.8	2.9	18.3	1103		
75	10	10.2	15.2	0.1			3.1	10.4	81.9	1.39	1.39	40.8		65.0	71.6	64.7			
100	0	10.6	14.5	0.2			3.6	3.9	87.4	2.34	2.34	2.4	23.7	0	12.2	-5	1074		
150	0	13.5	11.8	0.1			3.2	5.1	85.5	1.98	1.98	27.0	50.7	24.5	40.3	23.7	1105		
280	0	18.0	7.5	240p			2.9	6.9	84.3	1.28	1.28	46.8	76.4	45.2	60.0	44.7	1122		
500	0	19.4	5.5	90p			2.7	13.8	78.9	0.68	0.68	75.1	93.7	74.6	81.4	74.3	1115		

Table 20

COAL TYPE : P
 SR : 1.76
 BLAST O₂ CONCENTRATION : 21.1

BLAST TEMPERATURE : 1219
 FURNACE WALL TEMPERATURE : 1020

VELOCITY : 218
 INJECTOR NUMBER : 2

AD	HP	GAS ANALYSIS %						SOLID ANALYSIS %					DERIVED QUANTITIES					TEMP. °C
		CO ₂	O ₂	CO	H ₂	CH ₄	C ₂ H ₄	Vol.	Ash	C	H	C _x	H _x	T _x	Z _x	C _f		
25	0	5.2	21.8	0.2				3.6	3.0	88.8	2.65	-29	-12	-31	-14.0	-32.0	1155	
25	5	6.0	21.0	250p				3.8	5.4	86.9	2.74	29.9	38.1	29	52.4	-28.0		
25	10	10.4	15.5	70p														
50	0	5.6	21.0	0.2				2.7	3.7	88.7	1.87	-4.3	35.8	-5.6	30.6	-7.0	1103	
75	0	6.8	19.9	0.2				4.3	3.3	88.4	2.43	-16.6	6.5	-19.0	-24.0	-18.7	1066	
75	5	7.6	19.3	0.1				3.4	3.2	89.6	2.65	-21.0	0	-22.0	-1.0	-23.7		
75	10	9.2	17.5	180p				3.7	6.6	85.9	2.14	43.4	60.4	42.6	46.7	42.4		
100	0	8.2	18.2	0.13				2.9	2.8	89.6	2.68	-39.0	-21.0	-41.0	1.4	-42.7	1042	
150	0	9.6	16.6	0.05				3.4	3.0	89.4	2.62	-29.0	-10.9	-31.0	-7.8	-32.0	1030	
200	0	11.6	14.0	140p				3.3	5.9	85.0	1.93	37.2	50.4	35.3	46.8	34.7	1008	
500	0	10.8	14.2	80p				4.0	11.4	80.0	1.60	69.4	82.2	68.4	66.6	68.5	980	

Table 21

PLAHE NUMBER : 39

COAL TYPE : P

BLAST TEMPERATURE : 1042

VELOCITY : 210

SR : 1.87

FURNACE WALL TEMPERATURE : 783

INJECTOR NUMBER : 2

BLAST O₂ CONCENTRATION : 21.5

AD	HP	GAS ANALYSIS %						SOLID ANALYSIS %					DERIVED QUANTITIES					TEMP. °C
		CO ₂	O ₂	CO	H ₂	CH ₄	C ₂ H ₄	Vol.	Ash	C	H	C _x	H _x	T _x	Z _x	C _f		
25	0	4.9	18.8	0.09				4.6	5.0	86.9	2.61	24.4	36.3	22.9	12.5	23.4		
50	0	5.5	18.2	0.1				5.1	4.6	86.7	2.65	17.9	29.0	15.8	5.5	16.0		
100	0	5.8	17.5	0.12				4.8	4.7	87.1	2.53	19.4	34.3	17.7	15.4	19.2		
150	0	6.0	17.1	0.1				5.7	6.4	84.4	2.25	42.6	57.1	40.6	15.3	41.8		
200	0	7.0	16.2	0.1				6.6	7.8	82.7	1.90	53.8	70.3	52.0	19.5	53.5		
500	0	6.8	16.0	0.1														

Table 22

FLAME NUMBER : 40

COAL TYPE : EC
 SR : 1.08
 BLAST O₂ CONCENTRATION : 23.0

BLAST TEMPERATURE : 1012
 FURNACE WALL TEMPERATURE : 938

VELOCITY : 217
 INJECTOR NUMBER : 2

AD	HP	GAS ANALYSIS %						SOLID ANALYSIS %					DERIVED QUANTITIES					TEMP. °C
		CO ₂	O ₂	CO	H ₂	CH ₄	C ₂ H ₄	Vol.	Ash	C	H	C _x	H _x	T _x	Z _x	C _f		
25	0							17.0	10.6	76.8	2.6	42.8	69.9	43.3	67.3	31.5		
50	0	9.0	3.0	4.5			9.7	13.6	77.4	1.7	55.1	84.7	57.9	85.5	43.5			
75	0	16.0	2.7	1.0			12.9	12.9	78.0	2.1	52.3	80.0	54.6	79.6	42.3			
100	0	16.5	0.7	3.3			11.6	14.4	77.2	1.84	57.7	84.3	60.6	83.6	48.4			
150	0	16.5	2.0	1.2			7.4	15.9	78.3	1.08	61.1	91.7	64.4	90.4	51.6			
280	0	16.8	3.5	1.12			3.0	24.8	71.2	0.28	77.4	98.6	79.6	97.5	70.8			
500	0	16.4	4.2	300p			2.0	39.4	57.3	0.16	88.5	99.5	89.6	78.9	85.0			

Table 23

COAL TYPE : EC
 SR : 2.08
 BLAST O₂ CONCENTRATION : 21.1

BLAST TEMPERATURE : 933
 FURNACE WALL TEMPERATURE : 884

VELOCITY : 194
 INJECTOR NUMBER : 2

AD	HP	GAS ANALYSIS %						SOLID ANALYSIS %					DERIVED QUANTITIES					TEMP. °C
		CO ₂	O ₂	CO	H ₂	CH ₄	C ₂ H ₄	Vol.	Ash	C	H	C _x	H _x	T _x	Z _x	C _f		
50	0	7.3	9.0	9.4	3.9	2.0	0.5											
100	0	8.8	9.5	6.9	2.5	0.3	0.1	15.3	14.7	71.7	2.22	61.5	81.5	60.9	78.7	52.2		
100	5	7.9	14.4	1.5	0.4	0.1												
150	0	7.6	15.0	0.5				13.8	14.7	73.2	2.35	60.7	80.4	60.9	81.0	51.2		
280	0	8.8	14.0	0.1				8.9	23.1	67.4	1.87	77.0	90.1	77.6	92.1	70.5		
500	0	8.8	13.7	120p				6.3	35.6	55.9	1.05	87.6	96.4	88.0	96.3	83.6		

Table 24

Flame no.	T _B °C	Coal type	Fineness	SR	Blast O ₂	Injector	T _x % 1 m (10 ms)	T _x % 1.5 m (15 ms)
F-13	1170	EC	N	0.98	21	5	-	59
F-15	1185	EC	N	0.94	21	2	-	62
F-25	1188	EC	F	1.02	21	2	54	61
F-22	1030	EC	N	1.03	21	2	64	63
F-40	1012	EC	N	1.08	23	2	61	64
F-18	1177	EC	N	2.10	21	2	61	77
F-26	1179	EC	F	1.94	21	2	74	81
F-23	1011	EC	N	2.14	21	2	60	72
F-42	933	EC	N	2.08	21	2	61	61
F-28	1210	AR	N	1.01	21	2	65	62
F-29	941	AR	N	1.03	21	2	63	67
F-36	1218	NP	N	0.99	21	2	46	46
F-35	1212	NP	N	2.05	21	2	50	61
F-37	1218	P	N	0.90	21	2	0	24.5

TABLE 25 - COMPARISON OF PARAMETER EFFECT OF THE TOTAL BURN-OUT AT AXIAL DISTANCES OF 1.0 AND 1.5 METERS

FIGURES

=====

LIST OF FIGURES (continued)

Figure number

- 1 - IFRF furnace no. 1 with 6 cooling loops
- 2 - Blast air supply system
- 3 - Tuyere and blowpipe use for BF-C1
- 4 - IFRF pulverised coal feeding system
- 5 - Sampling grid for Hoogovens coal injection trial
- 6 - Half section of a blast furnace
- 7 - Calculated center line particle residence time as a function of axial position
- 8 - Axial solids burn-out: a. effect of injection size
b. effect of stoichiometric ratio
- 9 - Axial solids burn-out: a. effect of blast temperature with SR = 1
b. effect of blast temperature with SR = 2
- 10 - Axial solids burn-out: a. effect of particle size SR = 1
b. " " " " SR = 1
- 11 - Axial solids burn-out: a. effect of particle size SR = 2
b. effect of blast O₂ concentration
- 12 - Carbon/Hydrogen ratios for the Elk Creek flames: a. SR = 1
b. SR = 2
- 13 - Radial variation of measured quantities for F-15 (EC, T_b = 1200, SR = 1, N, I2)
- 14 - Radial variation of measured quantities for F-25 (EC, T_b = 1200, SR = 1, F, I2)
- 15 - Radial variation of measured quantities for F-26 (EC, T_b = 1200, SR = 2, F, I2)
- 16 - Radial variation of measured quantities for F-22 (EC, T_b = 1000, SR = 1, N, I2)
- 17 - Axial gas concentrations: a. EC, T_b = 1200, SR = 1, N, I2
b. EC, T_b = 1200, SR = 1, N, I5
- 18 - Axial gas concentrations: a. EC, T_b = 1200, SR = 2, N, I2
b. EC, T_b = 1200, SR = 1, F, I2
- 19 - Axial gas concentrations: a. EC, T_b = 1200, SR = 2, I2
b. EC, T_b = 1000, SR = 1, I2
- 20 - Axial gas concentrations: a. EC, T_b = 1000, SR = 2, I2
b. EC, T_b = 900, SR = 2, I2
- 21 - Axial temperatures for the Elk Creek flames: a. parameter effect
b. SR = 2
- 22 - Axial solids burn-out: a. Elk Creek vs. Armco coal, T_b = 1200 °C
b. " " " " " , T_b = 1200 °C

LIST OF FIGURES

Figure number

- 23 - Axial solids burn-out: a + b. Elk Creek vs. Armco coal; reduced blast temperature
- 24 - Radial variation of measured quantities for F-28 (AR, $T_b = 1200$, SR = 1, N, I2)
- 25 - Radial variation of measured quantities for F-29 (AR, $T_b = 900$, SR = 1, N, I2)
- 26 - Axial gas concentrations: a. AR, $T_b = 1200$, SR = 1, N, I2
b. AR, $T_b = 900$, SR = 1, N, I2
- 27 - Axial solids burn-out: a + b. Elk Creek vs. Norwich Park coal, SR = 1
- 28 - Axial solids burn-out: a + b. Elk Creek vs. Norwich Park coal, SR = 2
- 29 - Axial gas concentrations: a. NP, $T_b = 1200$, SR = 1, N, I2
b. NP, $T_b = 1200$, SR = 2, N, I2
- 30 - Axial solids burn-out for the Preussag coal
- 31 - Axial gas concentrations: a. P, $T_b = 1200$, SR = 1, N, I2
b. P, $T_b = 1200$, SR = 2, N, I2
- 32 - Axial gas burn-out for the heavy fuel oil flames
- 33 - Axial gas concentrations: a. Oil, $T_b = 1200$
b. Oil, $T_b = 950$
- 34 - Carbon/hydrogen ratios for Armco, Norwich Park and Preussag flames
- 35 - Axial temperatures for the various coals: a. SR = 1
b. SR = 2
- 36 - Axial temperatures for the reduced blast temperature flames

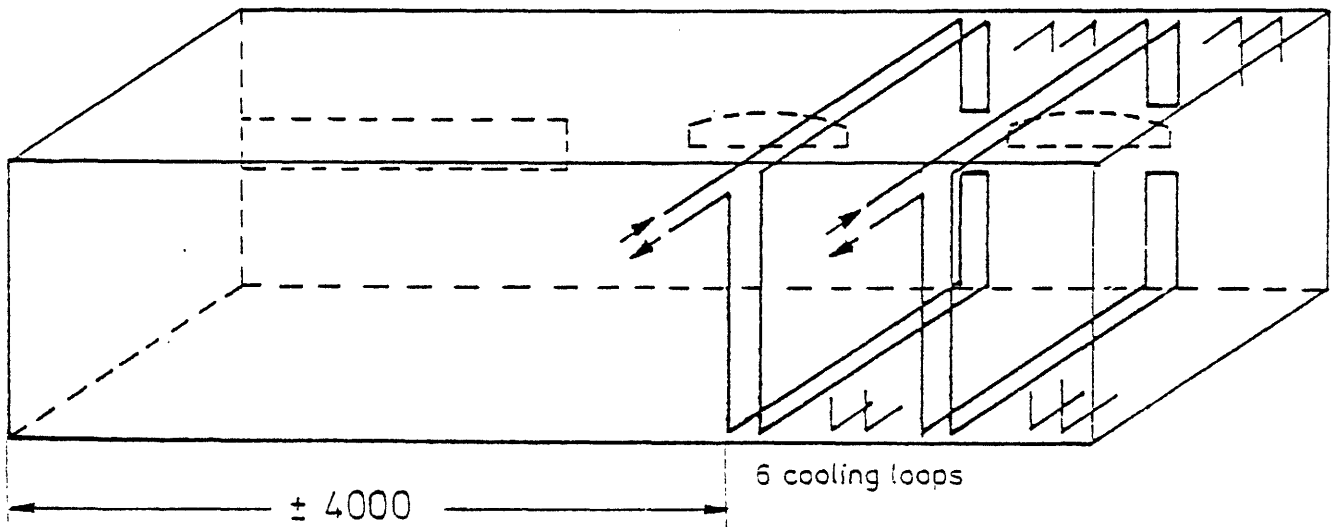
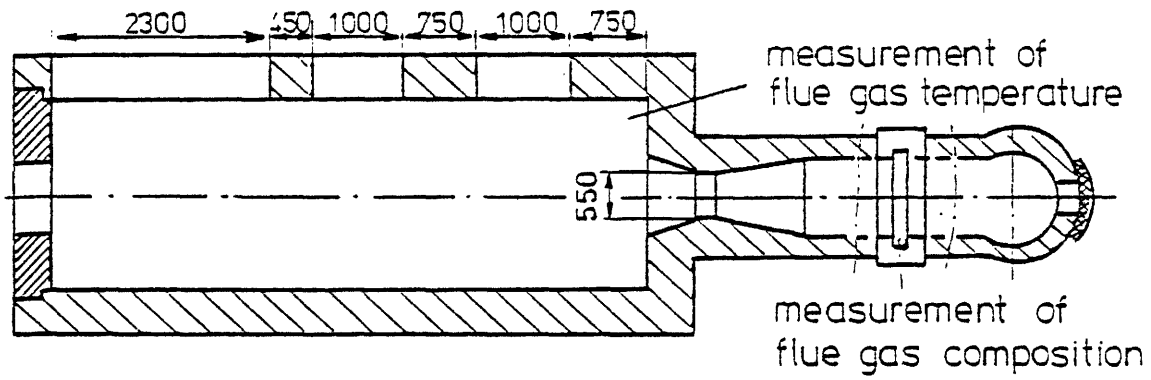
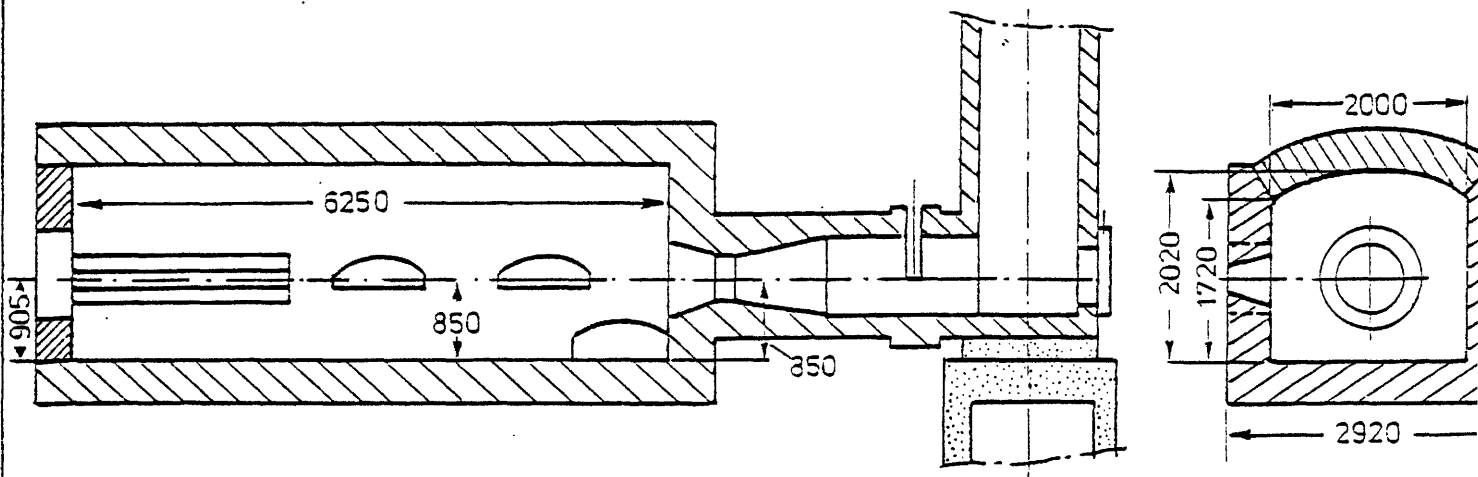


Fig. 1 IFRF furnace n^o 1 with 6 cooling loops



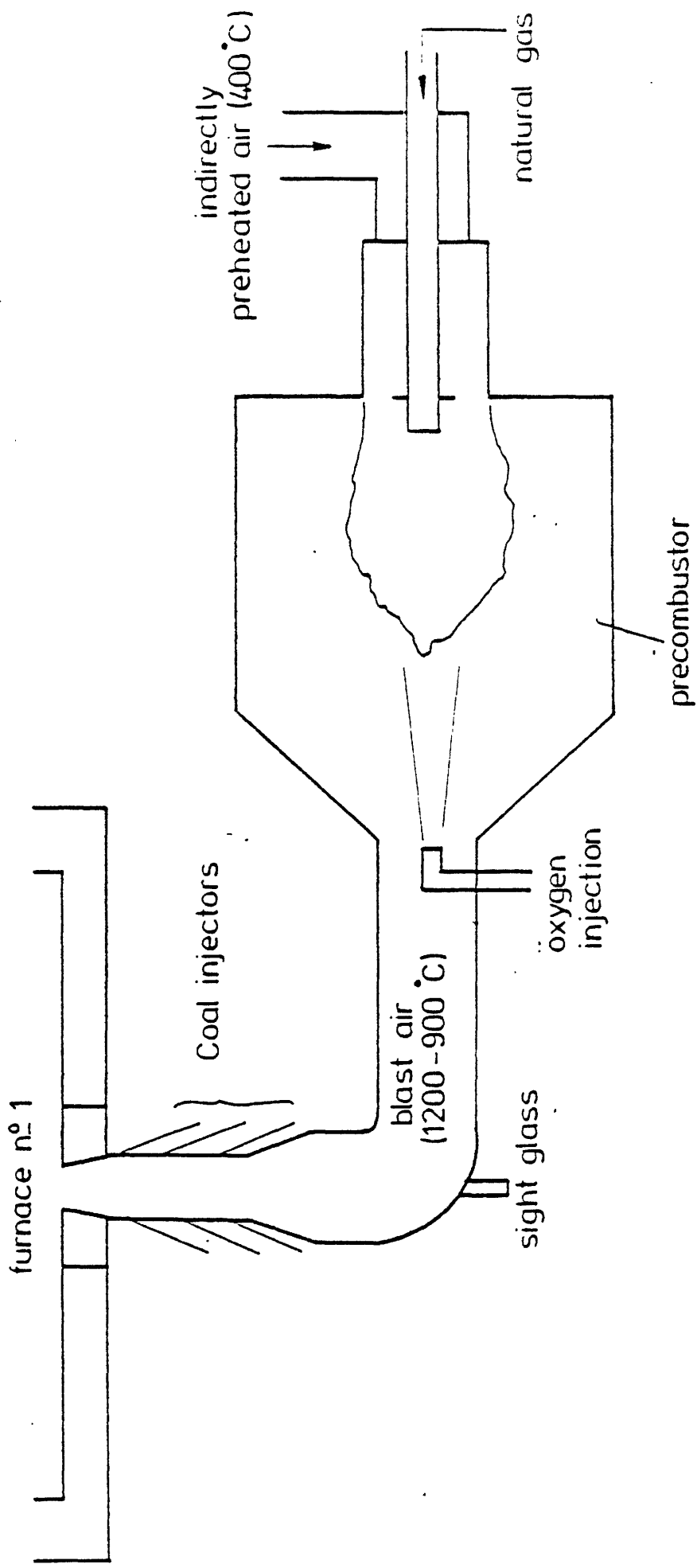


Fig. 2 Blast air supply system



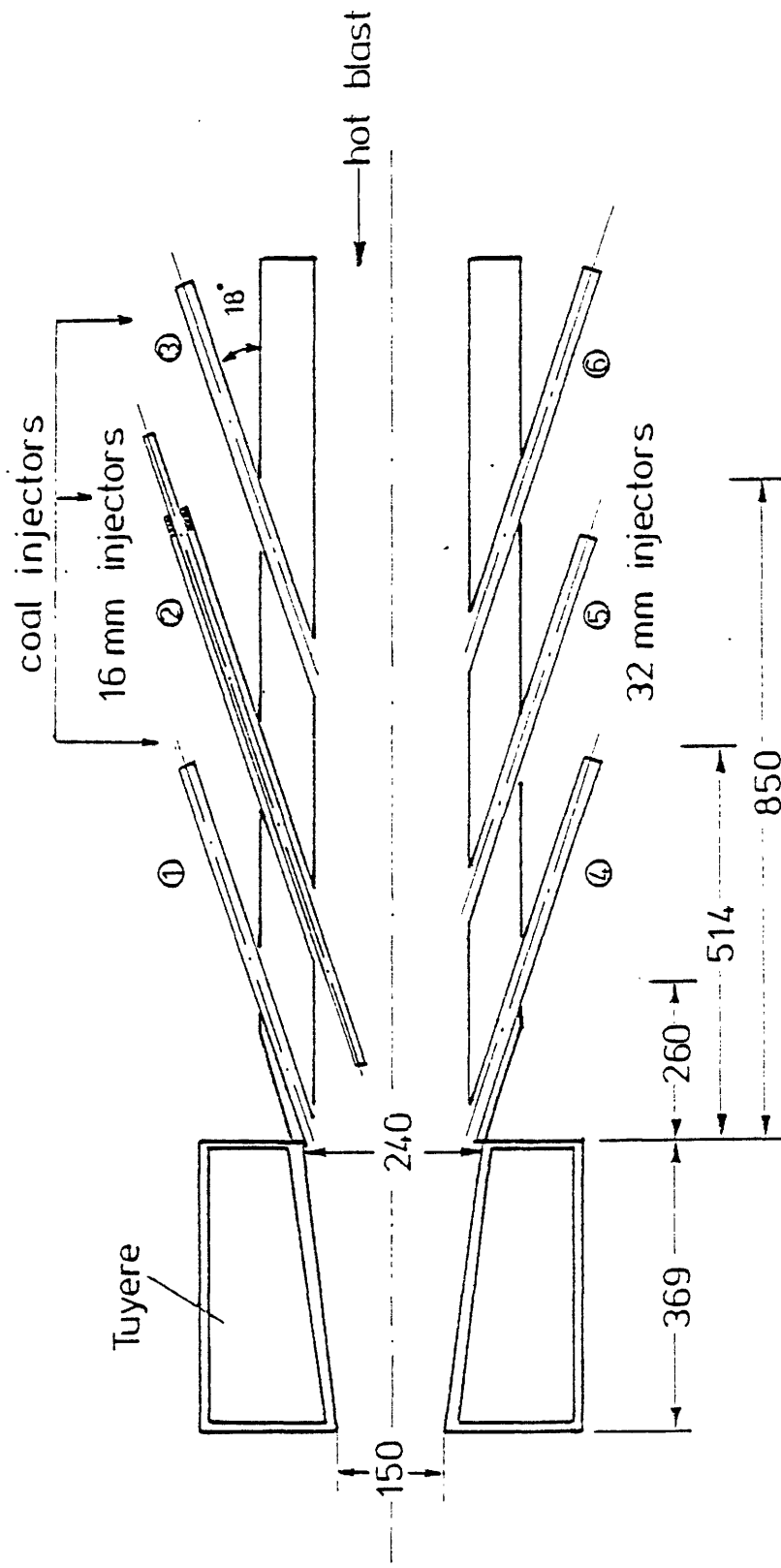


Fig. 3 Tuyere and blowpipe use for BF-C1



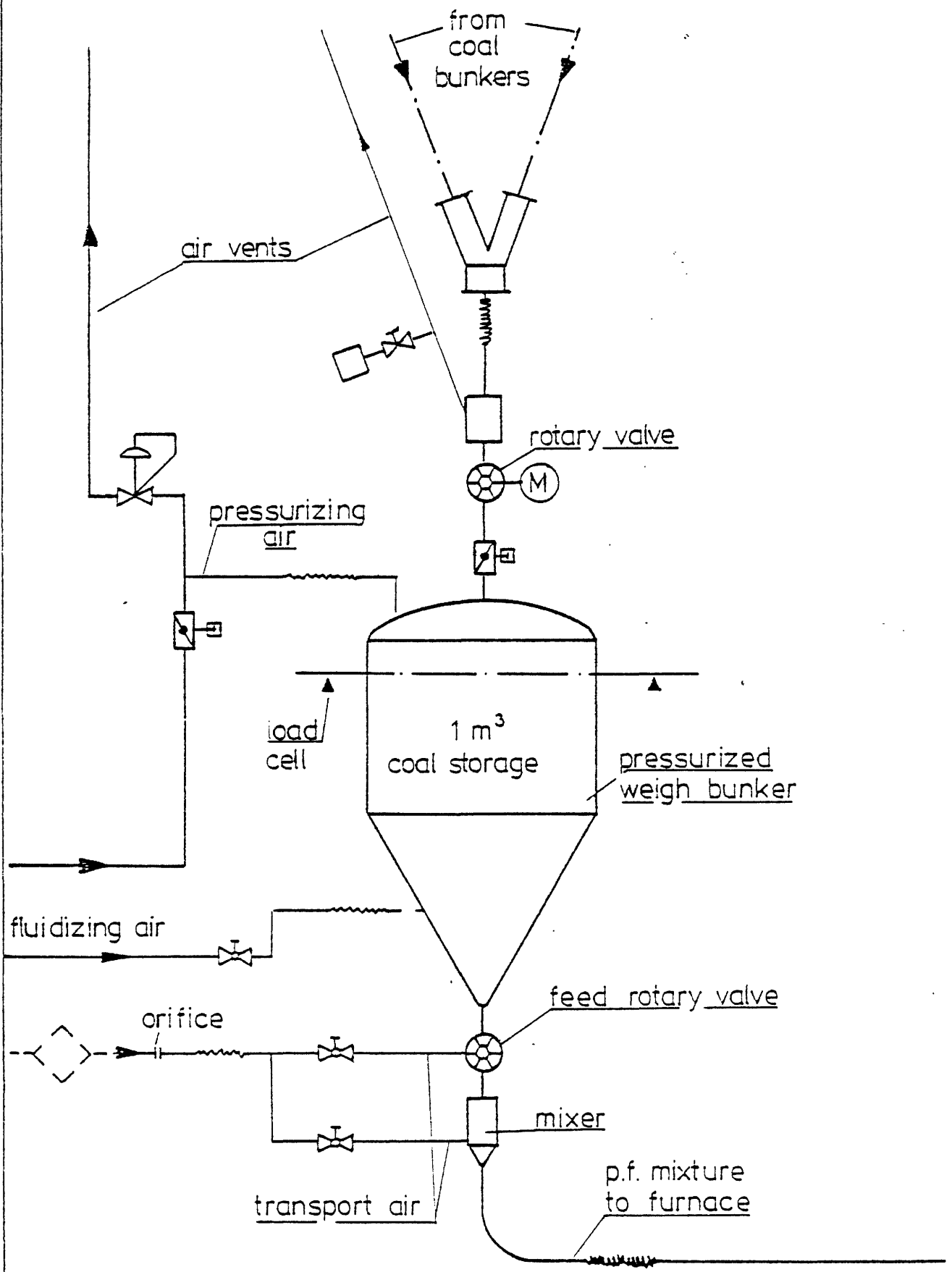


Fig. 4 IFRF Pulverised coal feeding system



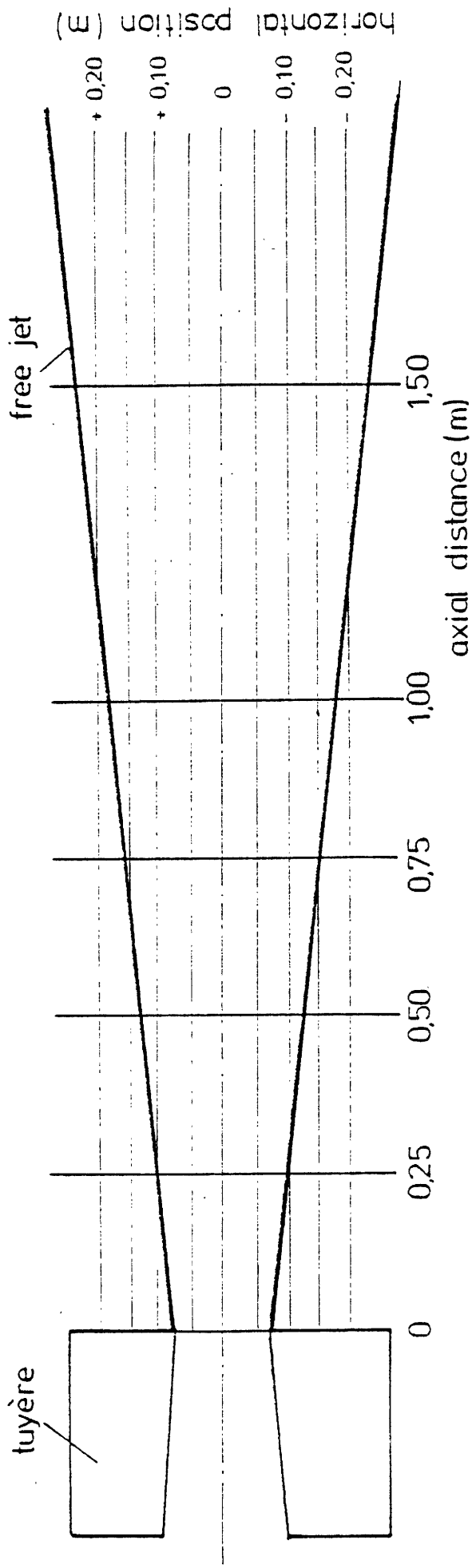


Fig. 5 Sampling _ grid for Hoogovens coal injection trial



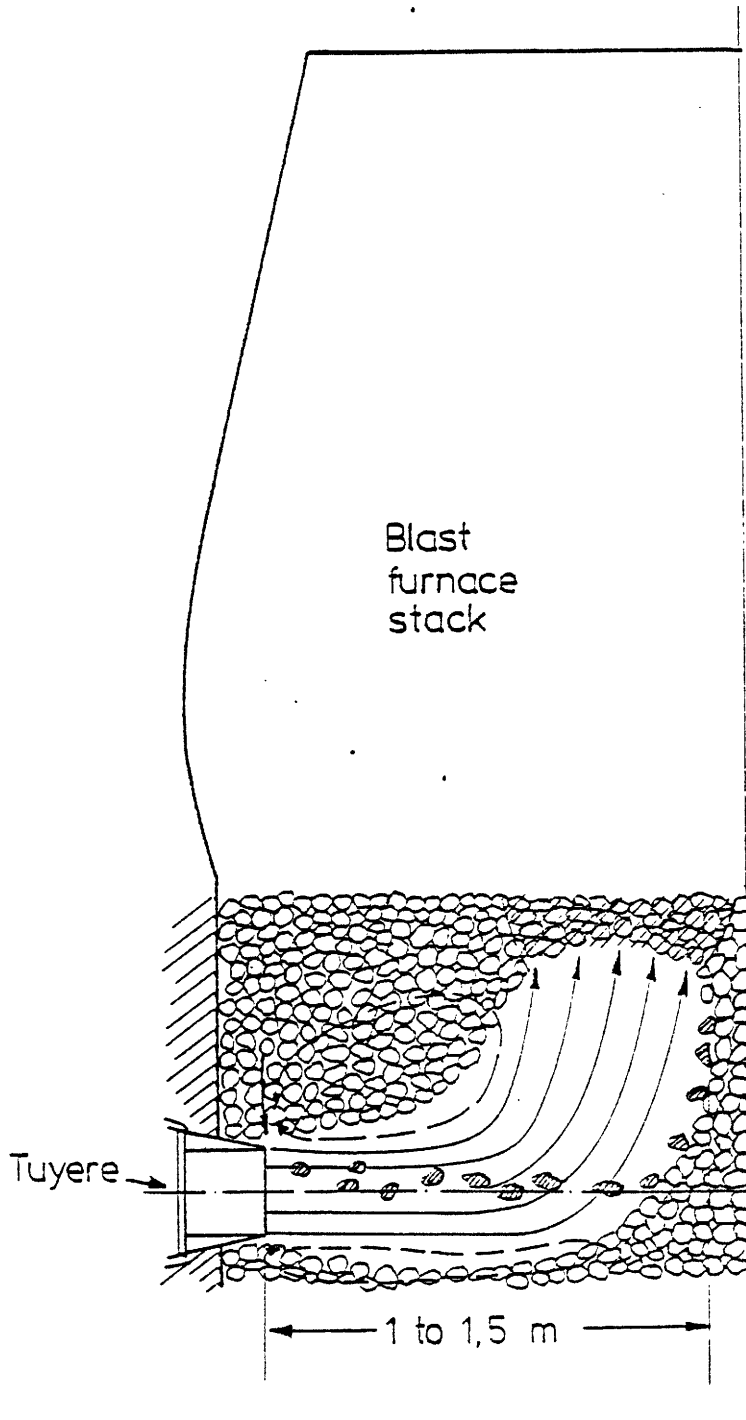


Fig. 6 Partial section of a Blast furnace

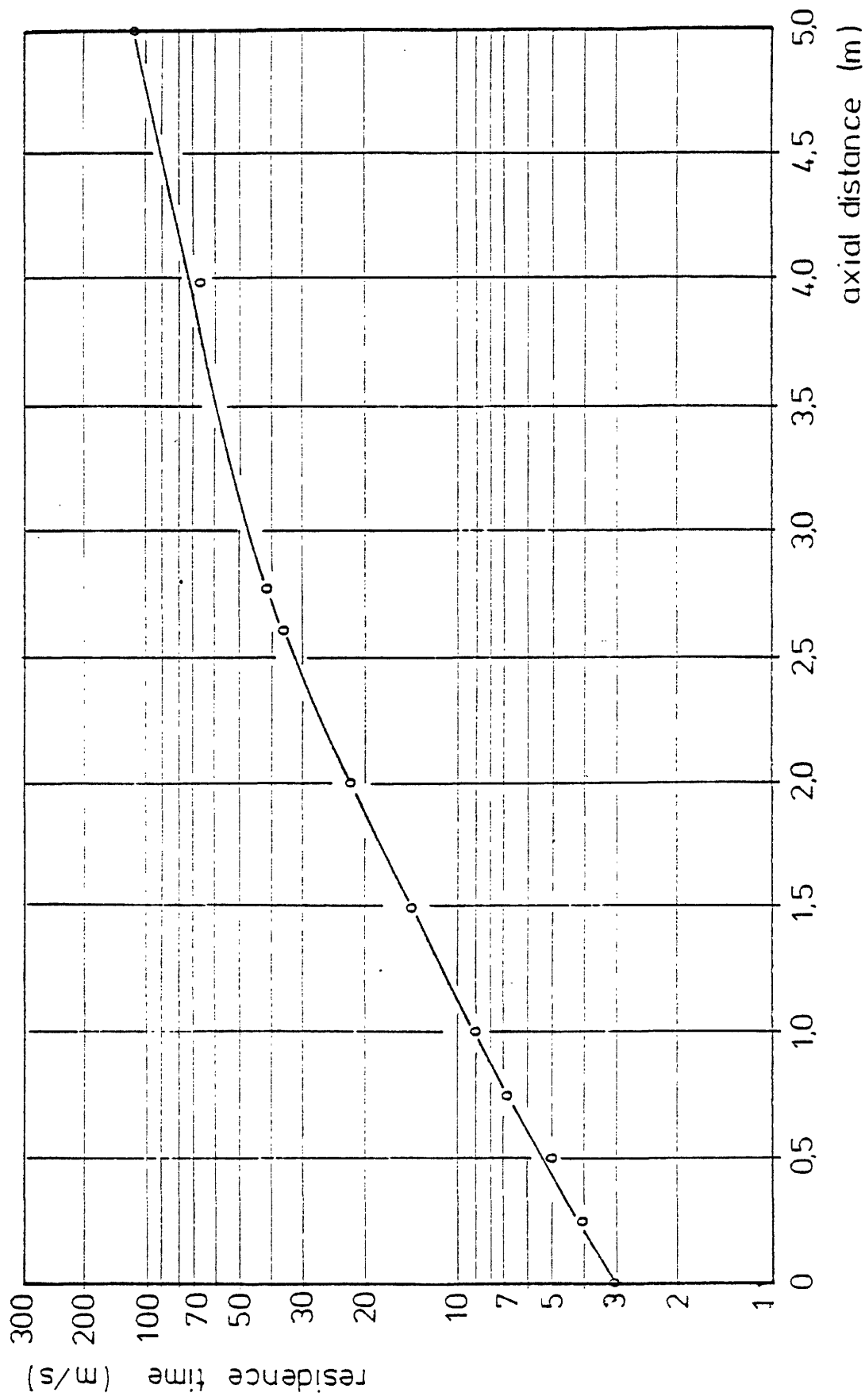


Fig. 7 Calculated center line particle residence time as a function of axial position



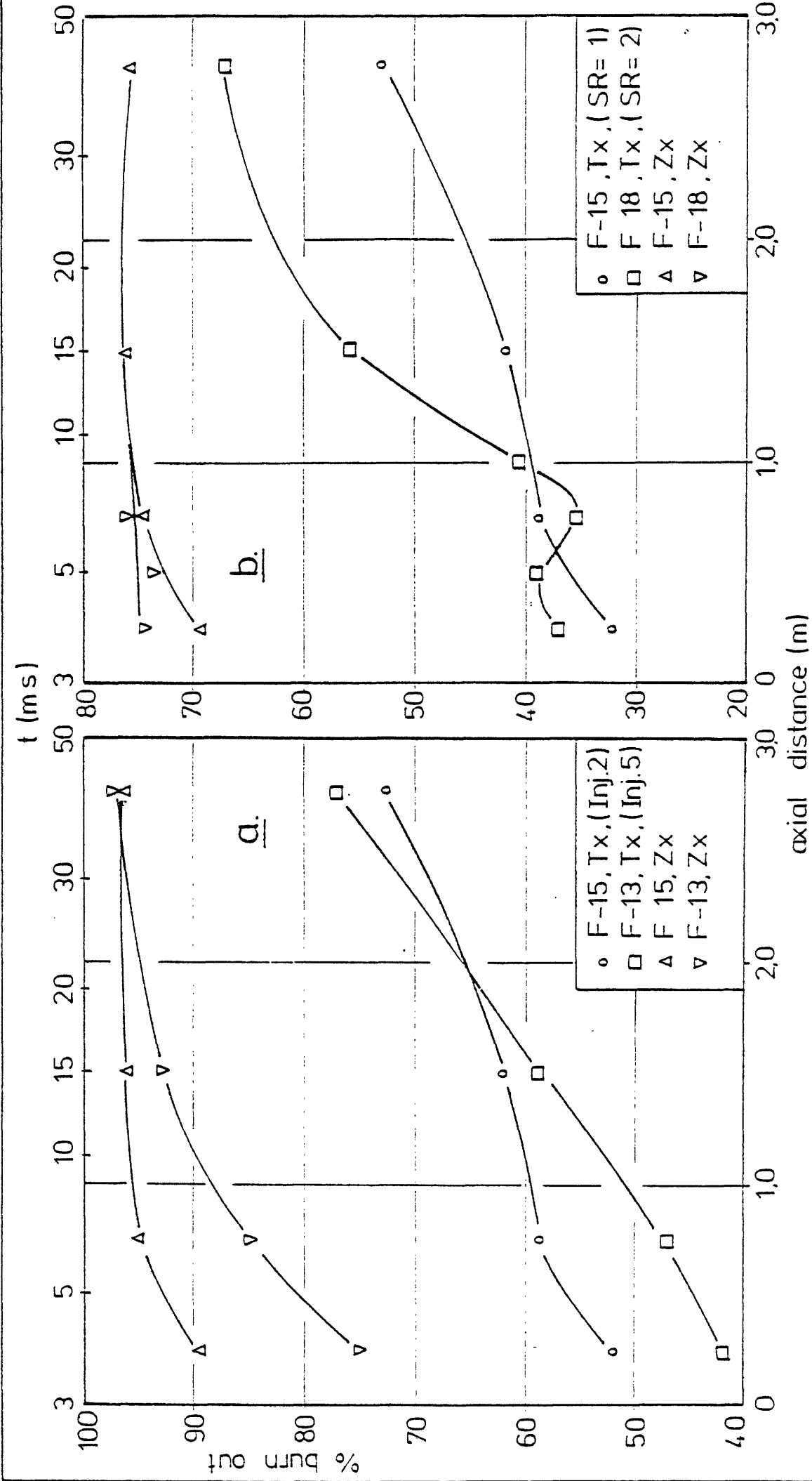


Fig. 8 Axial solids burn out; a: effect of injector size
 b: effect of stoichiometric ratio



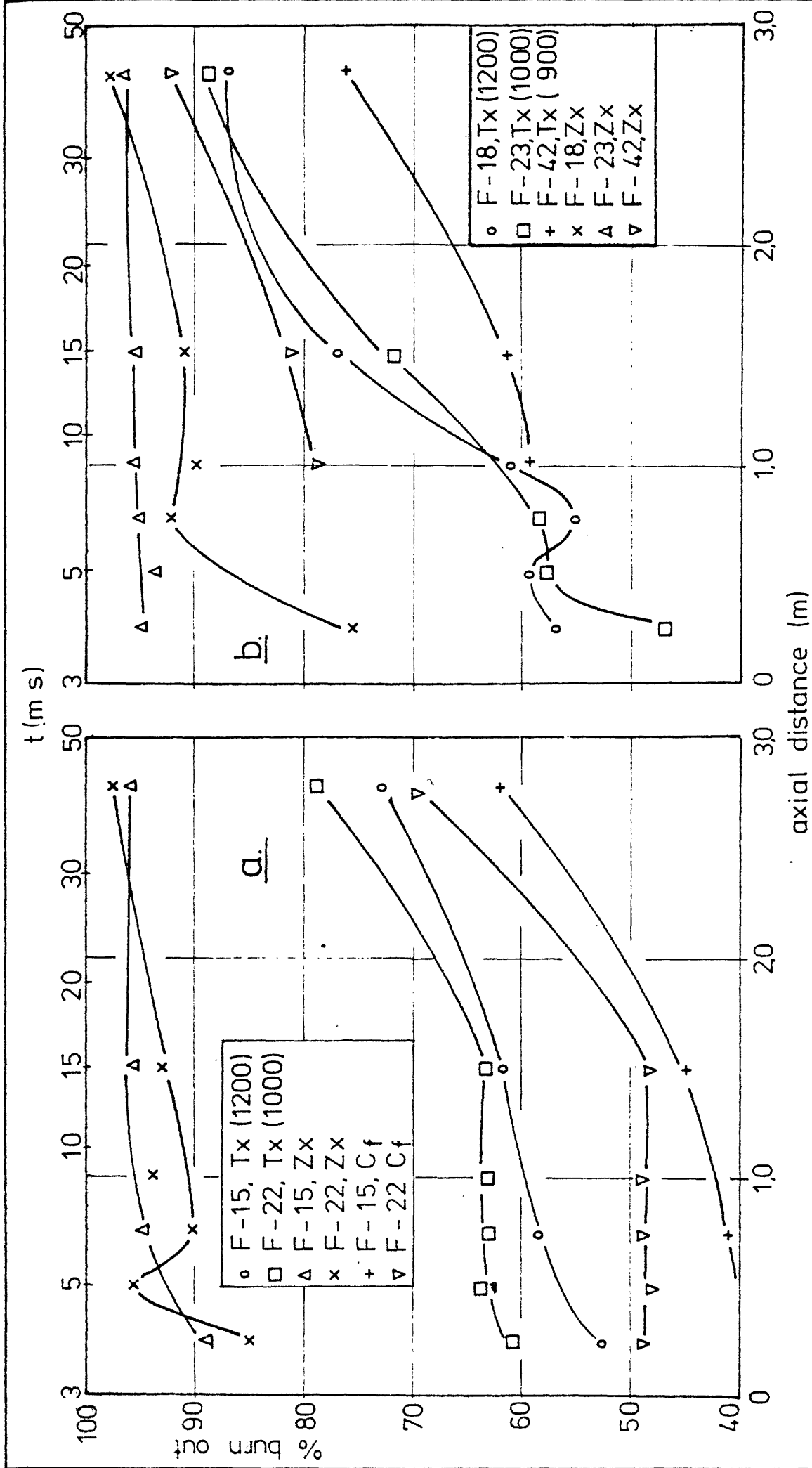


Fig.9 Axial solids burn out; a: effect of blast temperature with SR=1
b: effect of blast temperature with SR=2



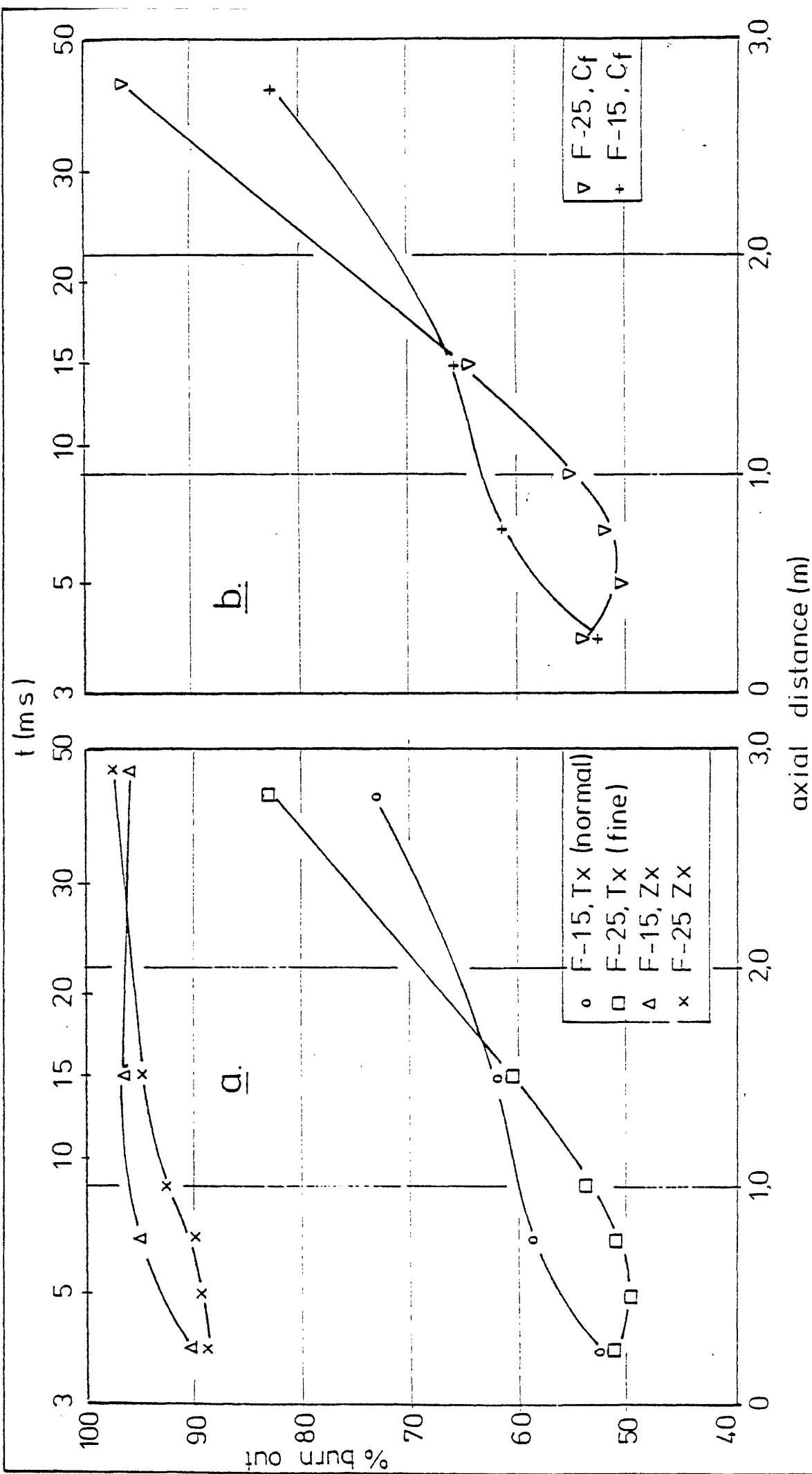


Fig. 10 Axial solids burn out; a,b: effect of particle size SR=1



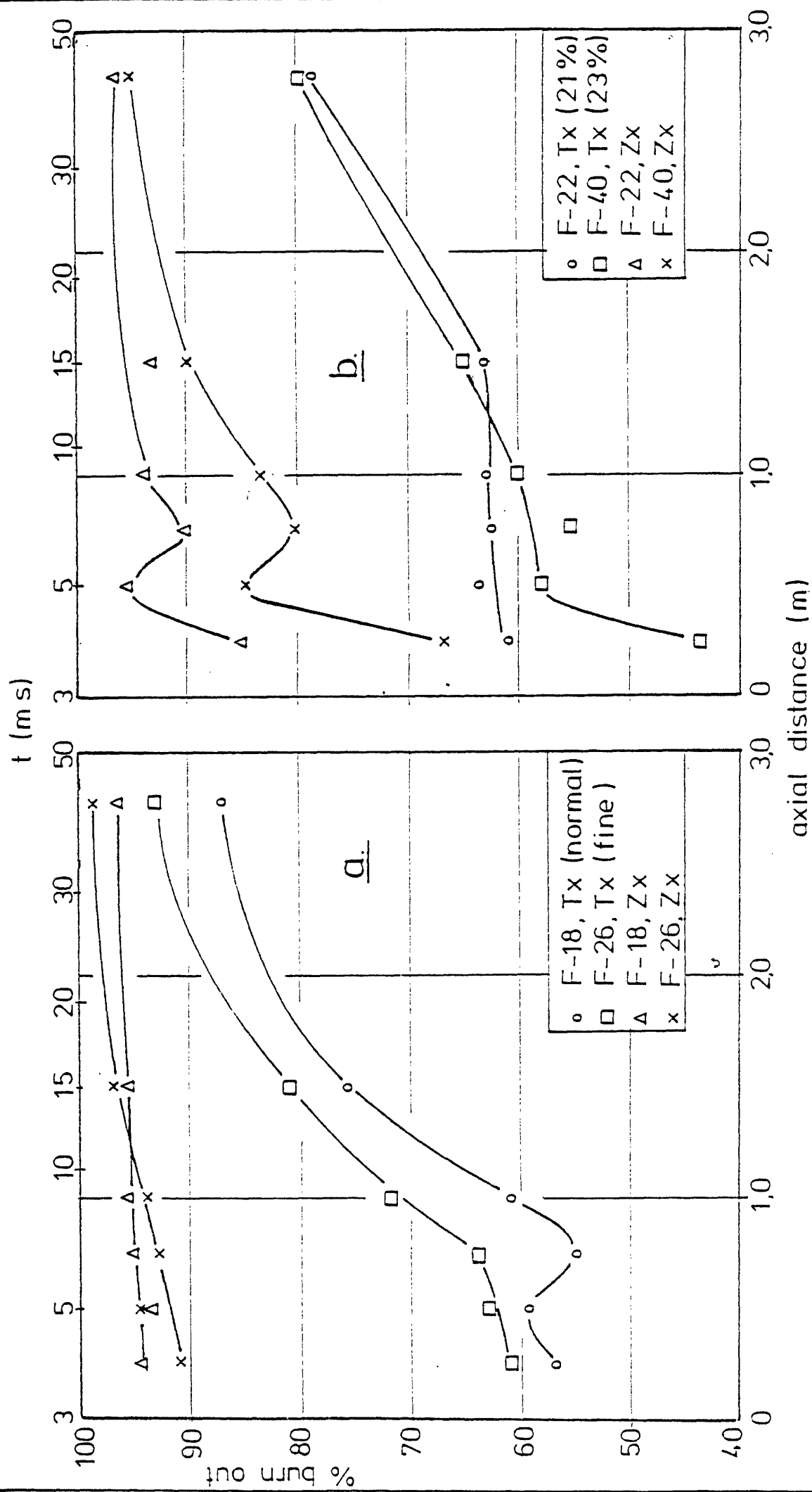


Fig. 11 Axial solids burn out ; a: effect of particle size SR=2
 b: effect of blast O₂ concentration



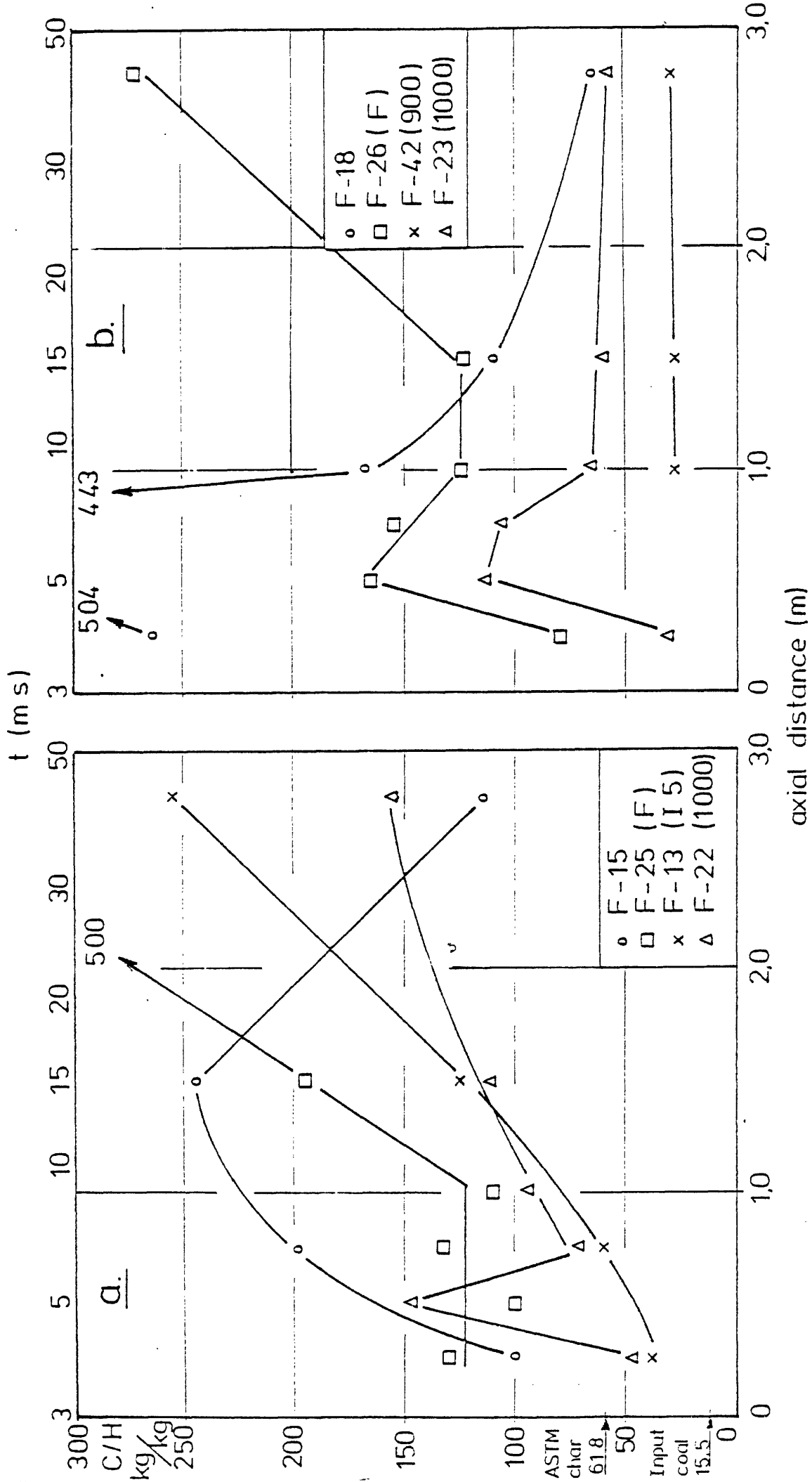


Fig. 12 Carbon/Hydrogen ratios for the Elk Creek flames
 a: SR=1 ; b: SR=2



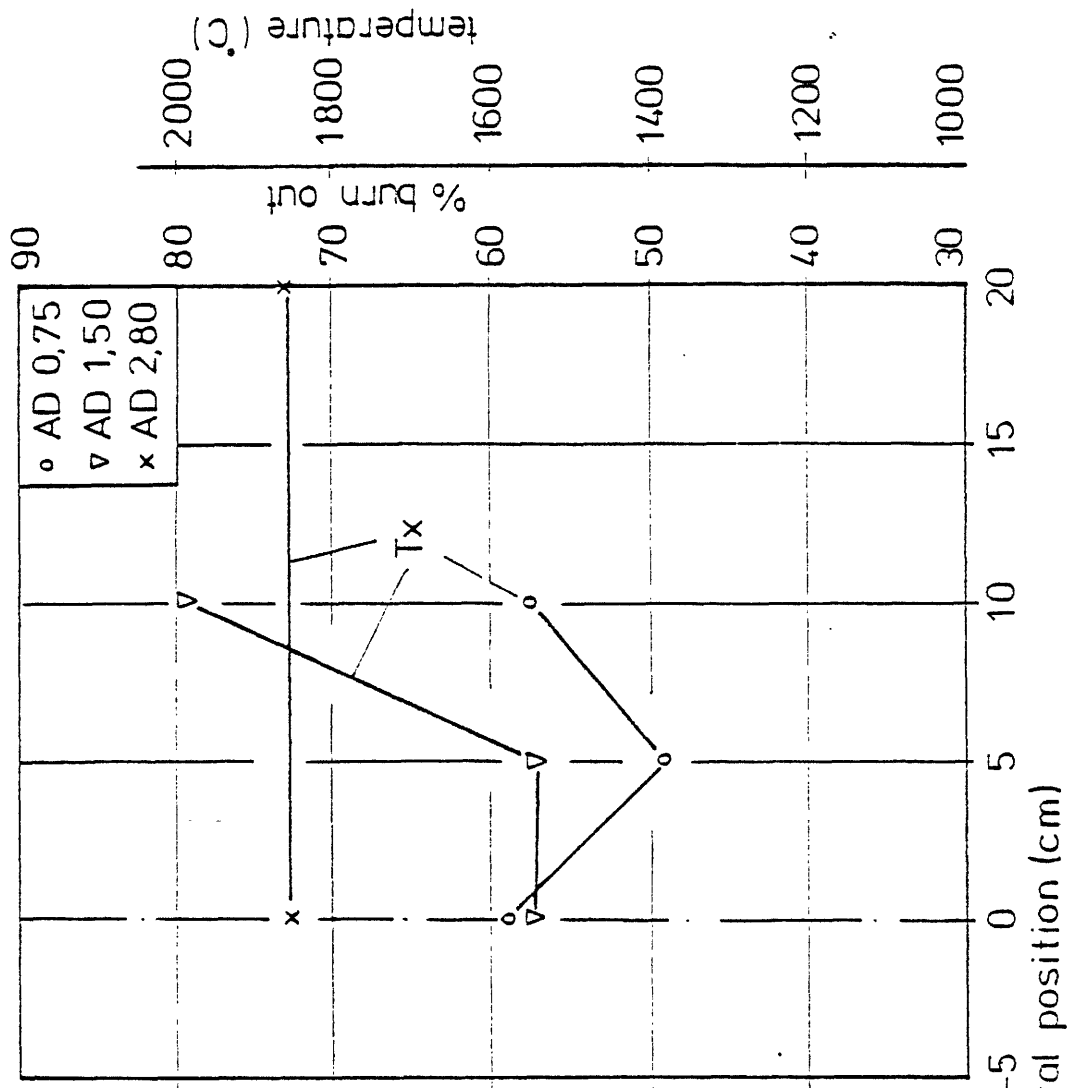
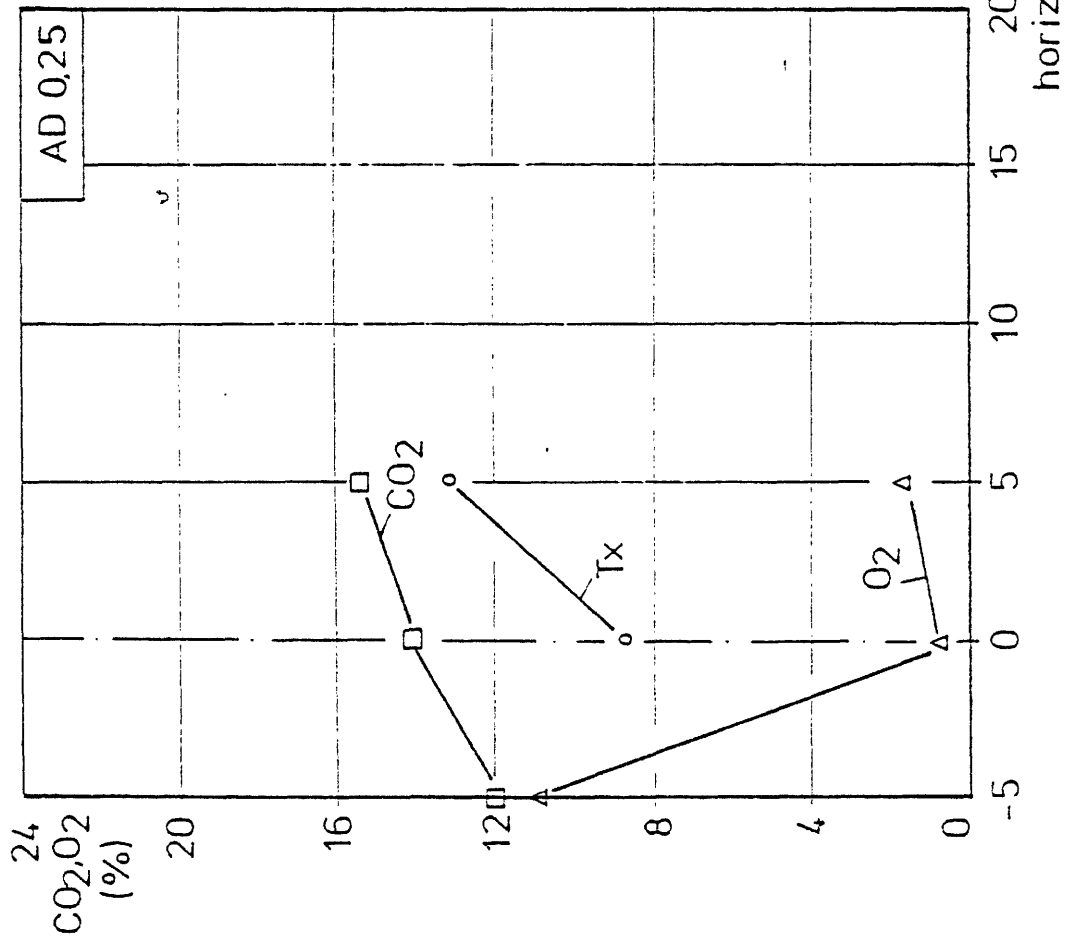


Fig. 13 Radial variation of measured quantities for F-15
 (EC, T_b = 1200, SR = 1, N, I2)



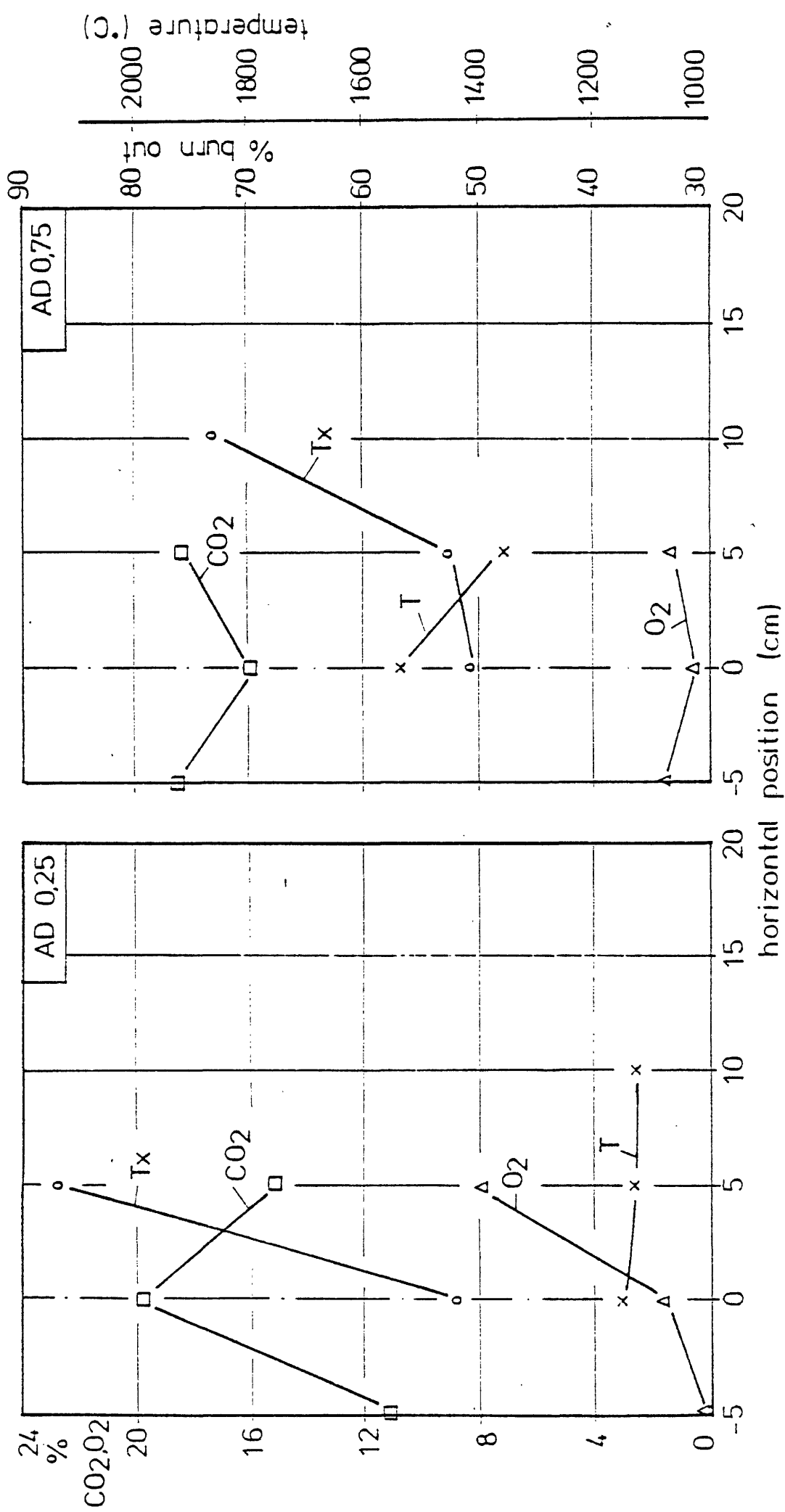


Fig. 14 Radial variation of measured quantities for F-25
 (EC, $T_b = 1200$, SR = 1, F, I2)



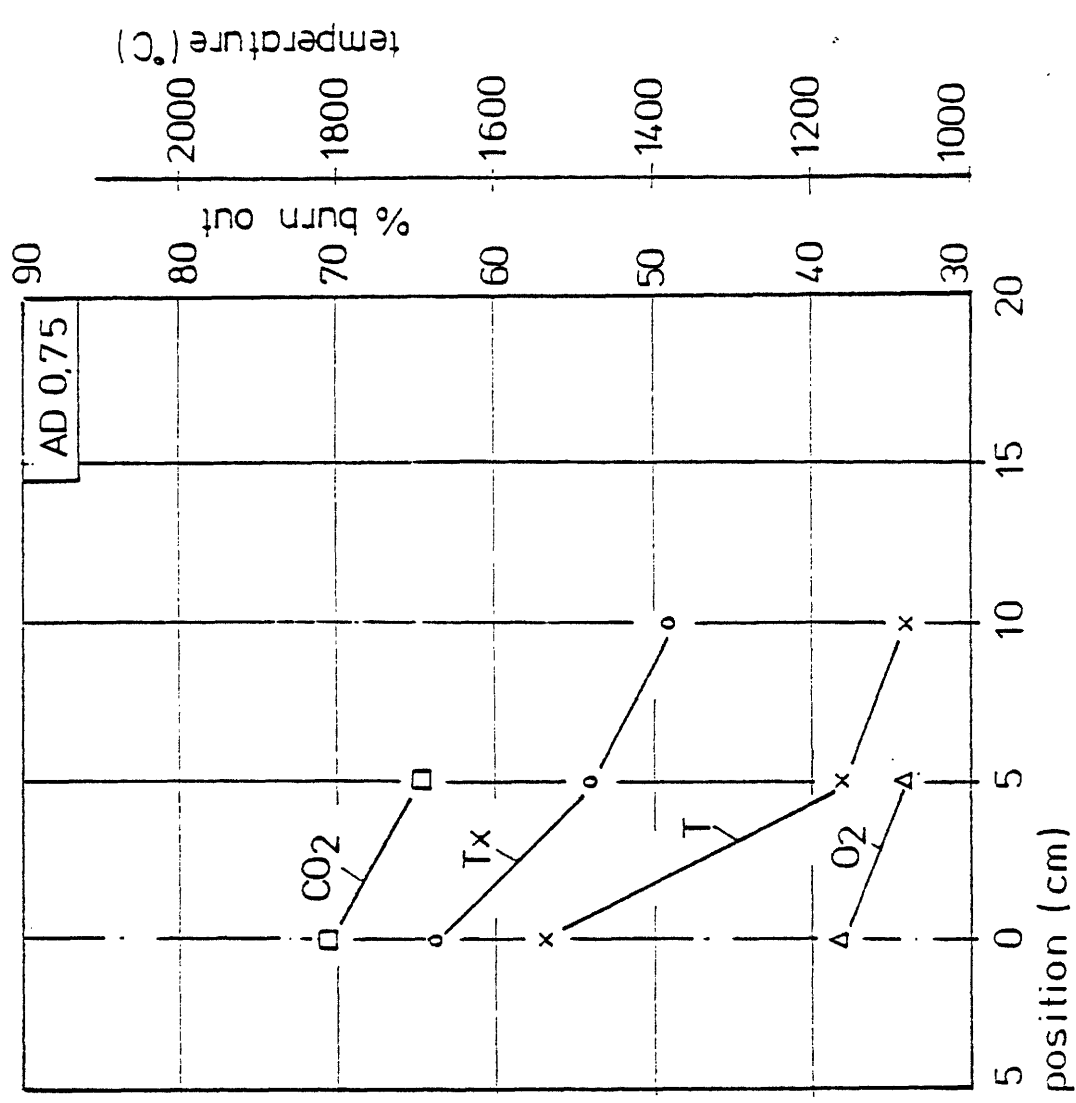
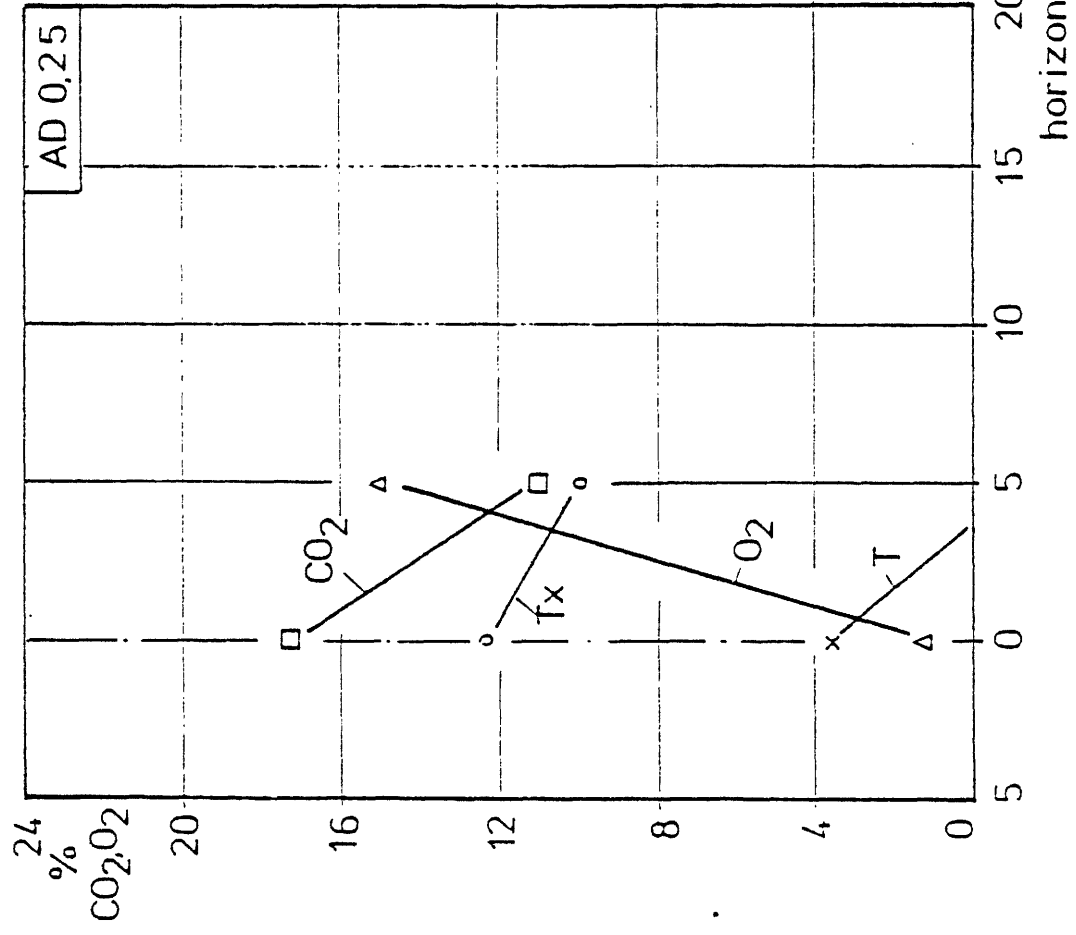


Fig. 15 Radial variation of measured quantities for F-26
 (EC, $T_b = 1200$, SR = 2, F, I 2)



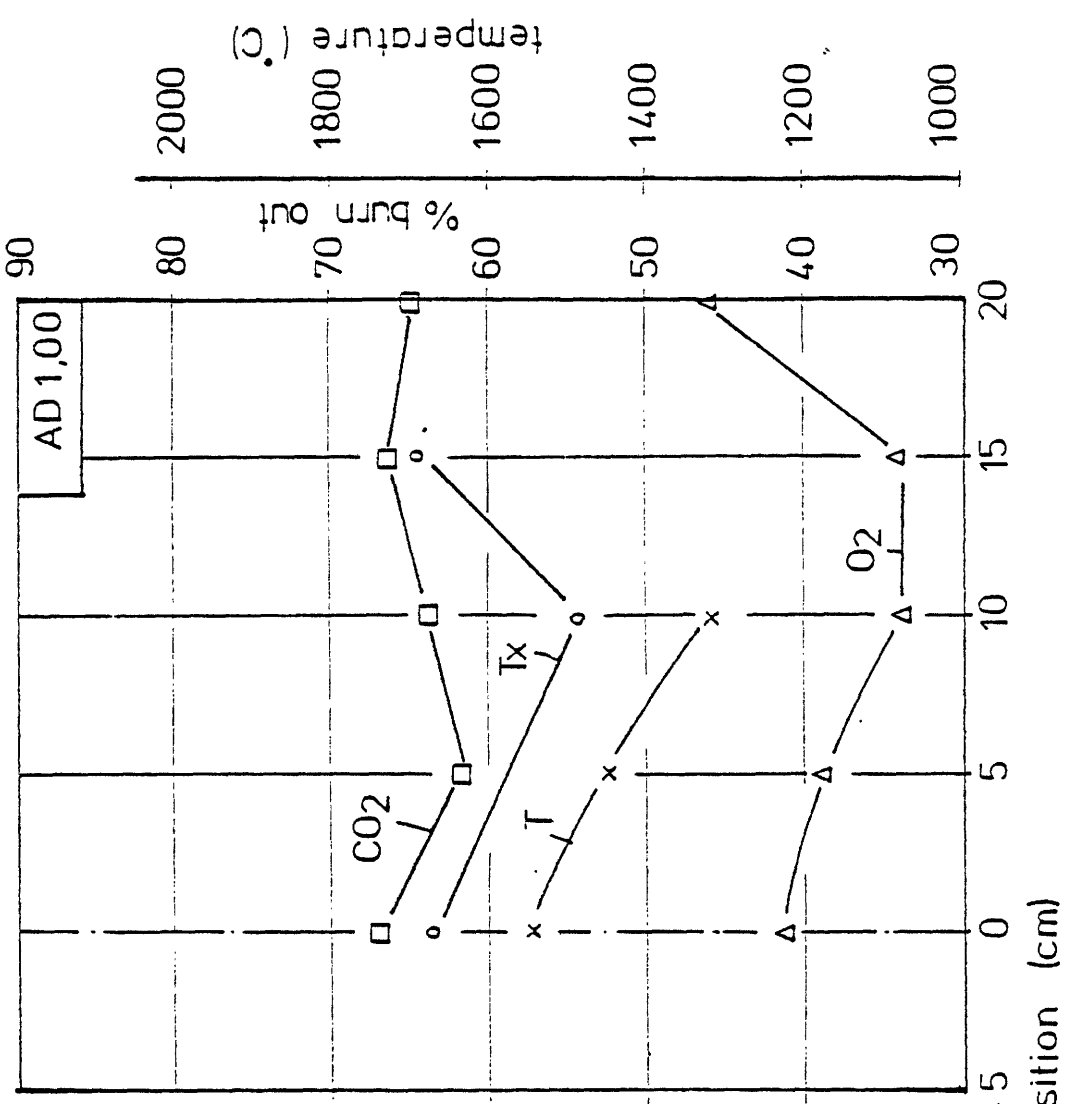
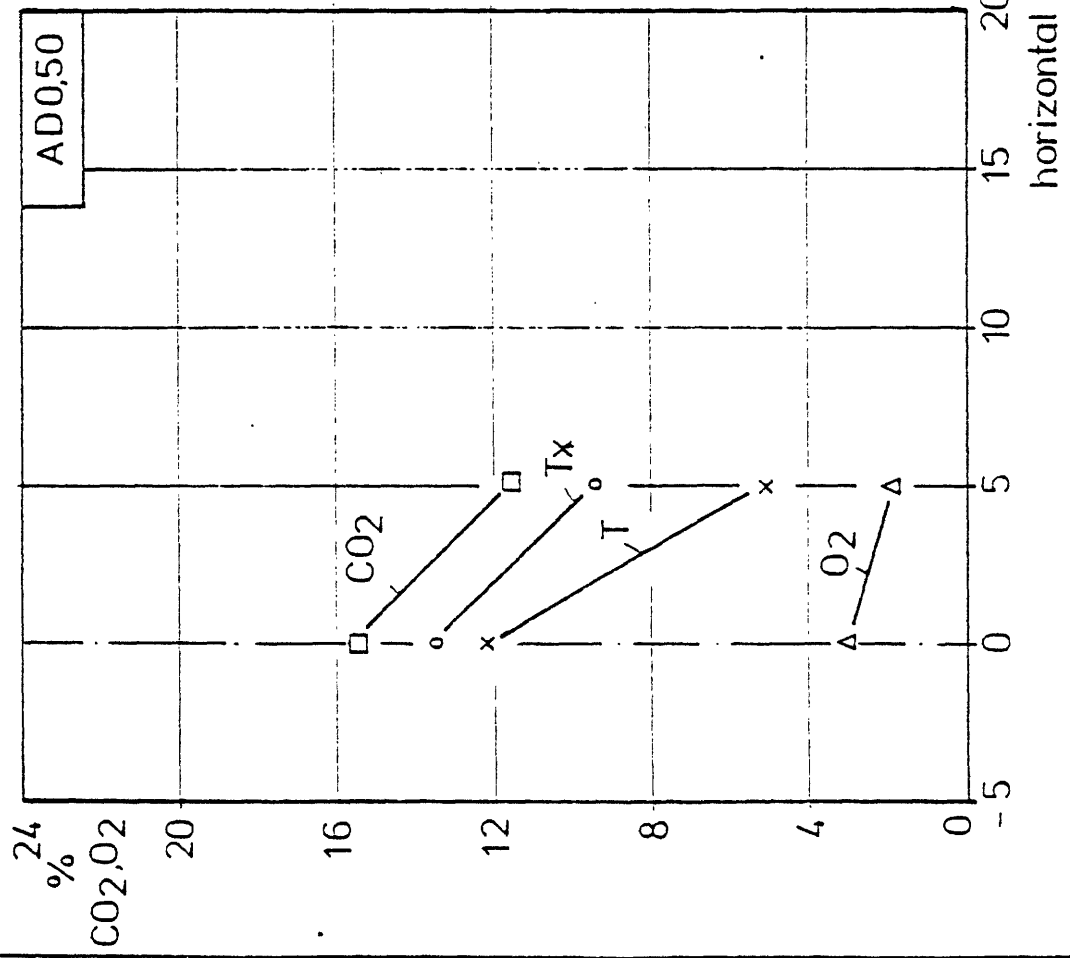
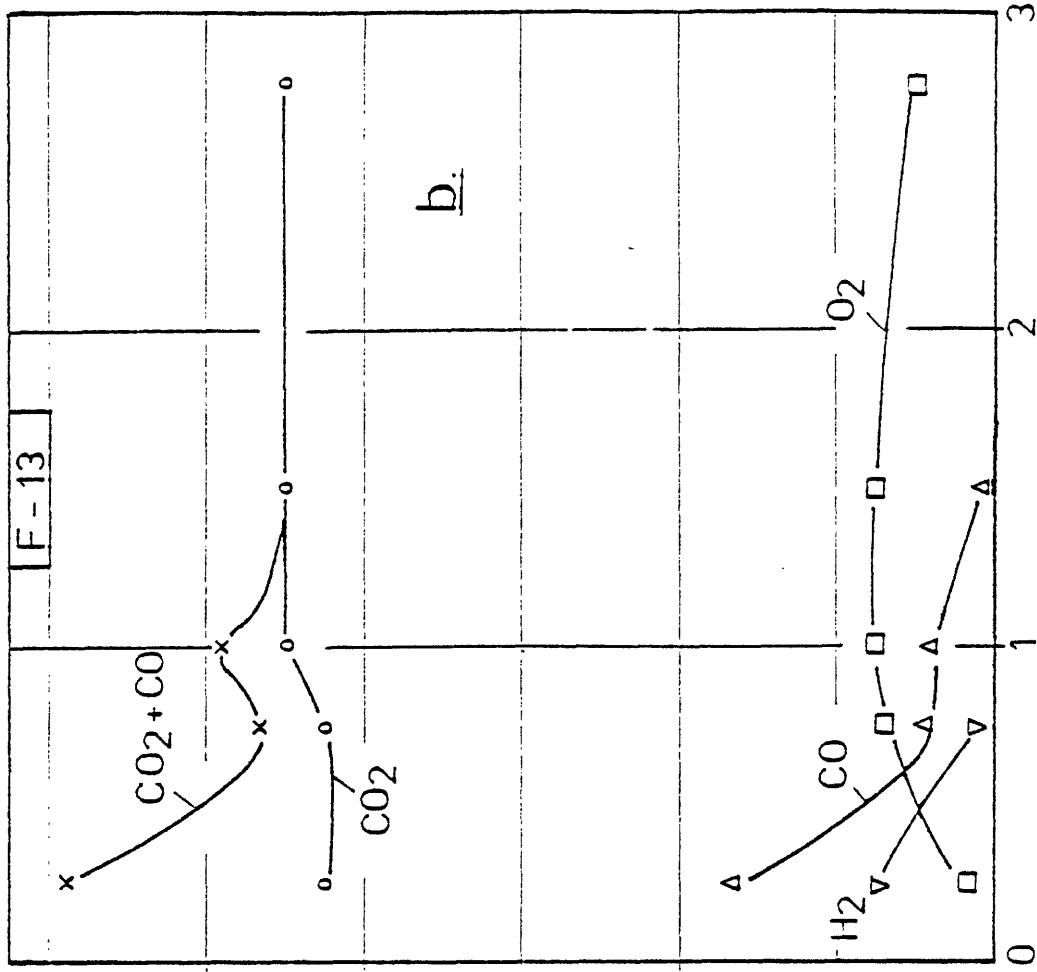
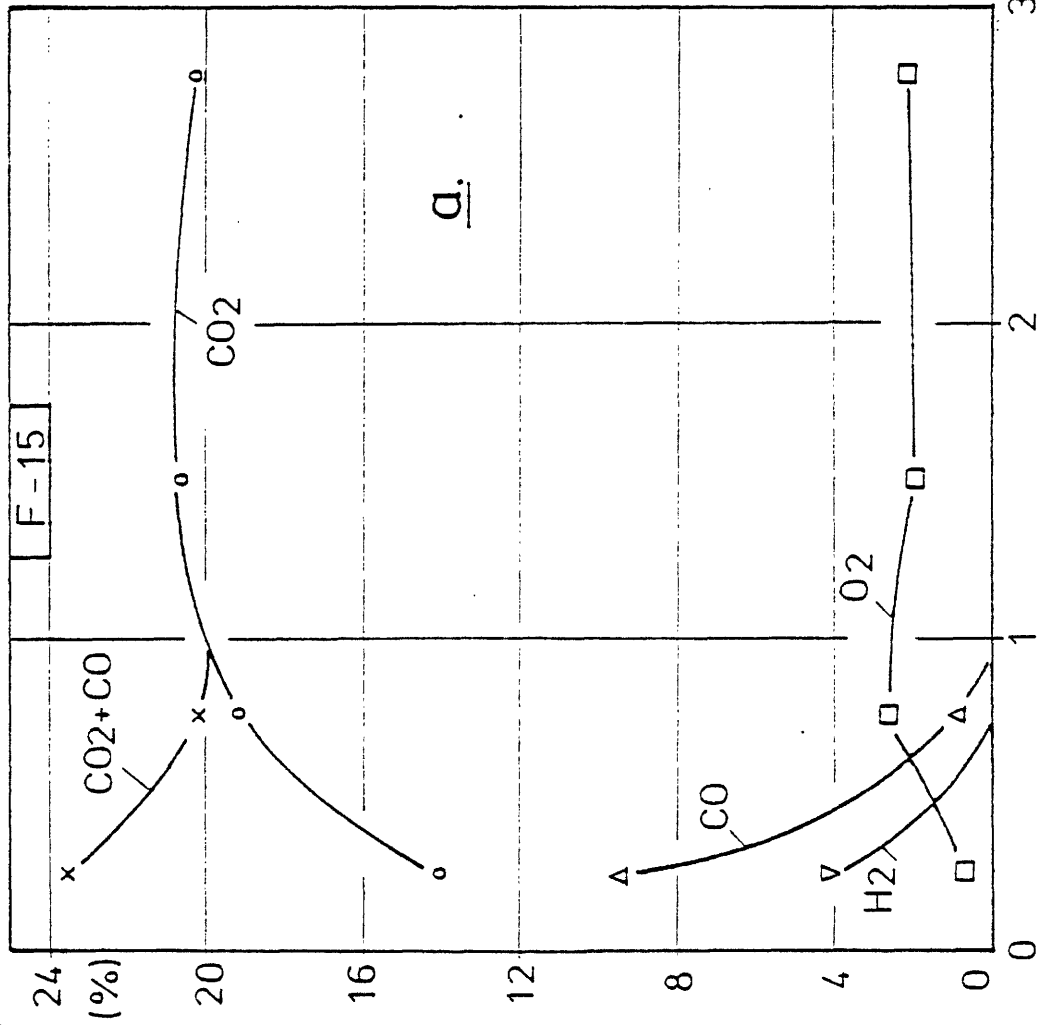


Fig. 16 Radial variation of measured quantities for F-22
 (EC, $T_b = 1000$, SR = 1, N, I2)





axial distance (m)

Fig. 17 Axial gas concentrations; a: $EC, T_b = 1200, SR = 1, N, I, 2$
 b: $EC, T_b = 1200, SR = 1, N, I, 5$



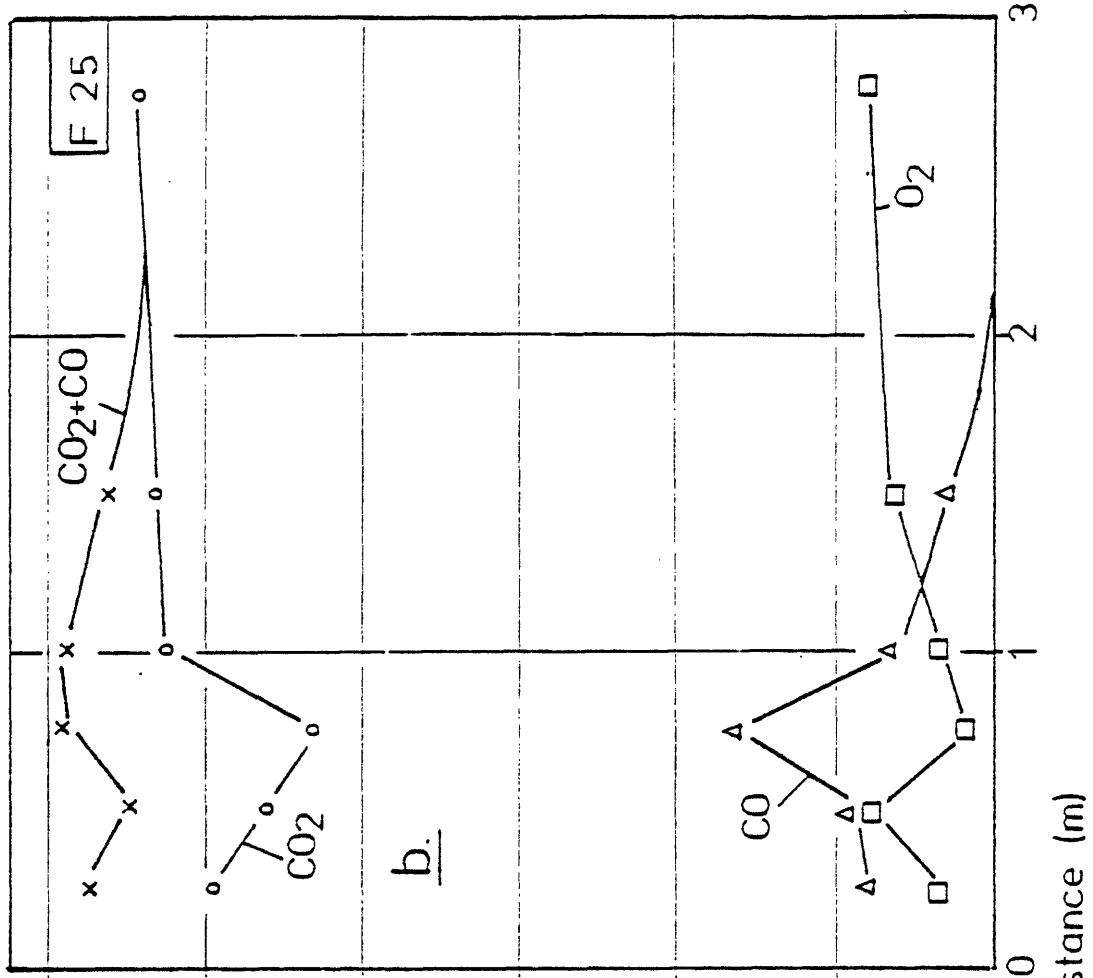
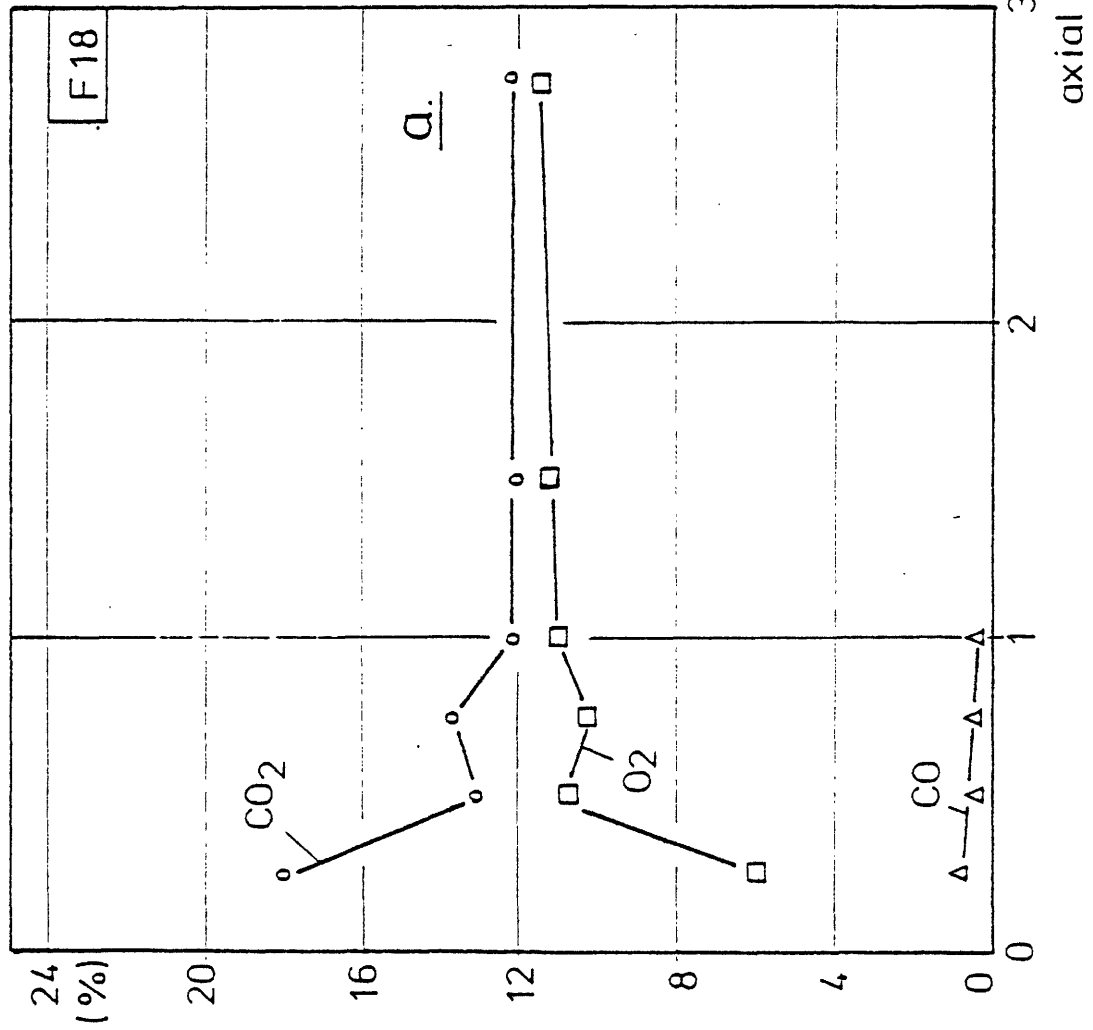


Fig. 18 Axial gas concentrations; a: EC, $T_b=1200$, SR=2, N, I2
 b: EC, $T_b=1200$, SR=1, F, I2



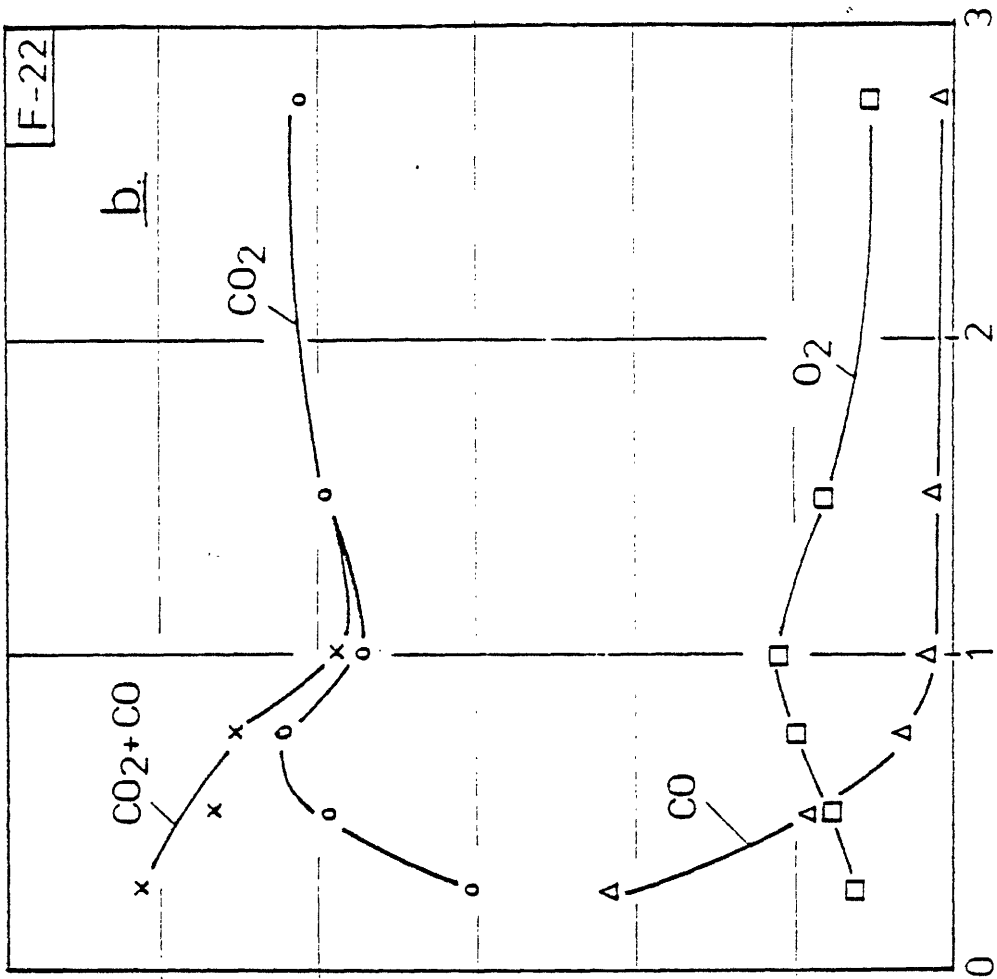
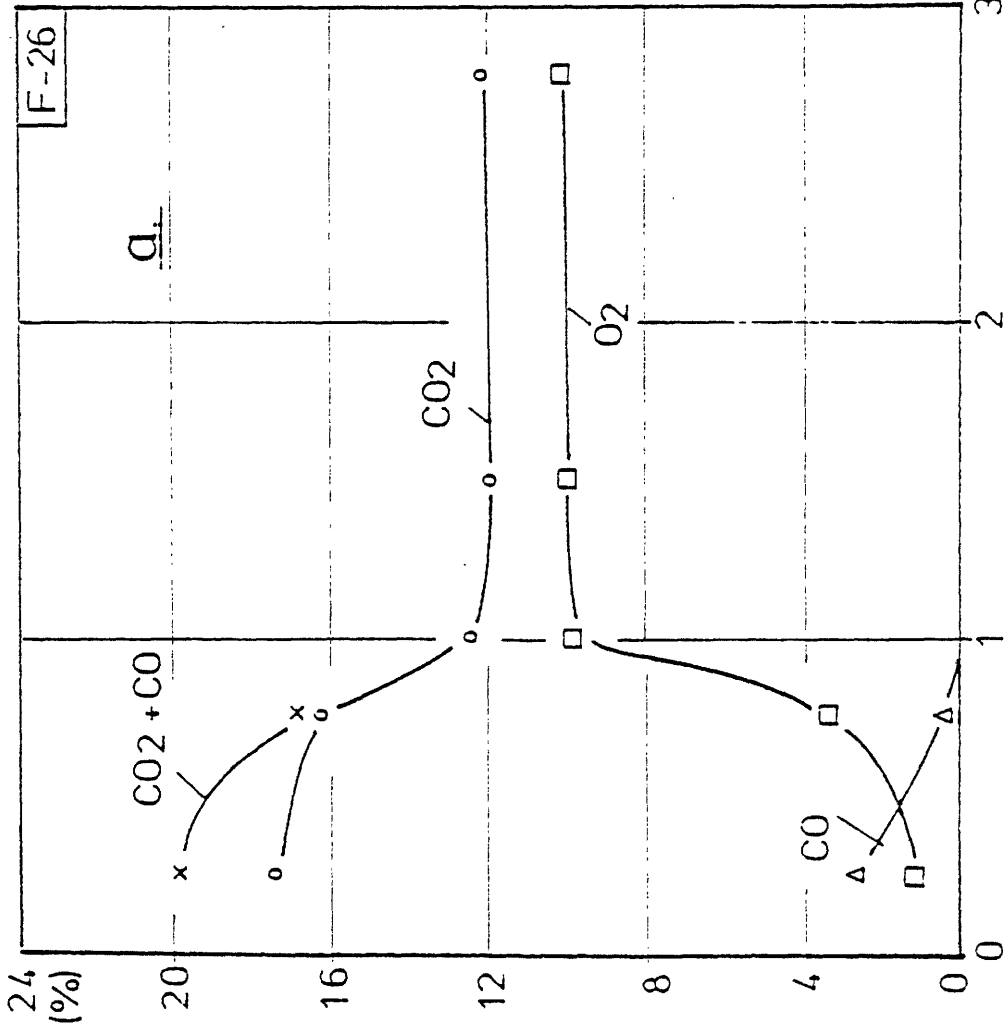


Fig. 19 Axial gas concentrations; a: EC, $I_b=1200$, SR=2, I2
 b: EC, $I_b=1000$, SR=1, I2



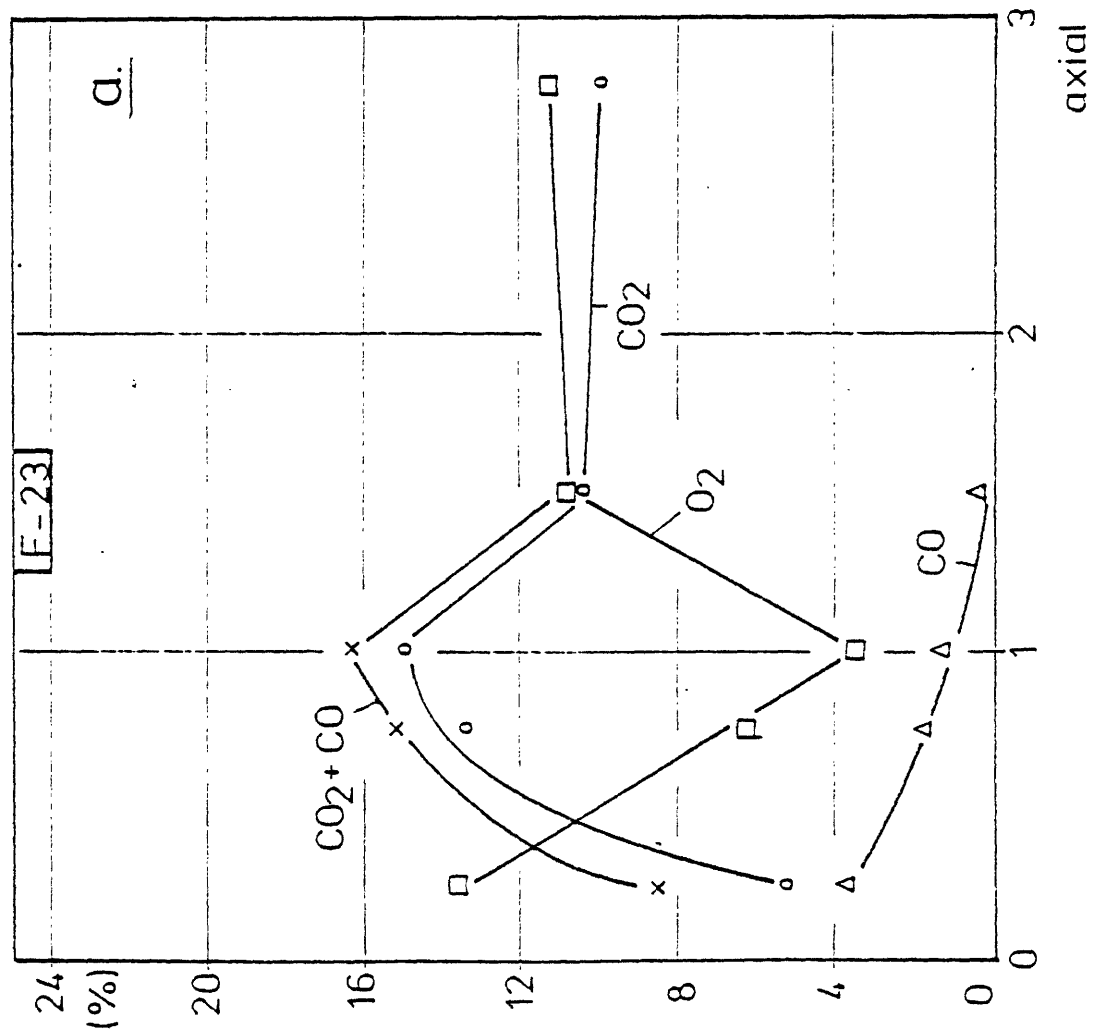
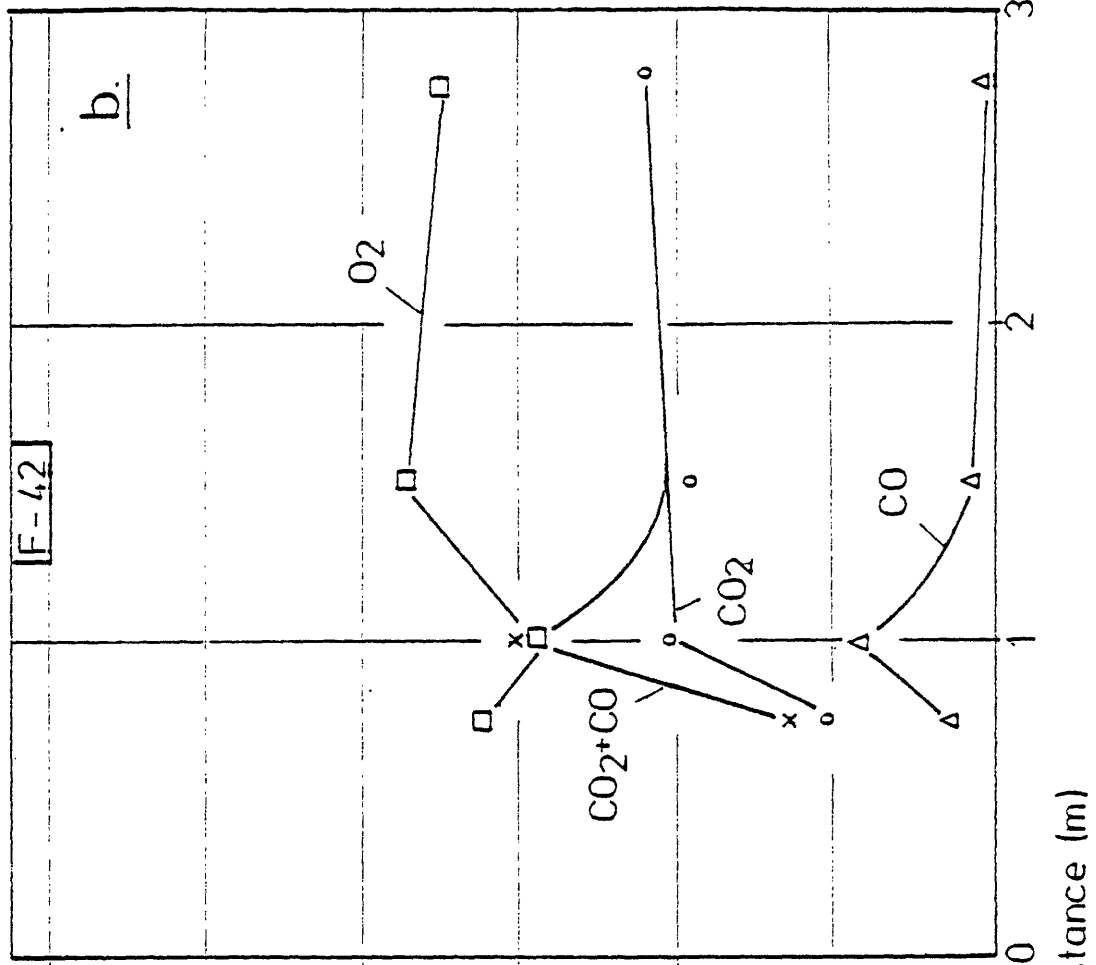


Fig. 20 Axial gas concentrations; a: EC, $T_b = 1000$, SR=2, I2
 b: EC, $T_b = 900$, SR=2, I2



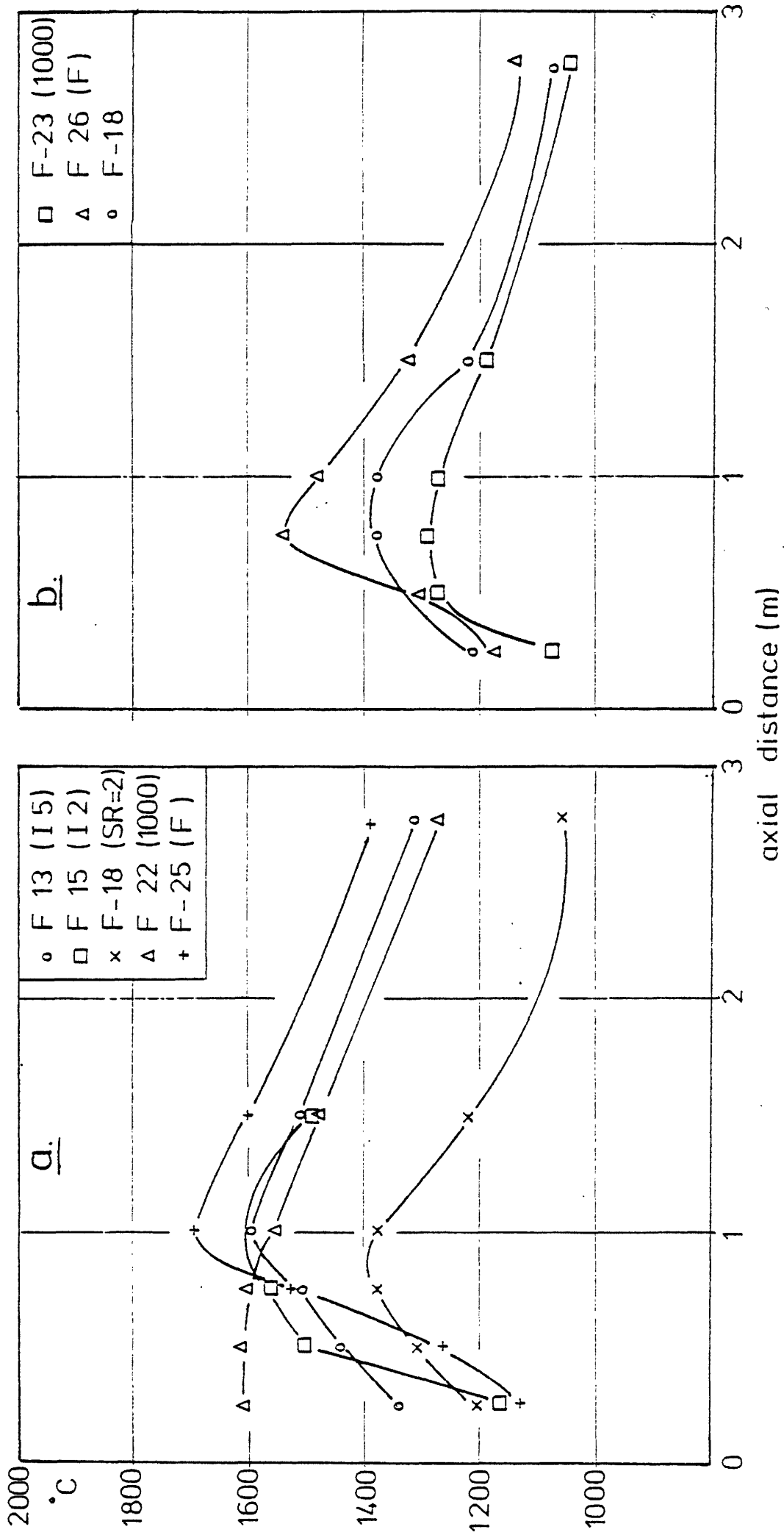


Fig. 21 Axial temperatures for the Elk Creek flames
 a: parameter effect ; b: SR=2



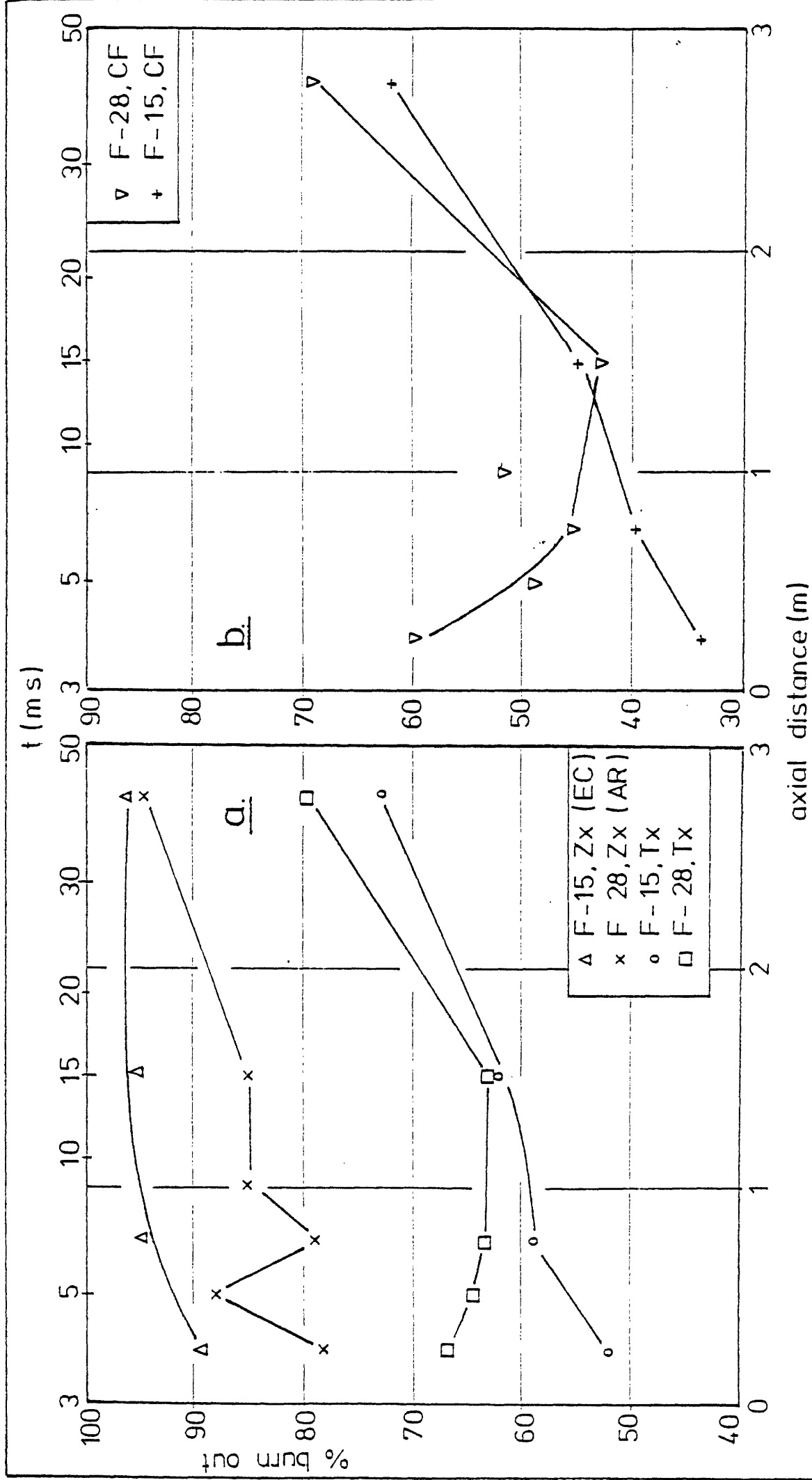


Fig. 22 Axial solids burn out; a,b: Elk Creek vs. Armco coal
 $T_b = 1200\text{ }^\circ\text{C}$



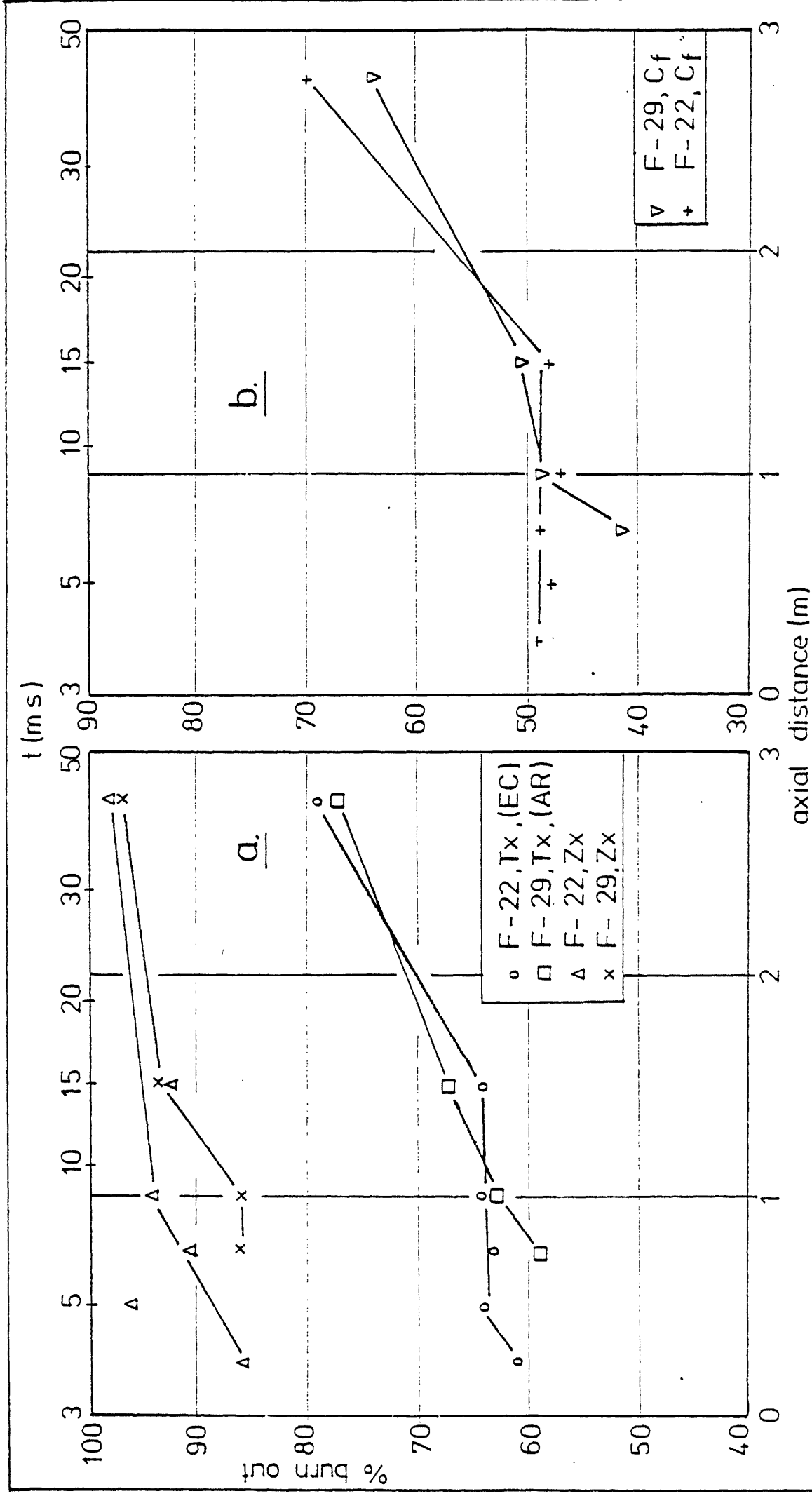


Fig. 23 Axial solids burn out ; a,b: Elk Creek vs Armco coal ;
 reduced blast temperature



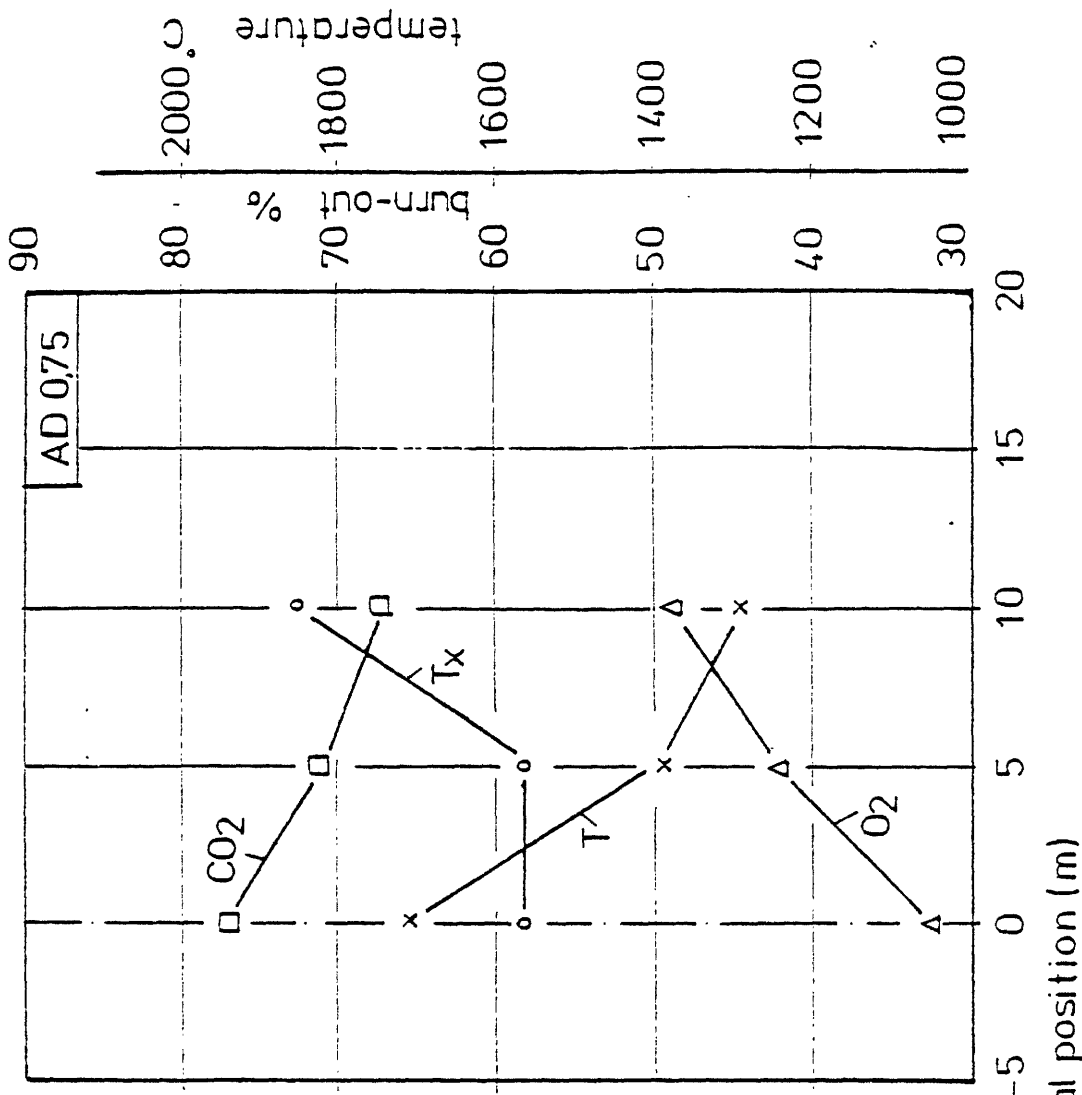
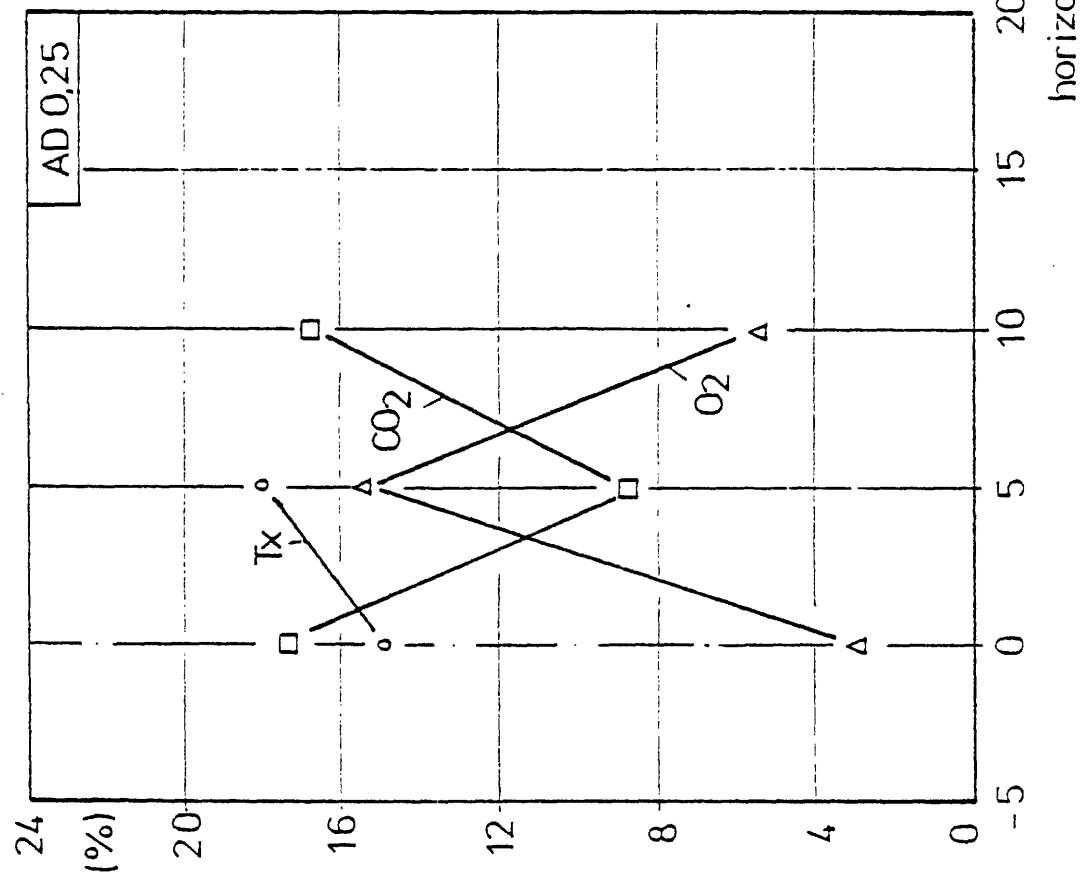


Fig. 24 Radial variation of measured quantities for F-28;
 (AR, $T_b = 1200$, SR=1, N, I2)



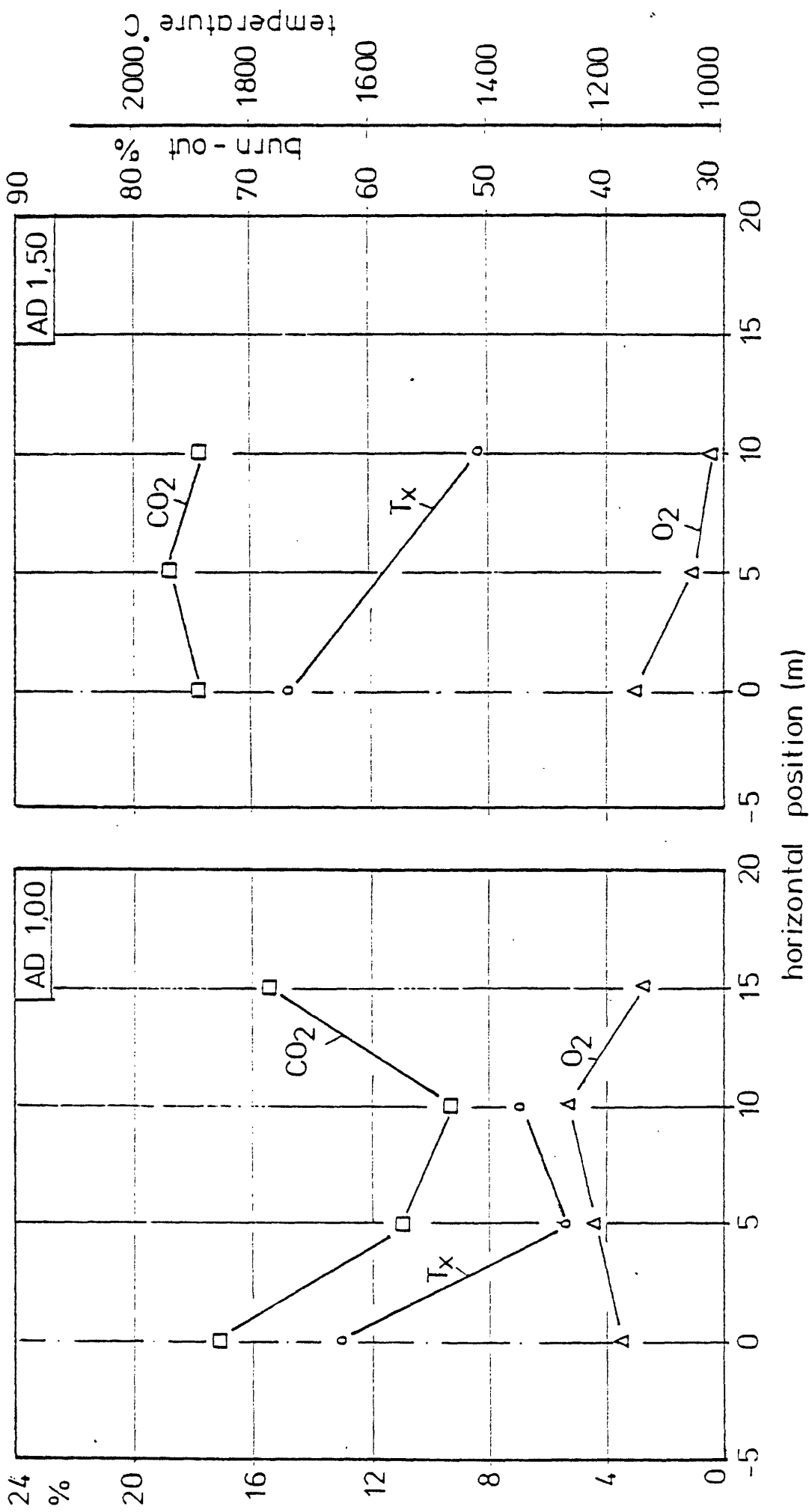


Fig. 25 Radial variation of measured quantities for F-29;
 (AR, $T_b = 900$, SR=1, N, I2)

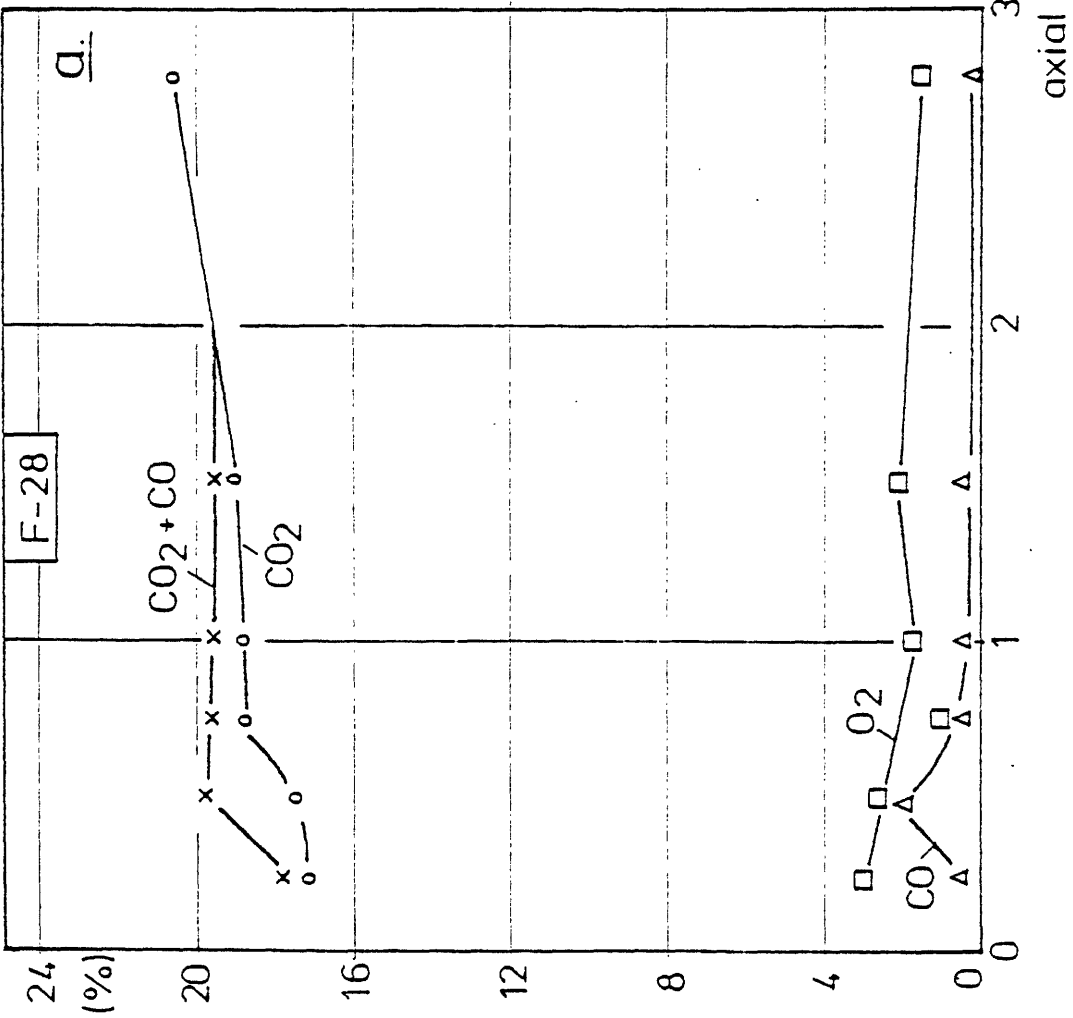
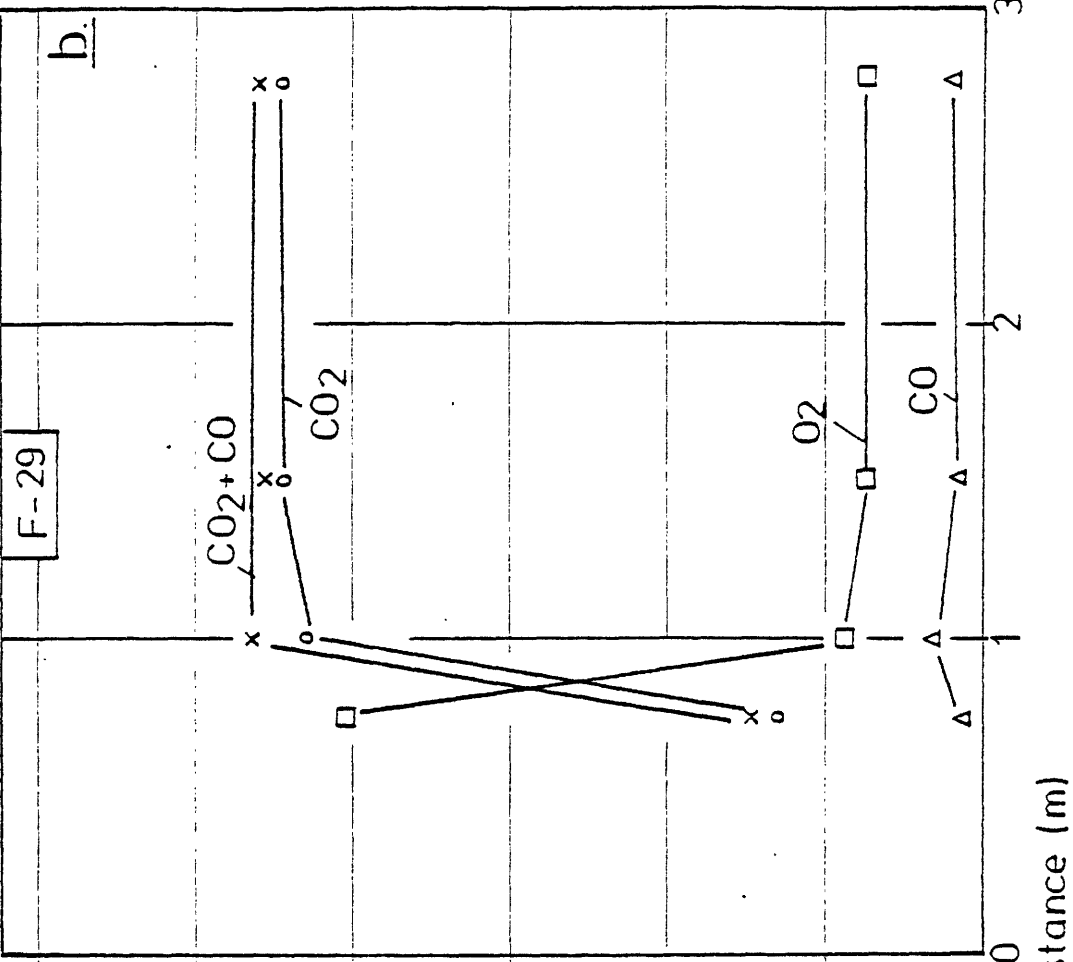


Fig. 26 Axial gas concentrations; a: AR, $T_b = 1200$, SR=1, N, I2
 b: AR, $T_b = 900$, SR=1, N, I2

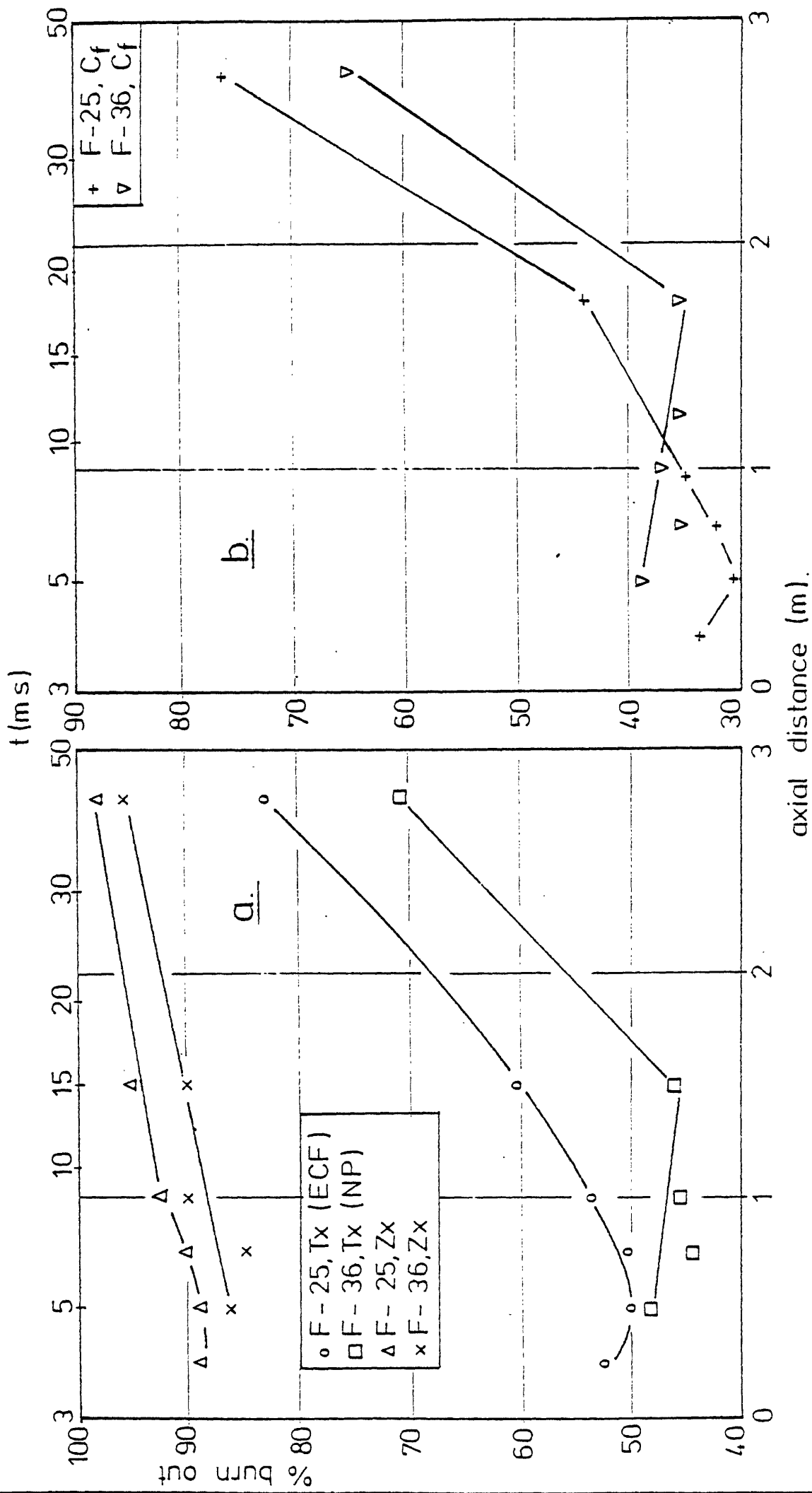


Fig. 27 Axial solids burn out; a,b: Elk Creek vs Norwich Park Coal;
SR = 1

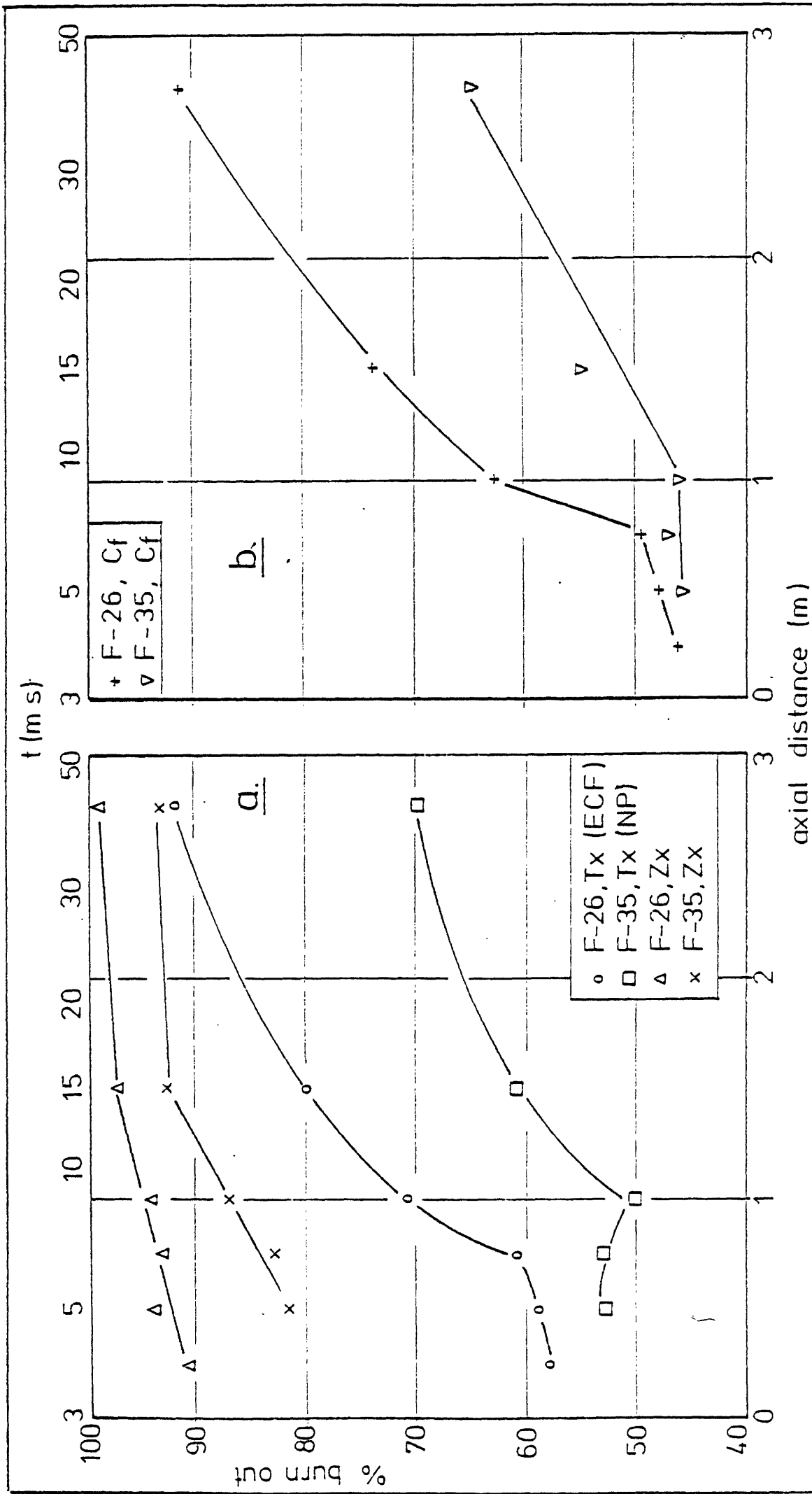


Fig. 28 Axial solids burn out; a,b: Elk Creek vs. Norwich Park Coal
 SR=2

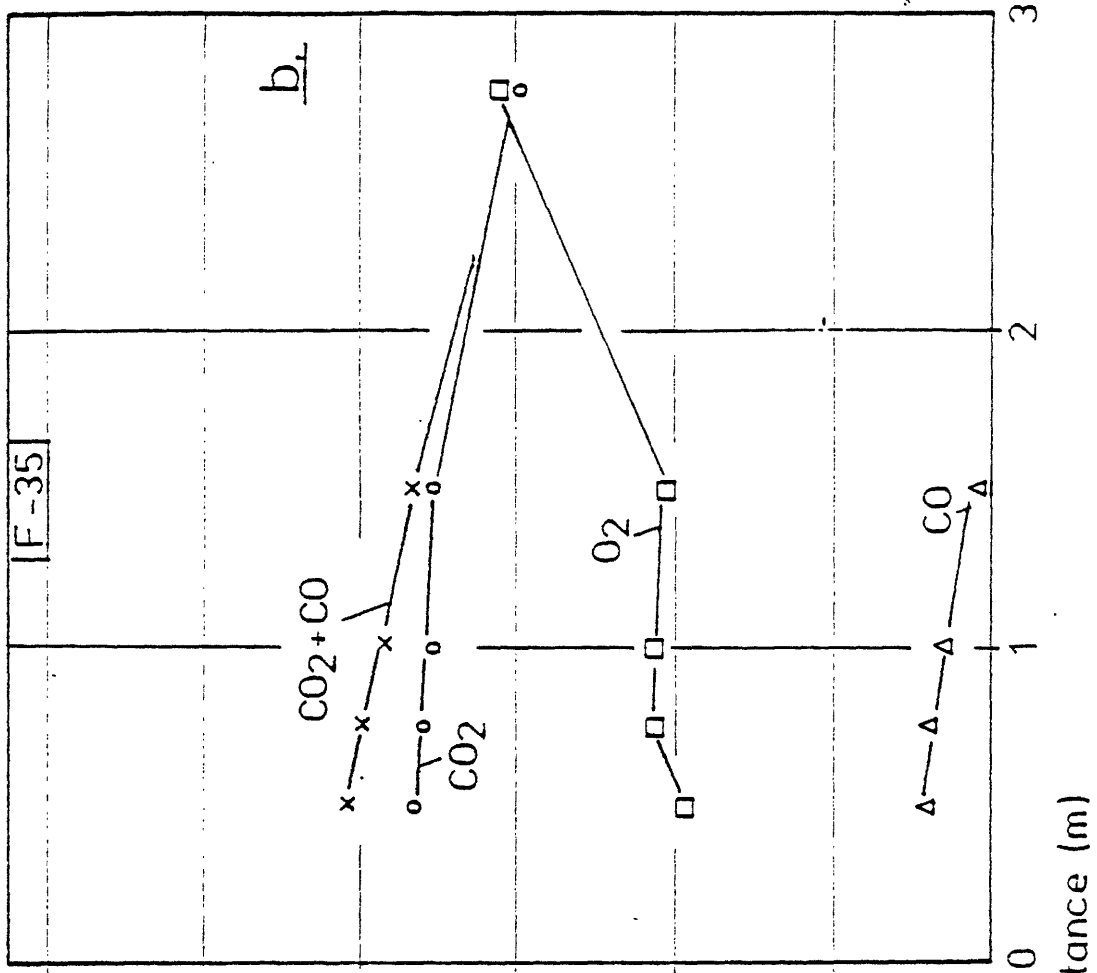
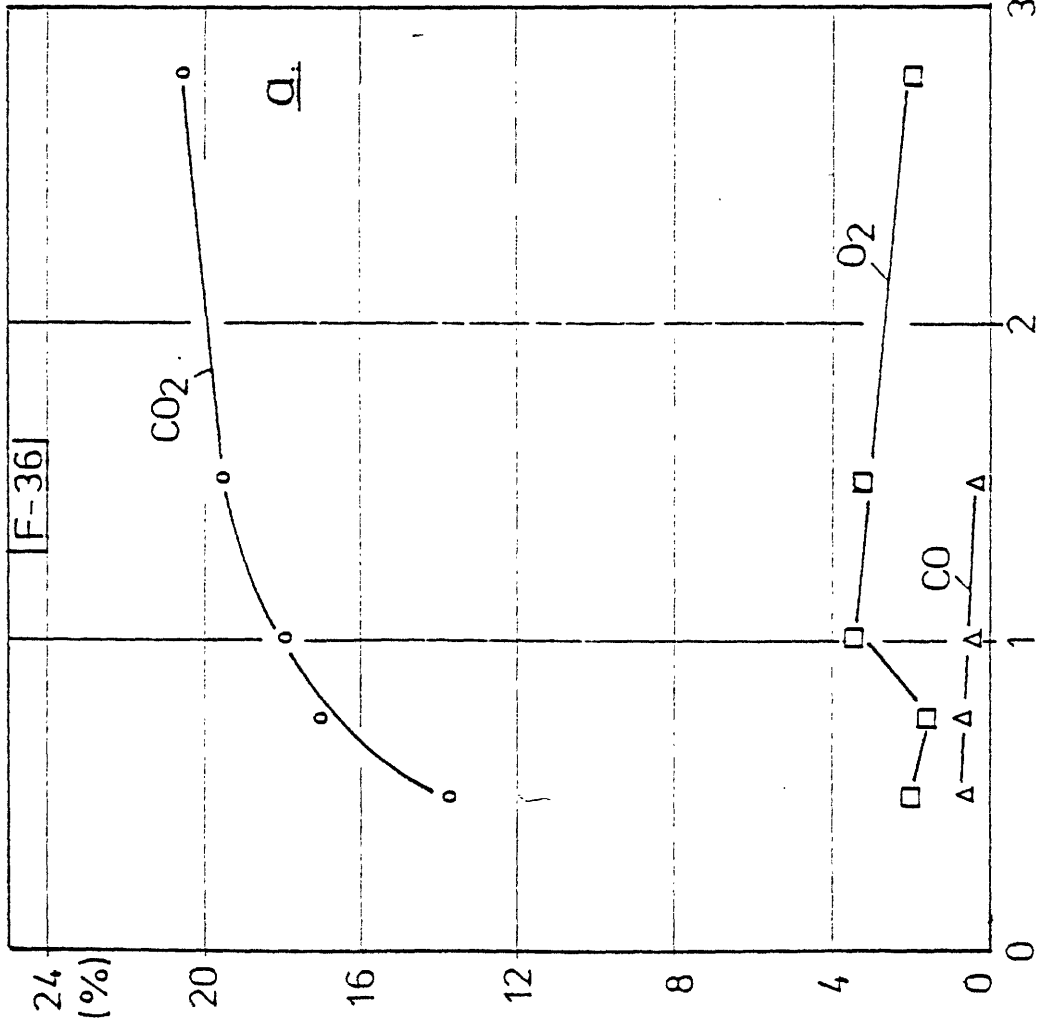


Fig. 29 Axial gas concentrations; a: NP, $T_b = 1200$, SR=1, N,I,2
 b: NP, $T_b = 1200$, SR=2, N,I,2

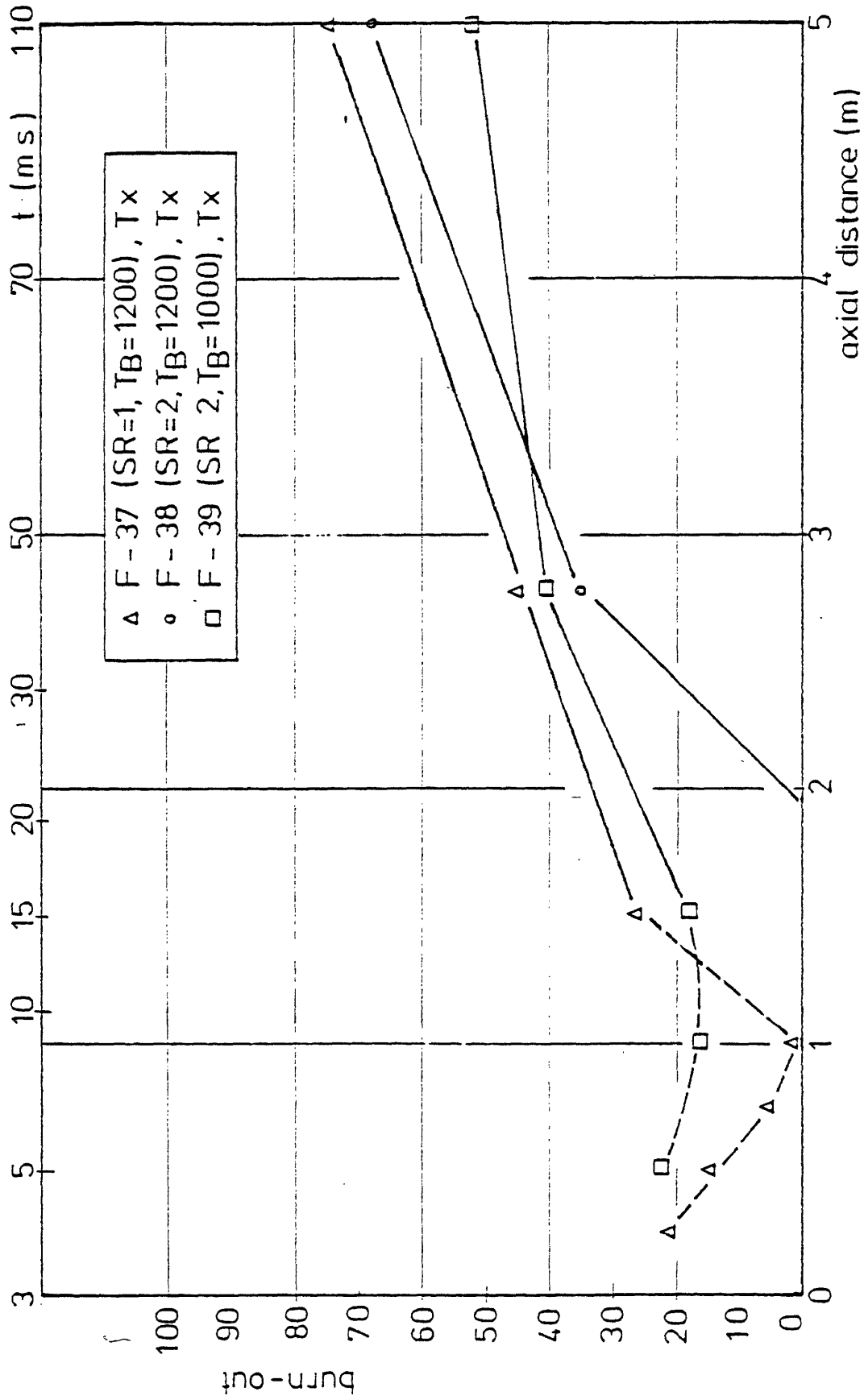


Fig. 30 Axial solids burn out for the Preussag coal

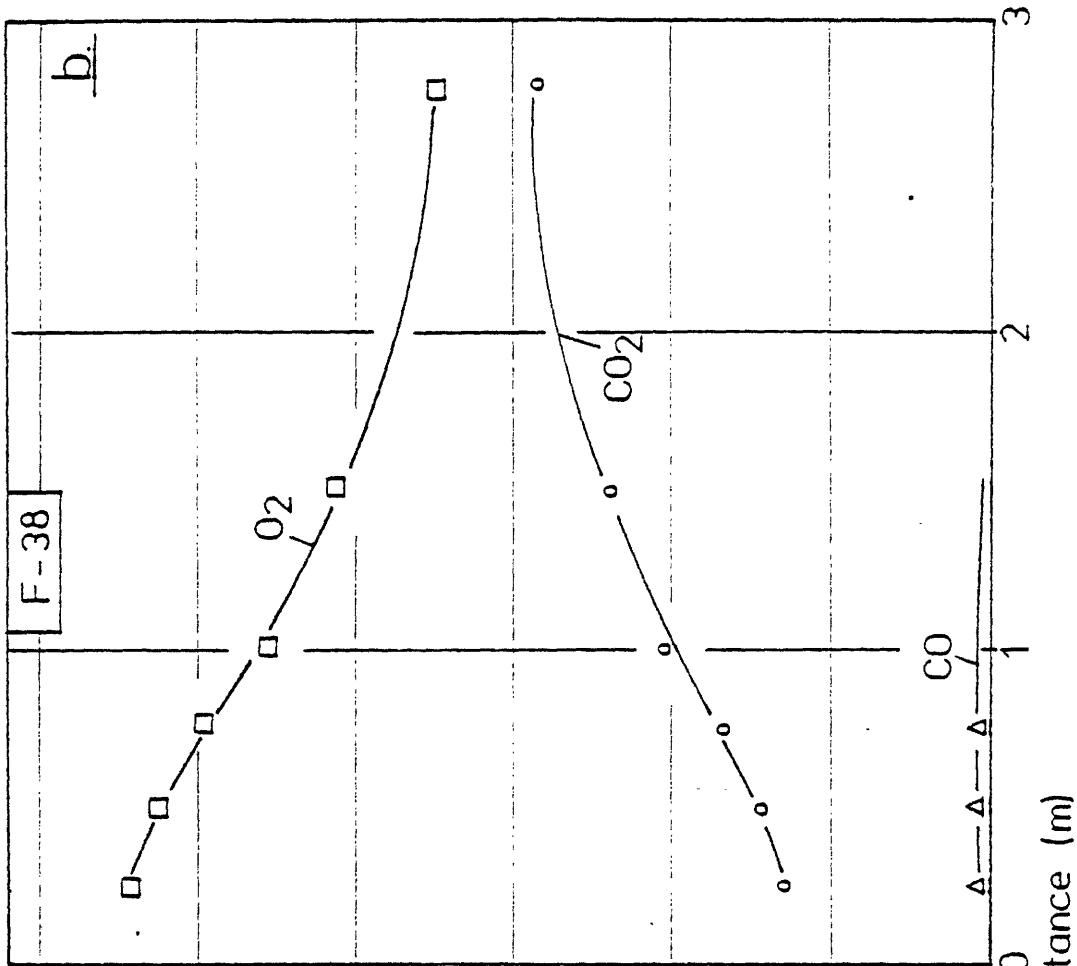
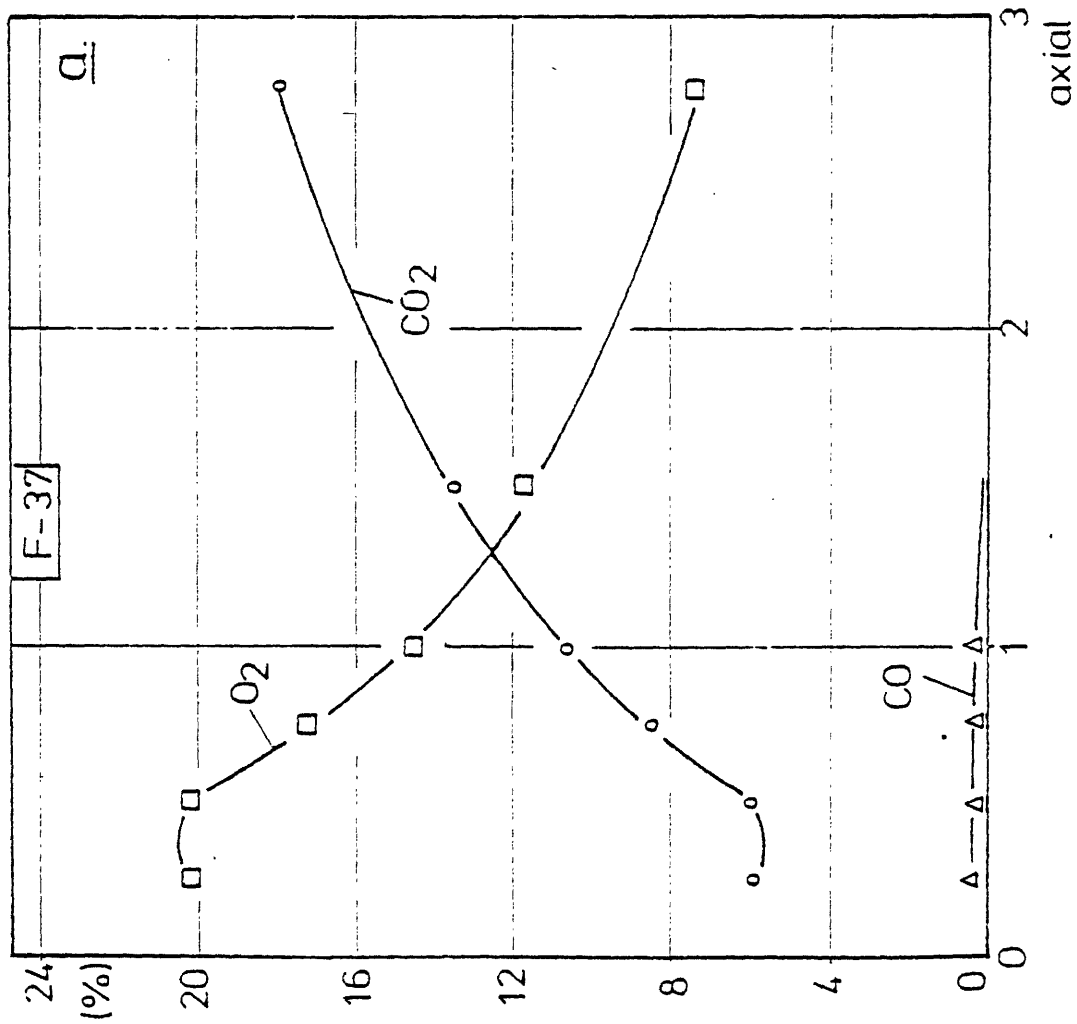


Fig. 31 Axial gas concentrations; a: $P, T_b = 1200, SR = 1, N, I2$
 b: $P, T_b = 1200, SR = 2, N, I2$

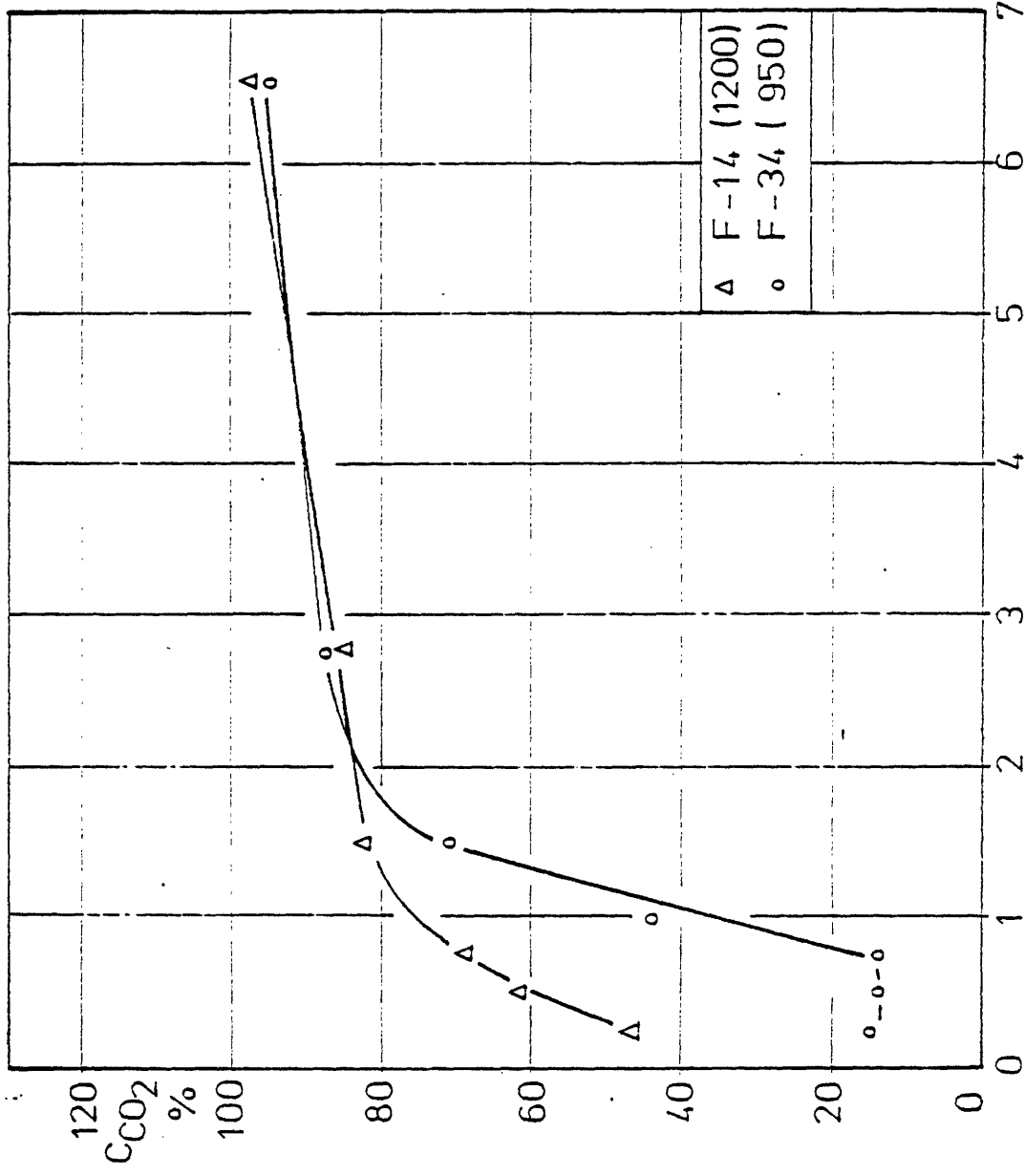


Fig. 32 Axial gas burn out for the heavy fuel oil flames

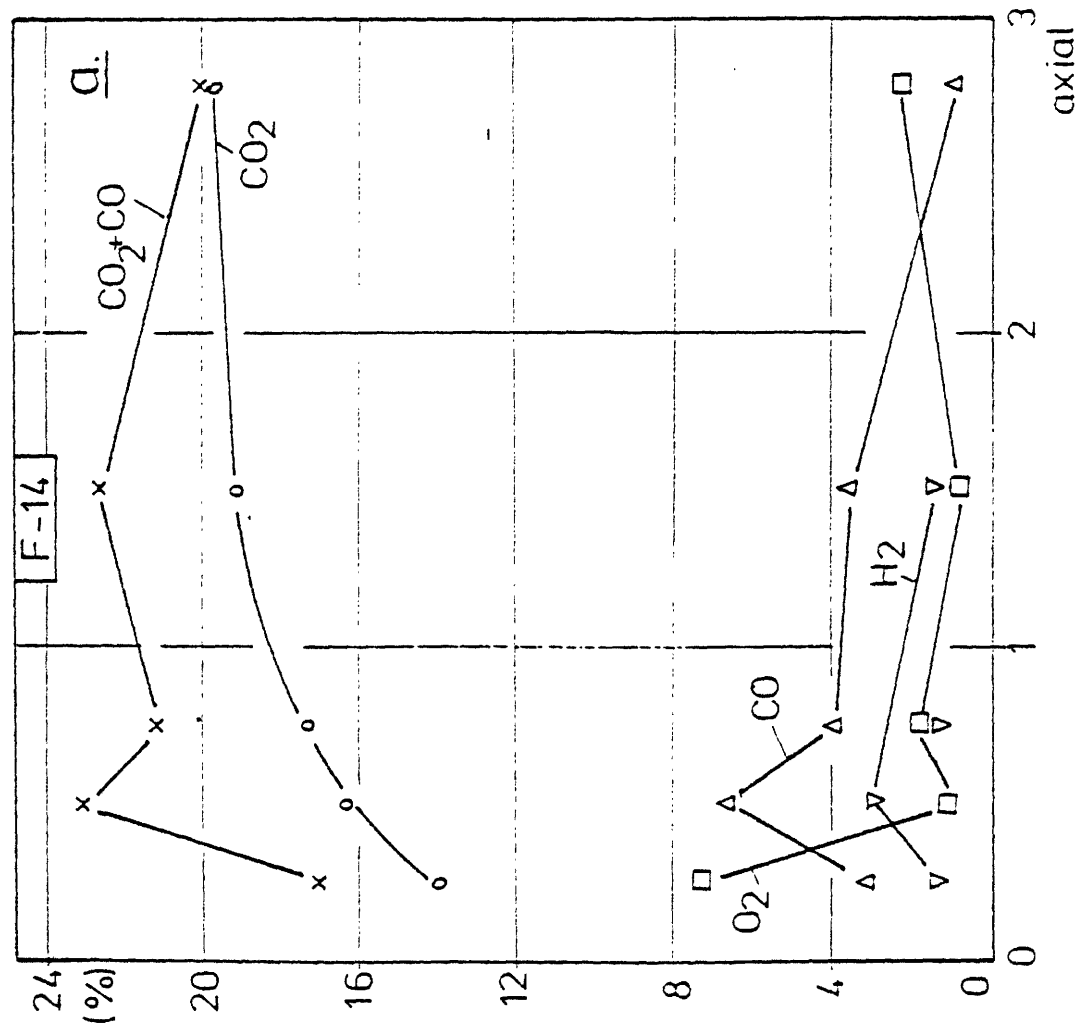
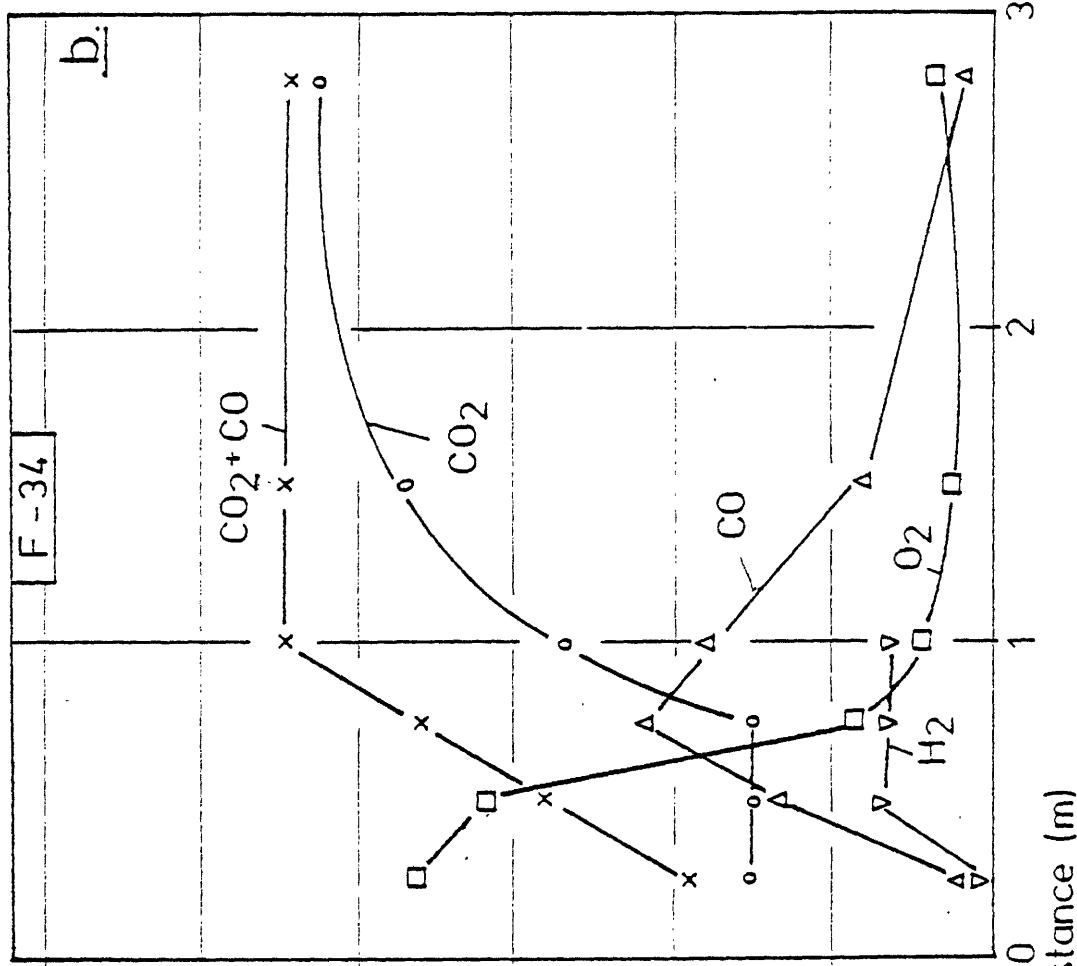


Fig. 33 Axial gas concentrations; a: Oil, $T_b=1200$
 b: Oil, $T_b=950$

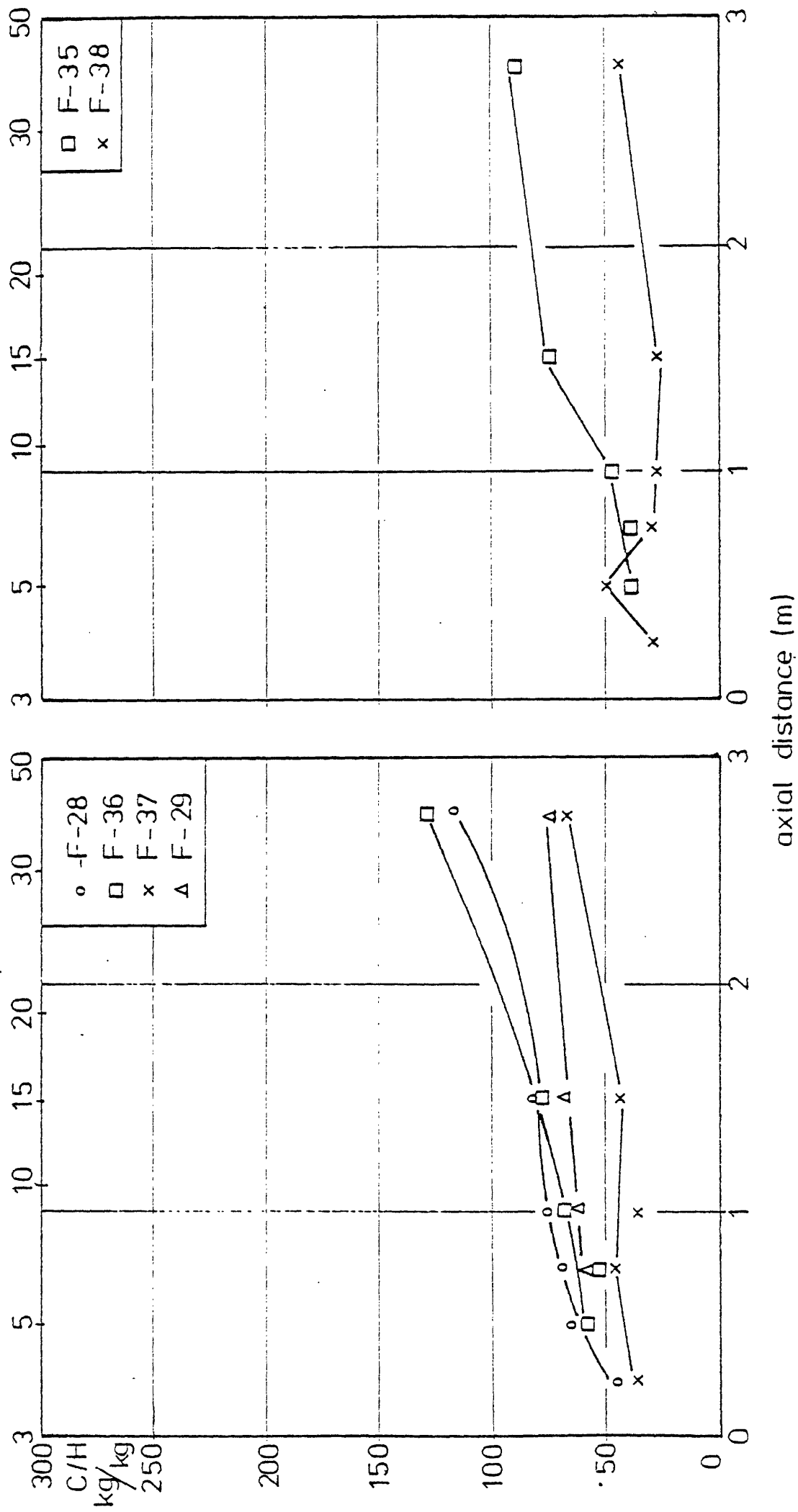


Fig. 34 Carbon/Hydrogen ratios for Armco, Norwich Park and Preussag flames

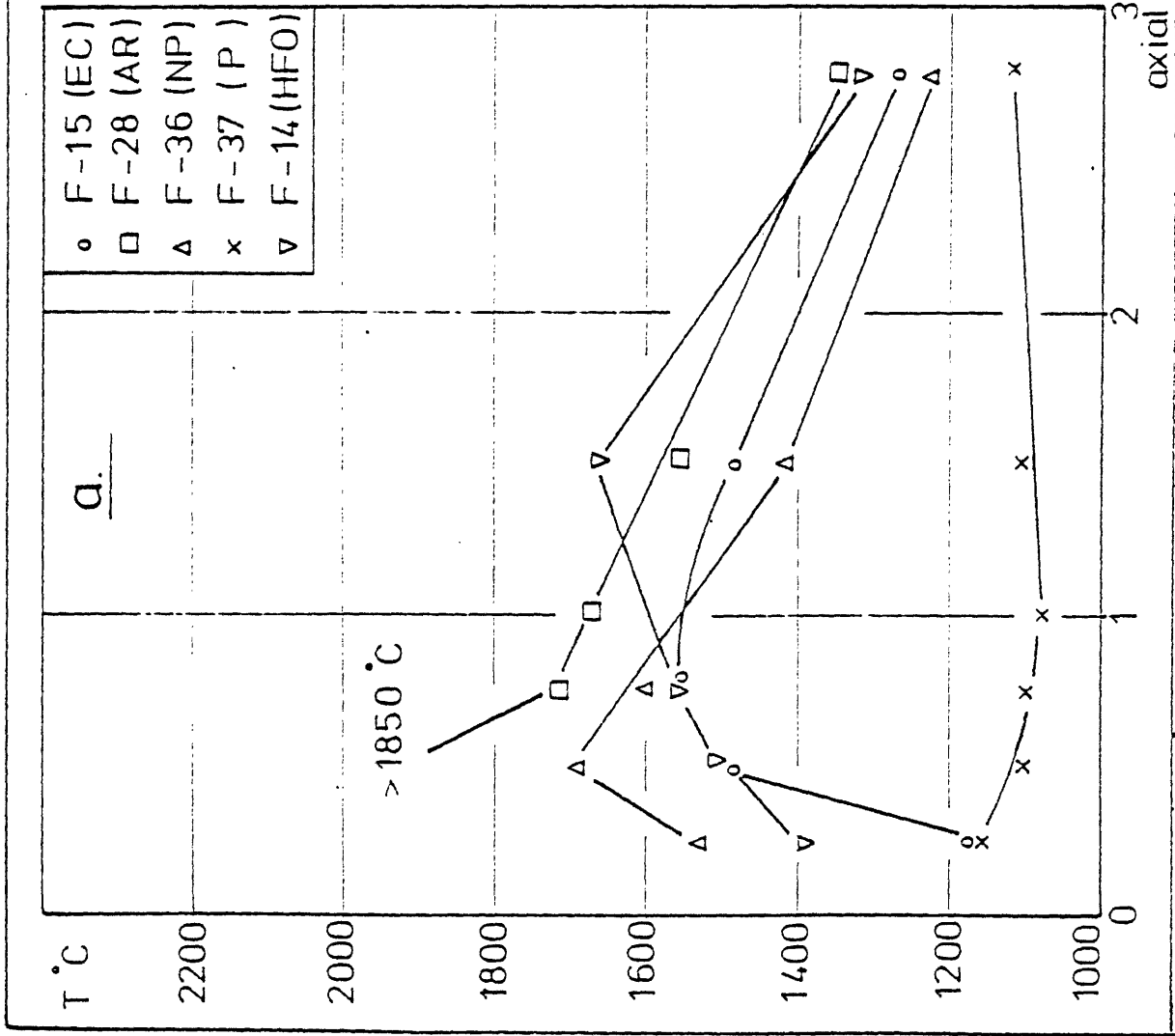
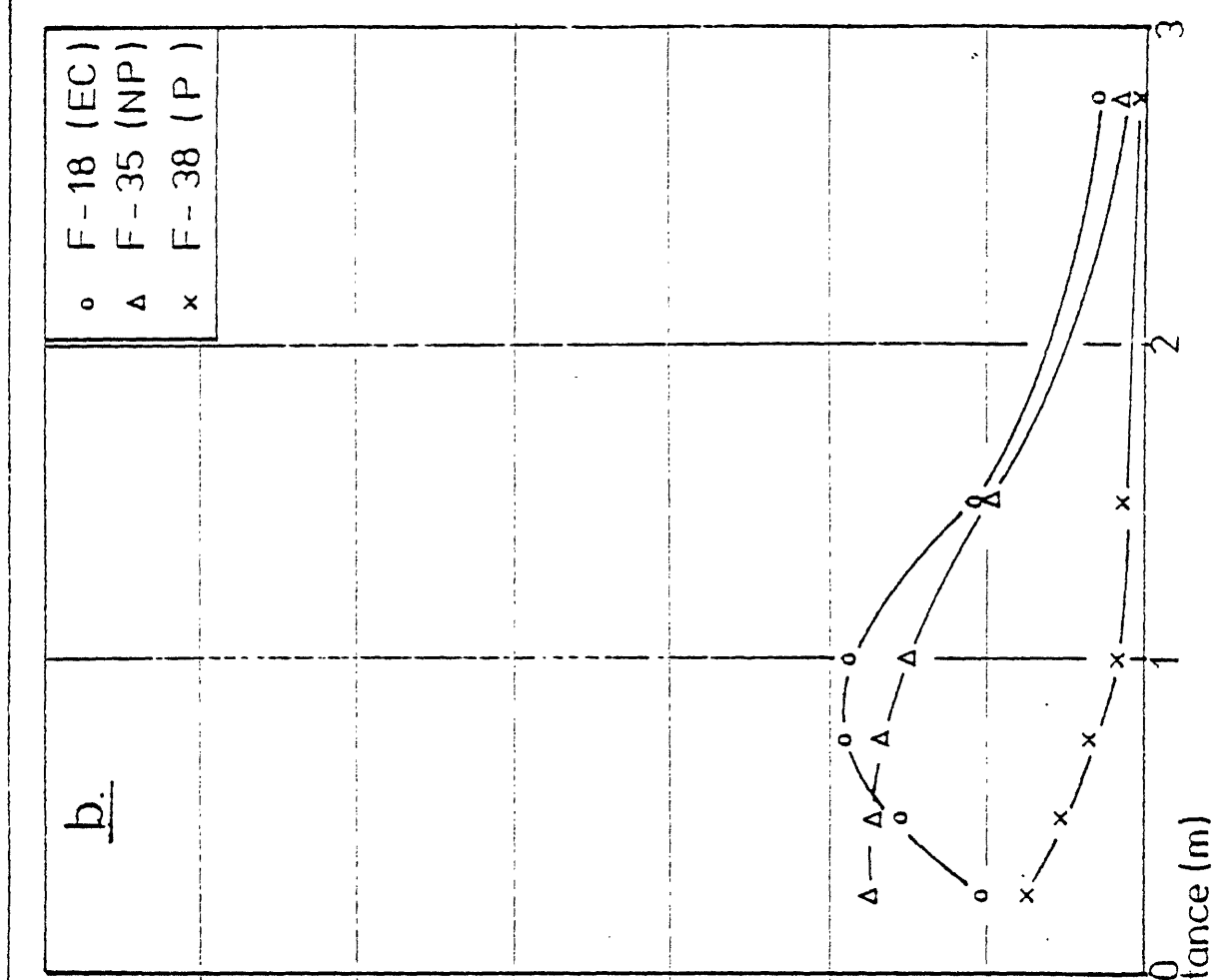


Fig. 35 Axial temperatures for the various coals; a: SR=1
b: SR=2



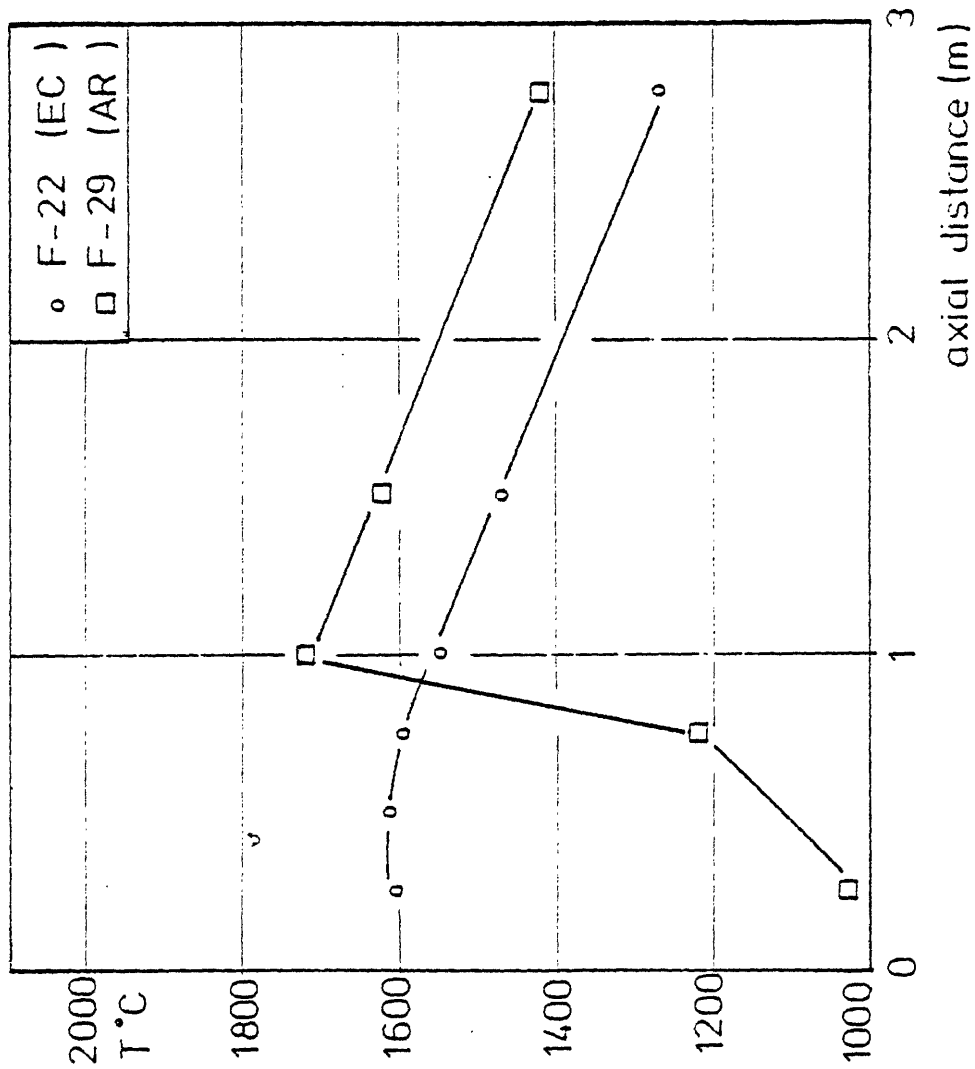
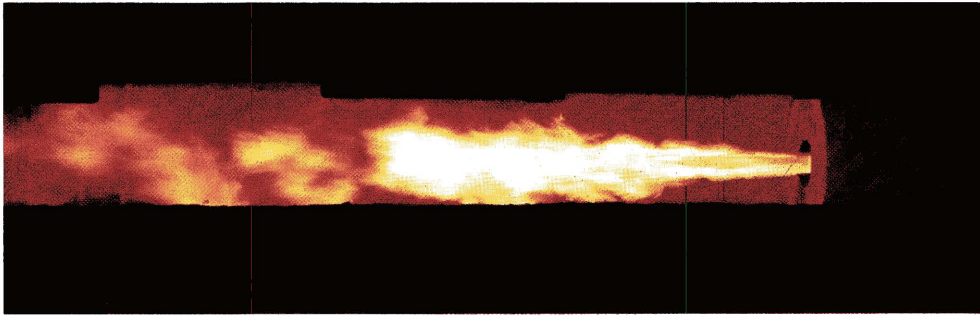


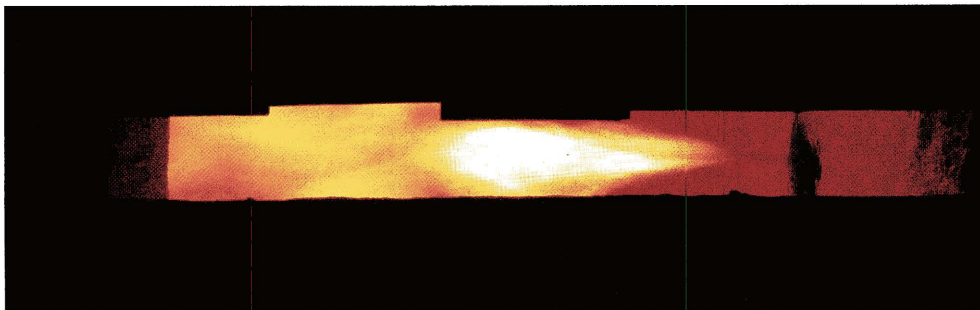
Fig. 36 Axial temperatures for the reduced blast temperature flames

PHOTOGRAPHS



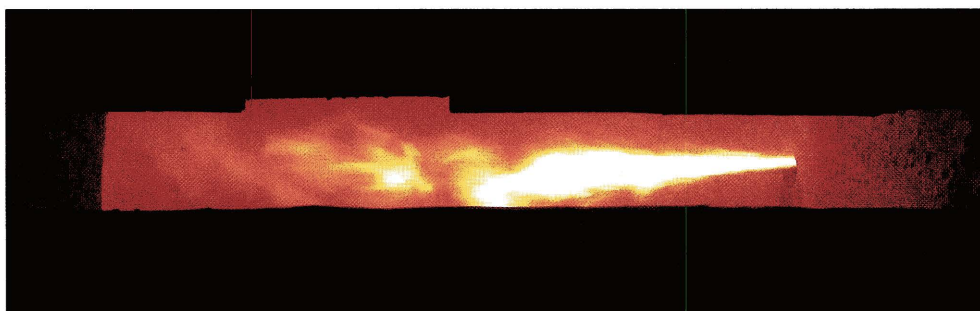
Photograph 1
Flame 14
Heavy Fuel Oil

SR = 1.05



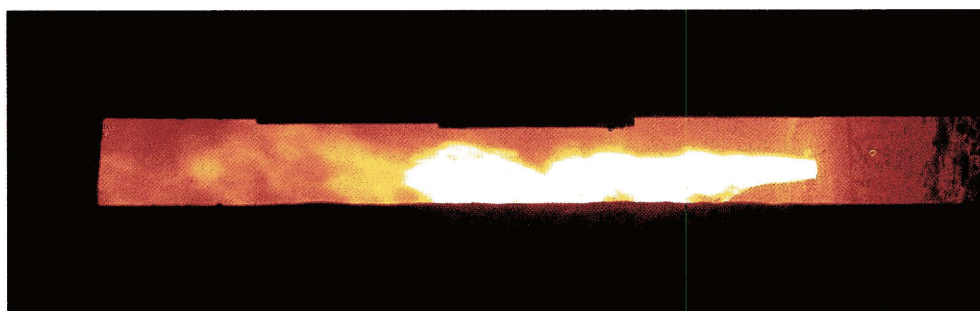
Photograph 2
Flame 34
Heavy Fuel Oil

$T_B = 950^\circ\text{C}$
SR = 1.09



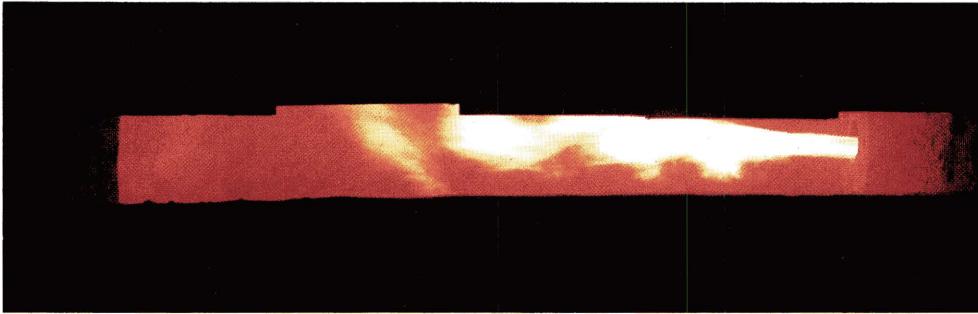
Photograph 3
Flame 4
Elk Creek Coal

$T_B = 1140^\circ\text{C}$
SR = 1.0
Injector 1

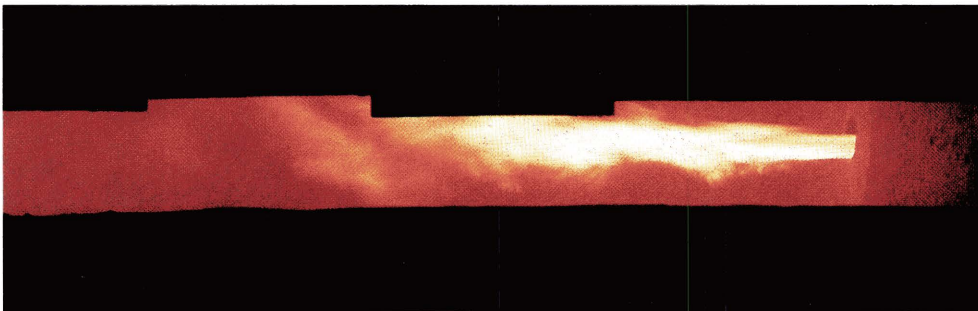


Photograph 4
Flame 3 and 15
Elk Creek Coal

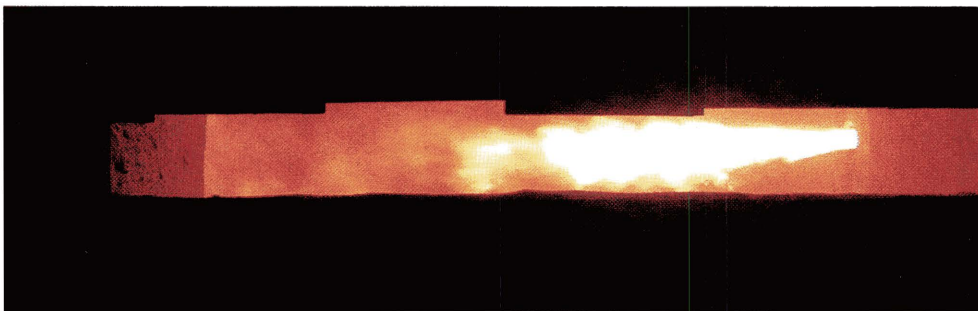
$T_B = 1190^\circ\text{C}$
SR = 1.0
Injector 2



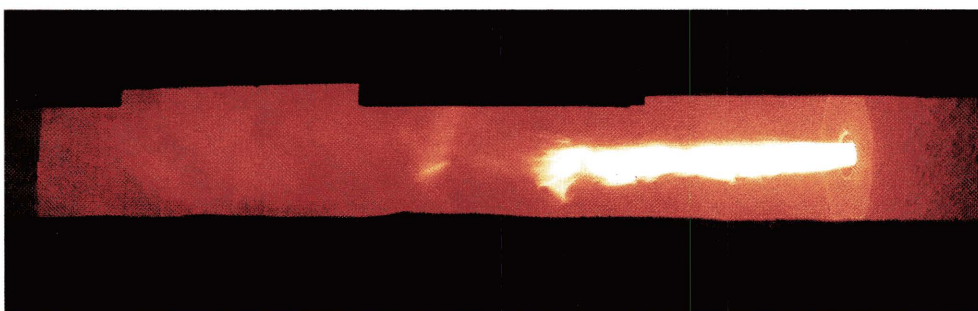
Photograph 5
Flame 5
Elk Creek Coal
 $T_B = 1190^\circ\text{C}$
SR = 1.0
Injector 4



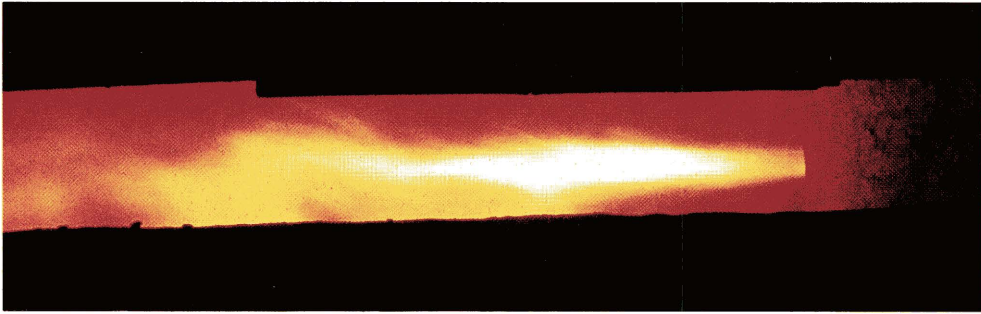
Photograph 6
Flame 6 and 13
Elk Creek Coal
 $T_B = 1160^\circ\text{C}$
SR = 1.0
Injector 5



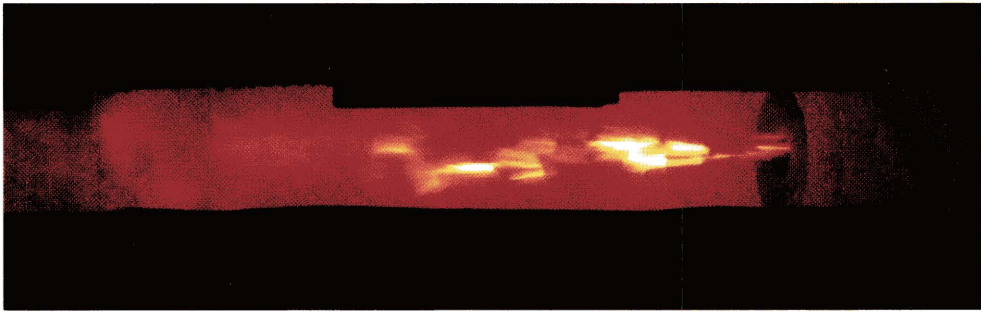
Photograph 7
Flame 25
Elk Creek Fine Grind
 $T_B = 1180^\circ\text{C}$
SR = 1.01
Injector 2



Photograph 8
Flame 26
Elk Creek Fine Grind
 $T_B = 1180^\circ\text{C}$
SR = 1.94
Injector 2



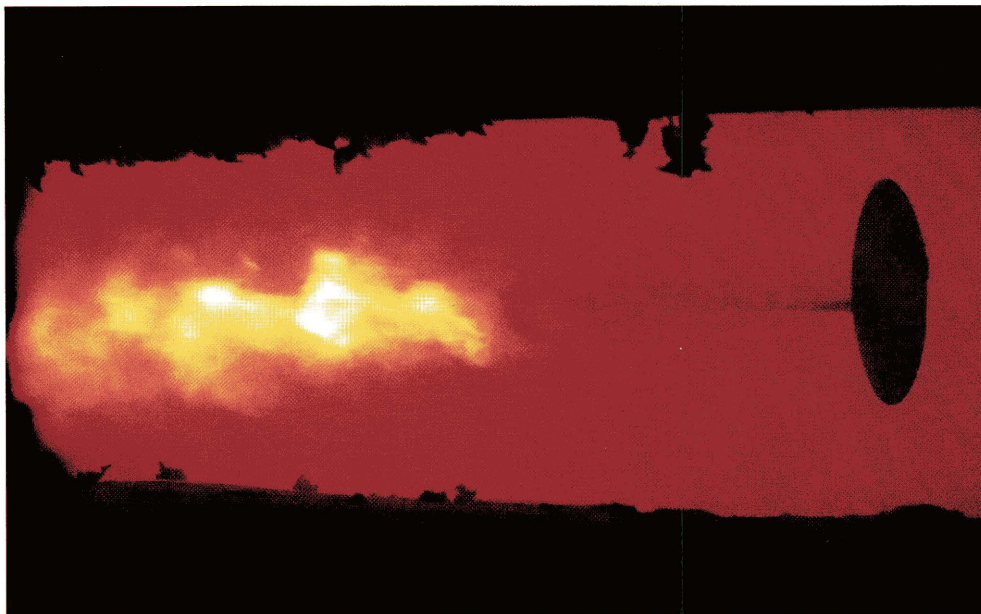
Photograph 9
Flame 22
Elk Creek Coal
 $T_B = 1030^\circ\text{C}$
SR = 1.0
Injector 2



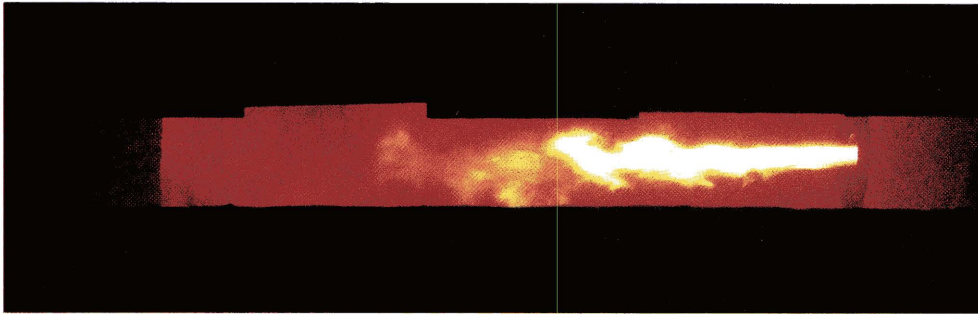
Photograph 10
Flame —
Elk Creek Coal
 $T_B = 990^\circ\text{C}$
SR = 2.0
Injector 2



Photograph 11
Flame 42
Elk Creek Coal
 $T_B = 930^\circ\text{C}$
SR = 2.0
Injector 2

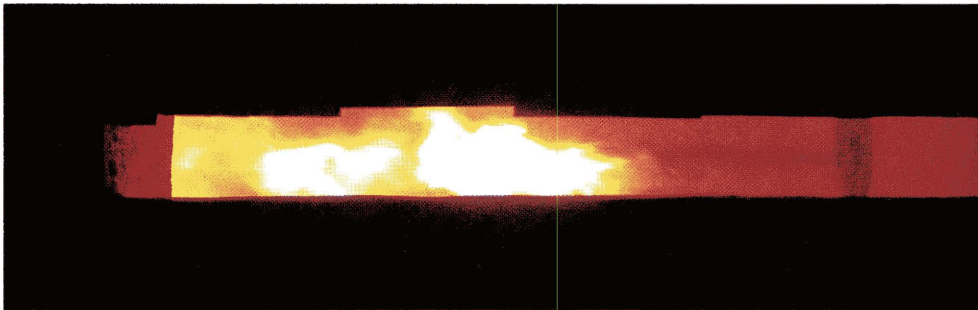


Photograph 12
Flame 29
Armco Coal
 $T_B = 940^\circ\text{C}$
SR = 1.0
Injector 2



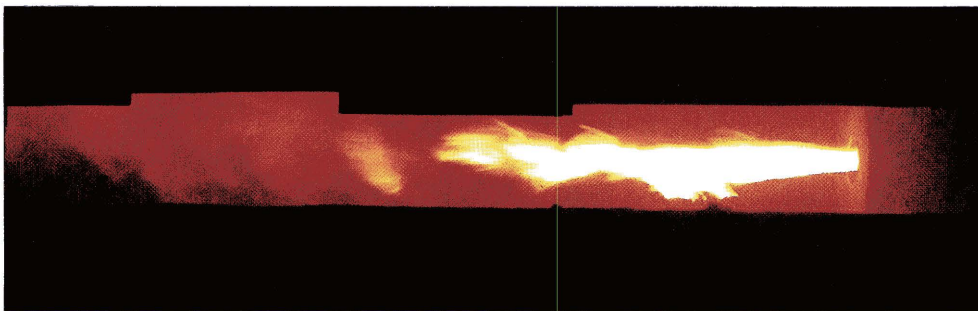
Photograph 13

Flame 28
Armco Coal
 $T_B = 1210^\circ\text{C}$
SR = 1.01
Injector 2



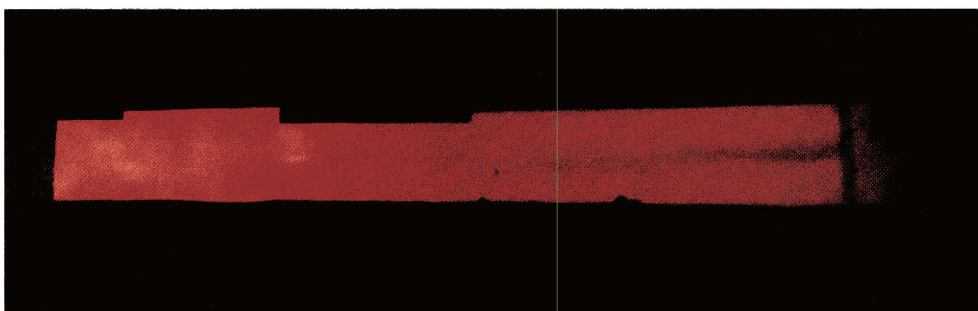
Photograph 14

Flame 29
Armco Coal
 $T_B = 940^\circ\text{C}$
SR = 1.03
Injector 2



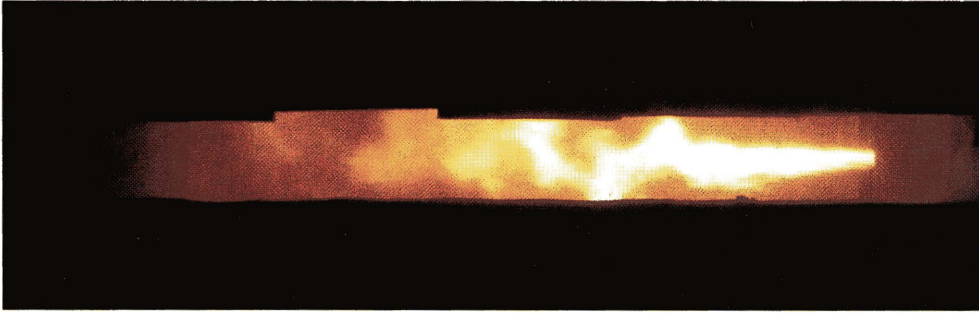
Photograph 15

Flame —
Armco Coal
 $T_B = 1200^\circ\text{C}$
SR = 2.0
Injector 2

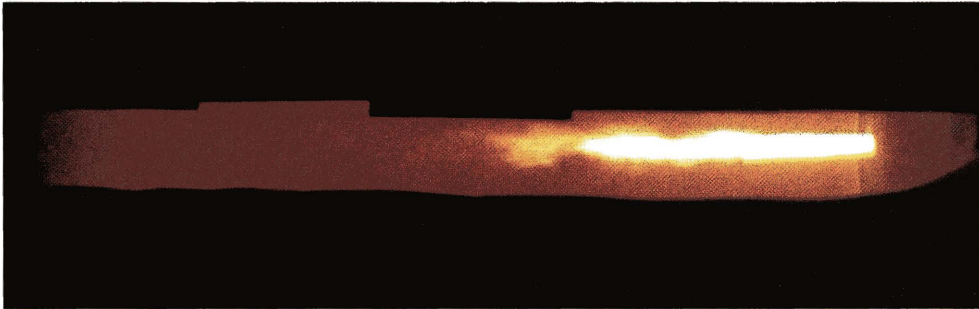


Photograph 16

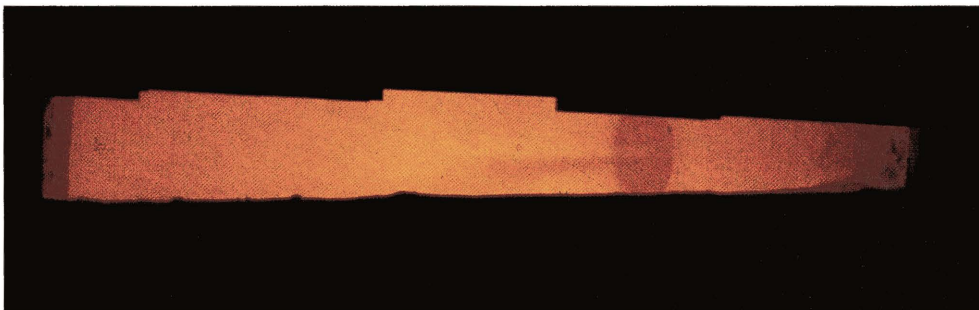
Flame —
Armco Coal
 $T_B = 930^\circ\text{C}$
SR = 2.0
Injector 2



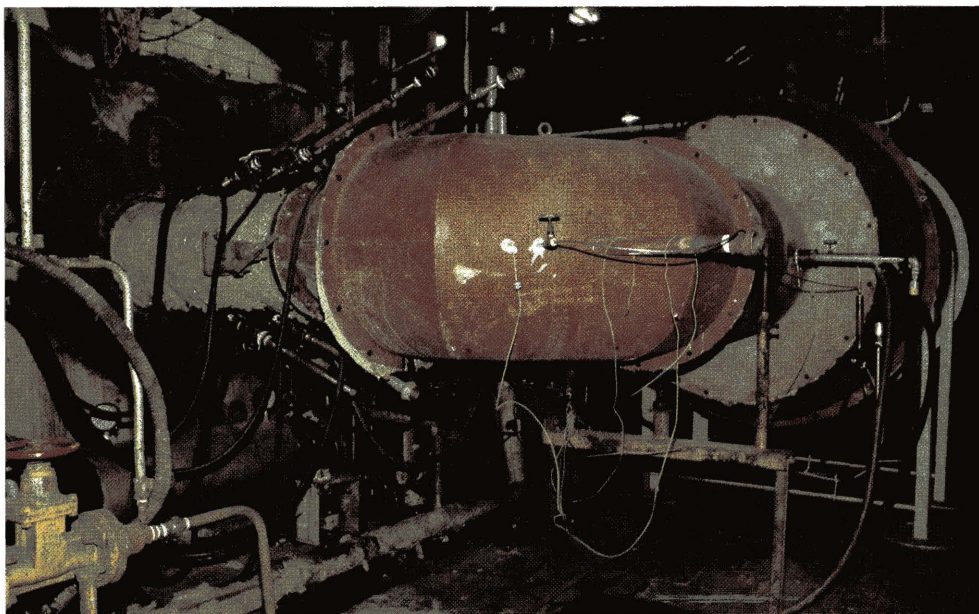
Photograph 17
Flame 36
Norwich Park Coal
 $T_B = 1220^\circ\text{C}$
SR = 0.99
Injector 2



Photograph 18
Flame 35
Norwich Park Coal
 $T_B = 1200^\circ\text{C}$
SR = 2.05
Injector 2



Photograph 19
Flame 37
Preussag Coal
 $T_B = 1220^\circ\text{C}$
SR = 0.90
Injector 2



Photograph 20
Air preheater
and blow pipe